New Synthetic Approaches to Triosmium Decacarbonyl Bisethoxide and the Systematic Design of Linked Triosmium Clusters via Bridging Diols

By
Robert E. Sommerhalter

A thesis submitted in partial fulfillment of the requirements for graduation with

HONORS IN CHEMISTRY

Examining Committee:

Mary-Ann Pearsall, Thesis Advisor
Chemistry

Alan Rosan, Member
Chemistry

Steve Surace, Member
Mathematics

Summer Harrison, Member
English and Environmental Studies

DREW UNIVERSITY
MAY 2016

Abstract

With the goal of developing systematic syntheses of linked triosmium carbonyl clusters, we report the substitution reactions of the dibridged cluster $Os_3(CO)_{10}(\mu^2\text{-}OEt)_2$ with the bifunctional ligand 1,5-pentanediol. Reaction of $Os_3(CO)_{10}(\mu^2\text{-}OEt)_2$ with 1,5-pentanediol affords the cluster $Os_3(CO)_{10}(\mu^2\text{-}O(CH_2)_5OH)_2$ as the major product. Over extended reaction periods, quantitative conversion to the cluster $H_4Os_4(CO)_{12}$ is observed. Linking of two triosmium carbonyl clusters via the 1,5-pentanediol bridging ligands has been achieved in the reaction of $Os_3(CO)_{10}(\mu^2\text{-}O(CH_2)_5OH)_2$ with one molar equivalent of $Os_3(CO)_{10}(\mu^2\text{-}OEt)_2$. A secondary product of this reaction has been characterized spectroscopically and is believed to be an intermediate in the formation of $H_4Os_4(CO)_{12}$. A synthetic route to $Os_3(CO)_{10}(\mu^2\text{-}OEt)_2$ via di-halogenated cluster intermediate $Os_3(CO)_{12}X_2$ or $Os_3(CO)_{10}(\mu^2\text{-}X)_2$ (X = Cl, Br, I) is also reported.

Table of Contents

Tables Page #

Figures Page #

Spectra Page #

Chapter 1 – Introduction

In this work the chemistry of osmium carbonyl clusters of the form $Os_3(CO)_{10}(\mu^2\text{-}X)_2$ will be discussed (figure 01).

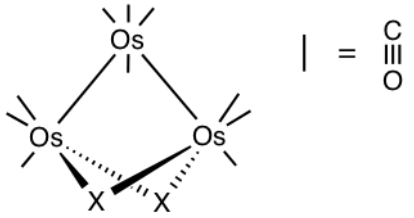

Figure 01 – Structure of a cluster with formula $Os_3(CO)_{10}(\mu^2\text{-}X)_2$. Line bonds from metal centers will be used to represent carbonyl ligands (CO) throughout this work.

A metal cluster is an organometallic complex having three or more transition metal centers with substantial bonding between metal centers.[1] It is neither a mononuclear complex nor a bulk metal – two well established structures in chemistry – but it possesses structural features of both. As with mononuclear complexes, a metal cluster has ligands which may be exchanged (figure 02). Unlike mononuclear complexes, however, clusters are unique due to the presence of metal-metal bonds – a feature that was previously thought reserved for bulk metals. For these reasons, metal clusters may offer unique physical and chemical properties to the development of new materials.

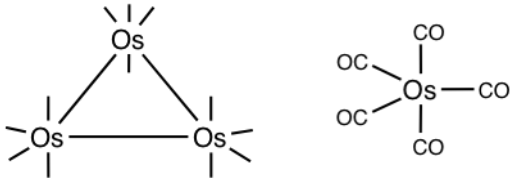

Figure 02 – Structure comparison of a cluster, $Os_3(CO)_{12}$ (left), and a mononuclear complex, $Os(CO)_5$ (right).

There are two important considerations when interpreting structure and reactivity of organometallic complexes – its ligands and electron count. The 18-electron rule is a

concept which applies to organometallic complexes.[2] In the typical organometallic complex, one may observe that to each valence orbital of the metal center there is two electrons. This is to utilize all nine available orbitals in bonding interactions. Having all nine valence orbitals of the metal engaged in bonding stabilizes the complex. For example, chromium hexacarbonyl $Cr(CO)_6$ has 6 valence electrons from the metal (Cr [Ar]$3d^6$) plus 2 electrons for each CO ligand to a total electron count of 18 (figure 03).

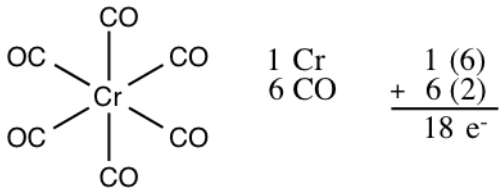

Figure 03 – Structure of chromium hexacarbonyl and its electron count demonstrating the 18-electron rule.

When applied to clusters, the 18-electron rule allows us to predict the number of M–M bonds. Figure 04 shows the electron count for the cluster $Os_3(CO)_{10}(\mu^2\text{-}OEt)_2$. Although an electron count of 54 is required by the 18-electron rule, only 50 are accounted for in the figure. This means that the cluster is coordinatively unsaturated, and will engage in M–M bonding to satisfy the 18-electron rule. Thus the structure in figure 04 satisfies the 18-electron rule by forming two Os–Os bonds. By using this simple electron counting method one may predict a few major structural features of the cluster.

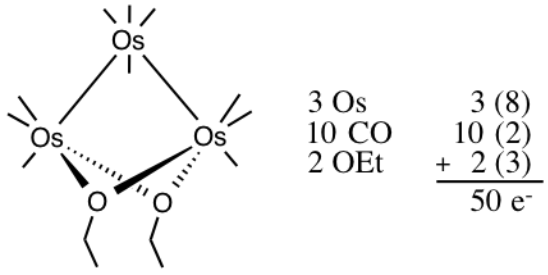

Figure 04 – Structure of $Os_3(CO)_{10}(\mu^2\text{-}OEt)_2$ and its electron count demonstrating how the 18-electron rule applies to metal clusters.

The ligands of a transition metal complex affect the reactivity of the complex. There are several types of ligand-metal interactions; the simplest of which is the σ-donor.[2] Transition metals are electron deficient, that is, they have fewer electrons than the number of valence orbitals available. As such, they have vacant orbitals to accept electrons from a ligand. A σ-type interaction refers to *end-on* orbital overlap. Conversely, a π-type interaction refers to *side-on* orbital overlap. There are two types of π-type interactions: π-acceptor and π-donor (figure 05).[2]

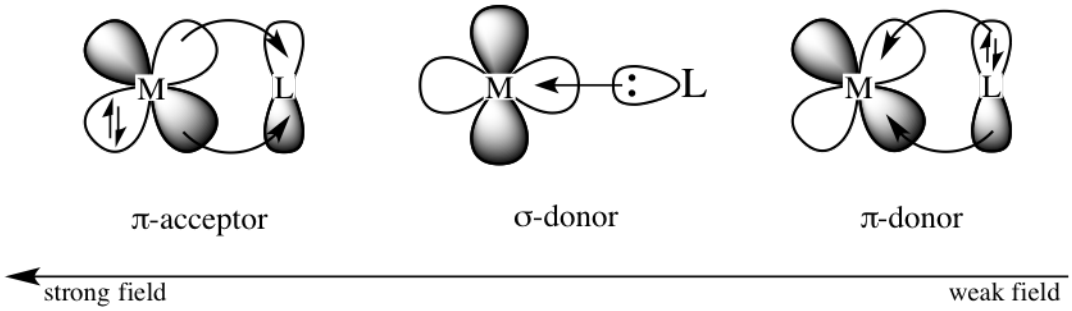

Figure 05 – Simple metal-ligand interactions in classical coordination complexes.

One of the most common ligands in organometallic complexes is carbon monoxide (CO). When coordinated to a metal center, carbon monoxide is called a carbonyl ligand. As a ligand, carbon monoxide engages in σ-donor, π-acceptor interactions with the metal center (figure 06).

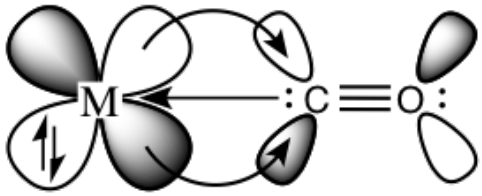

Figure 06 – Model of the metal-ligand interactions for a carbon monoxide ligand.

A M—CO bond involves two orbital interactions. Electrons in the CO non-bonding σ 2p orbital are donated into a vacant d orbital of the metal for a σ-type interaction. Additionally, a π-type interaction occurs between a filled metal d orbital and the antibonding π* orbital of the ligand. This form of π-acceptor interaction is referred to as *back-donation* from M(nd) to L(π*).

Carbon monoxide is considered to be a *strong field ligand*. The designations strong and weak field ligand stem from ligand field theory.[2] It refers to the relative effect that each M—L orbital interaction has on the splitting of metal d orbitals. The energy gap between nd orbitals split by an octahedral field is a quantity called Δ_{oct}. In the carbon monoxide example, back-donation from M(nd) to CO(π*) stabilizes the d_{xy}, d_{xz}, d_{xy} orbitals of the metal and destabilizes the π* orbitals of the ligand. The σ-donor interaction destabilizes the d_z^2 and $d_{x^2-y^2}$ orbitals of the metal, and stabilizes the σ orbitals of the ligand. Thus both π-acceptor and σ-donor ligands will effectively increase Δ_{oct} (figure 07).

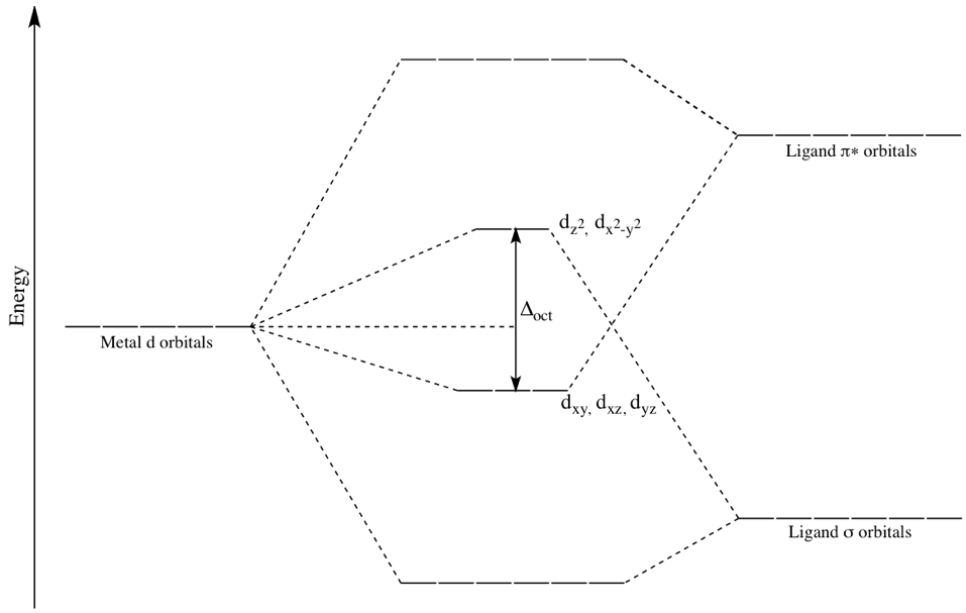

Figure 07 – Molecular orbital energy diagram of a transition metal in an octahedral field of π-acceptor ligands.

Following a similar approach, one would find that π-donor ligands reduce Δ_{oct} and are thus designated *weak field ligands*. These ligand classifications are supported by experimental evidence, which resulted in the *spectrochemical series* – a series of the relative strong or weak field character for common ligands.[2] The splitting of metal nd orbitals by Δ_{oct} may have a net stabilization effect, called *Ligand Field Stabilization Energy* (LFSE). Each electron contributes some fraction of Δ_{oct} to the LFSE. The sign of each electron contribution depends on which d orbital the electron occupies. Changes to LFSE through a ligand exchange reaction mechanism will influence activation energy.

Unfortunately, a molecular orbital approach to M–L bonds in a metal cluster is much more complicated than in mononuclear complexes. As such, the ways in which one might come to understand metal cluster bonding are relatively limited. Computational modelling of the molecular orbitals in a metal cluster offers insight into possible M–L interactions. Alternatively, an observational approach on a cluster's reactivity with small organic molecules offers a different form of understanding.

Fundamental understanding of how small organic molecules interact with and coordinate to the metal core is necessary to the eventual design of functional clusters. By investigating the interactions of simple organic molecules with the metal core this research aims to develop a basis for the synthetic design of novel osmium clusters.

One area of interest for the design of functional clusters is in catalysis. Catalysis is a process in which a catalyst facilitates a reaction with an otherwise insurmountable energy barrier or that cannot be achieved directly.[2] In a catalytic cycle, the active catalyst is regenerated and will continue to actively convert substrate to product. There is an

interesting parallel between mononuclear and bulk metal catalysts. Mononuclear catalysts generally have greater selectivity than does the bulk metal. This parallel becomes clear by comparison of two catalysts which effectively facilitate the same substrate modification. For example, Wilkinson's catalyst $RhCl(PPh_3)_3$ and Raney-Nickel are both known to catalytically hydrogenate alkenes.[3,4] In the presence of hydrogen, Raney-Nickel will hydrogenate most unsaturated hydrocarbons.[4] Wilkinson's catalyst, however, has high specificity for unhindered alkenes due to the steric bulk of the triphenylphosphine groups.[3]

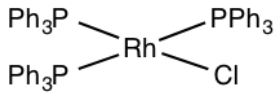

Figure 08 – The structure of Wilkinson's catalyst.

As was mentioned previously, a metal cluster may be thought of as a mononuclear-bulk metal hybrid because it has some features of both metal structures. This is one of the reasons why researchers study the chemistry of metal clusters. Metal clusters might be developed into new catalysts to lower the cost of manufacturing pharmaceuticals and other chemical products.

Osmium Carbonyl Clusters

In 1968, the English chemist Professor the Lord Jack Lewis discovered a new synthetic route to triosmium dodecacarbonyl—a discovery that enabled the rigorous study of osmium carbonyl cluster chemistry.[5] Lewis reported $Os_3(CO)_{12}$ in high yields from the reaction osmium tetroxide (OsO_4) with carbon monoxide in methanol under high pressure (75 atmos.) and temperature (175 ˚C) (figure 09).[5]

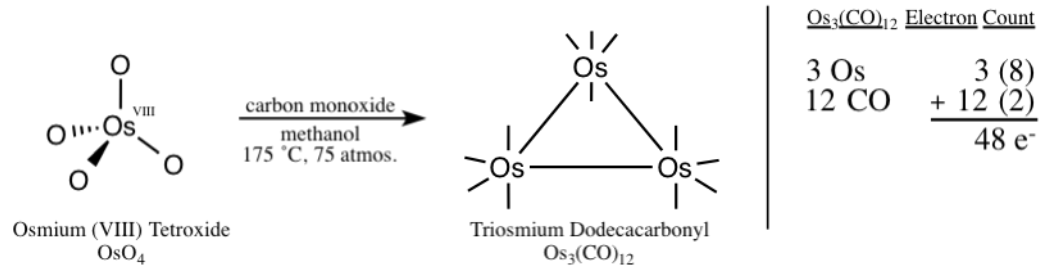

Figure 09 – Scheme of $Os_3(CO)_{12}$ synthetic route by Lewis (left) and electron count of $Os_3(CO)_{12}$ (right).

While Lewis' discovery was not the first reported occurrence of $Os_3(CO)_{12}$, his synthetic route afforded the greatest yield of the cluster.[5,6] Many chemists at the time recognized that derivatization of $Os_3(CO)_{12}$ would mean the development of an entire new class of compounds.[7] Pioneers of this research thought that these clusters might have unique physical and chemical properties. With Lewis' new route, the parent cluster to the study triosmium carbonyl clusters was made accessible.

Structure and bonding in $Os_3(CO)_{12}$ may be interpreted via the 18-electron rule. This cluster has an overall charge of zero. As such, each osmium center has oxidation state zero and coordinated electron configuration Os $[Xe]4f^{14}5d^8$ (in complexes the energy of 6s lies above 5d). So each osmium contributes 8 valence electrons to the electron count. With three metal centers, a total of 54 electrons are required to satisfy the 18-electron rule. Counting each carbonyl as a two electron donor, 48 electrons are accounted for in M–L bonding. With a deficiency of 6 electrons, three Os–Os bonds are predicted.

Triosmium dodecacarbonyl is a triangular structure with three Os–Os bonds – a rather unique feature of group VIII transition metal clusters.[6] The significance of this molecule is realized with the presence of these Os–Os bonds and its capacity to be

functionalized with organic molecules. Looking at the functionalization of triosmium carbonyl cluster derivatives, one may begin to appreciate the versatility of metal clusters.

Several unique ligand coordination modes are observed in organometallic chemistry.[2] What coordination mode a ligand will assume depends on the electronic nature of the ligand and also the availability of the binding site. Three of the most well established ligand coordination modes are discussed below.

A ligand is often referred to as a *terminal* ligand if it is coordinated to just one metal center.[2] These are the ligands that occur most frequently in classical coordination complexes. Carbon monoxide is an example of a terminal ligand in the cluster $Os_3(CO)_{12}$. Clusters introduce additional functionality with new ligand coordination options. For example, some ligands may bridge a M–M edge of the cluster. These ligands are referred to as being *bridging*. In the cluster $(\mu^2\text{-H})Os_3(CO)_{10}(\mu^2\text{-Cl})$ there are two types of bridging ligands: a bridging hydride and a bridging chloride (figure 10).[8] The Greek letter μ (*mu*) in a cluster formula indicates that the ligand is bridging, and the superscript specifies the number of metal centers to which the ligand is coordinated. This terminology and formalism will be used throughout this work.

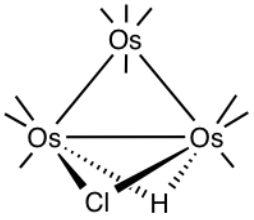

3 Os	3 (8)
10 CO	10 (2)
1 Cl	1 (3)
1 H	+ 1 (1)
	48 e⁻

Figure 10 – The structure of $(\mu^2\text{-H})Os_3(CO)_{10}(\mu^2\text{-Cl})$ demonstrates the three common types of ligand coordination modes in metal cluster chemistry.

Over the past few decades, hundreds of new triosmium carbonyl derivatives have been synthesized.[9] Many of these clusters offer promising utility to the synthetic design of new catalysts and materials. There are several ways to generate functionalized osmium carbonyl clusters from $Os_3(CO)_{12}$. The first method is via the direct reaction of $Os_3(CO)_{12}$ with an appropriate organic molecule to achieve the desired functionality.[10] An alternative method is to introduce a labile ligand, thereby creating an activated cluster.[11] The use of such an activated cluster allows for milder reaction conditions. Examples of each of these approaches and their flaws will be discussed.

A major obstacle to the study of triosmium carbonyl clusters is the low reactivity of $Os_3(CO)_{12}$.[12] In general, functionalization of $Os_3(CO)_{12}$ via direct reaction with organic molecules requires high temperature and pressure. These heightened reaction conditions often result in cluster decomposition and affords multiple undesirable byproducts. For example, the reaction of $Os_3(CO)_{12}$ with isobutanol affords a total of six unique cluster products (figure 11).[13]

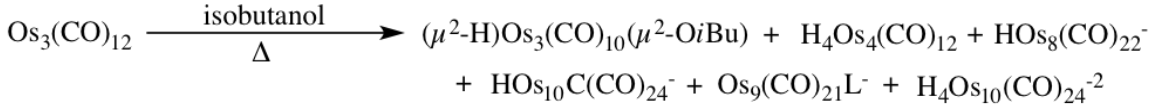

Figure 11 – Scheme of the reaction of $Os_3(CO)_{12}$ with isobutanol at elevated temperature.

To avoid severe reaction conditions, a labile ligand may be introduced to $Os_3(CO)_{12}$ for the synthesis of functionalized triosmium carbonyl clusters.[11] This approach is better suited for multistep synthesis of triosmium cluster derivatives as it reduces the risk of thermal decomposition. There are several activated clusters that are regularly used in the literature. The acetonitrile cluster $Os_3(CO)_{10}(MeCN)_2$ is one of the most frequently used

activated clusters.[9] Its synthesis involves the reaction of $Os_3(CO)_{12}$ with trimethylamine N-oxide in the presence of acetonitrile (figure 12).[12]

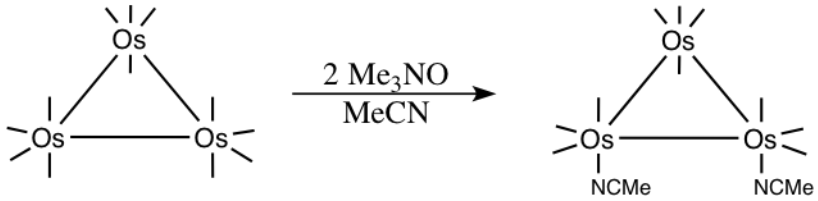

Figure 12 – Scheme of reaction of $Os_3(CO)_{12}$ with trimethylamine N-oxide in the synthesis of $Os_3(CO)_{10}(MeCN)_2$.

As an intermediate to functionalized clusters, $Os_3(CO)_{10}(MeCN)_2$ has been demonstrated to undergo ligand exchange in very mild conditions.[12] Acetonitrile ligands are readily replaced and so this cluster acts as entry into different modes of functionalization. For example, synthesis of clusters of the form $(\mu^2\text{-H})Os_3(CO)_{10}(\mu^2\text{-OR})$ (R = H, Me, Et) is achieved with addition of HOR to $Os_3(CO)_{10}(MeCN)_2$.[12] Bridging alkoxide clusters are different in that they are functionalized with bridging ligands bearing unique reactivity. For example, a new bridging ligand may be introduced to this cluster via displacement of the bridging OR ligand. Ligand exchange has been demonstrated for many different ligands, including other alcohols (HOR') (figure 13).[14]

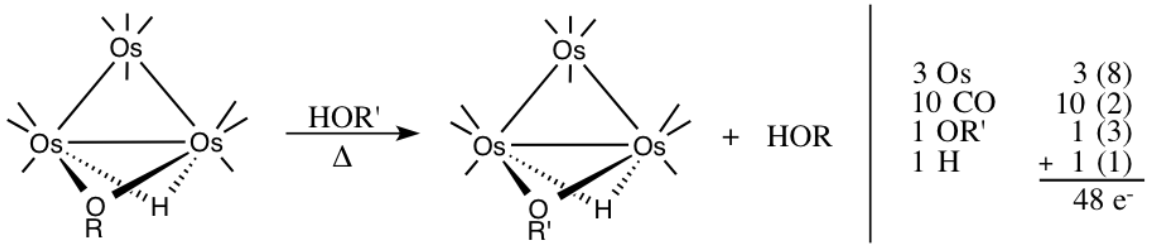

Figure 13 – Scheme of substation reaction of a cluster $(\mu^2\text{-H})Os_3(CO)_{10}(\mu^2\text{-OR})$ with an alcohol HOR' to produce $(\mu^2\text{-H})Os_3(CO)_{10}(\mu^2\text{-OR'})$ (left). Electron count of this type of cluster (right).

Bridging hydride ligands are present in the majority of known triosmium carbonyl derivatives.[9] The quintessential cluster of this type is triosmium decacarbonyl dihydride.

Hydrogenation of $Os_3(CO)_{12}$ affords the deep purple cluster $(\mu^2\text{-}H)_2Os_3(CO)_{10}$ in high yield (figure 14).[15]

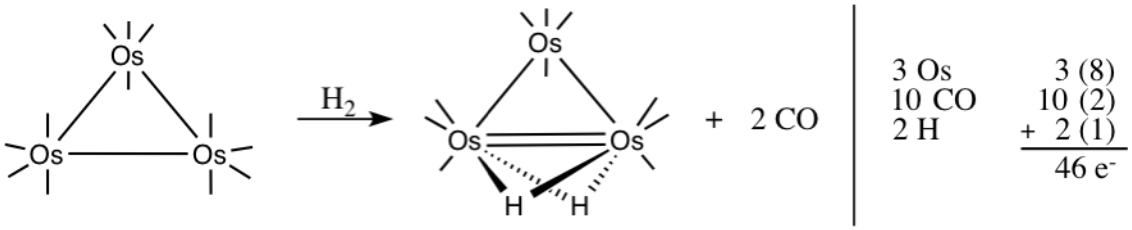

Figure 14 – Scheme of hydrogenation of $Os_3(CO)_{12}$ to produce the cluster $(\mu^2\text{-}H)_2Os_3(CO)_{10}$ (left) and the product electron count (right).

The deep purple color of $(\mu^2\text{-}H)_2Os_3(CO)_{10}$ is rather unique as most triosmium carbonyl clusters appear visibly orange-yellow. On applying the electron counting method to $(\mu^2\text{-}H)_2Os_3(CO)_{10}$ the cluster is coordinatively unsaturated by 8 electrons. This means that four Os–Os bonds are predicted by the 18-electron rule. This requirement is satisfied by the presence of an Os=Os double bond that is unusually reactive.

As a starting compound, $(\mu^2\text{-}H)_2Os_3(CO)_{10}$ reacts with 1,3-dioxol-2-one to give an interesting cluster $(\mu^2\text{-}H)Os_3(CO)_{10}(\mu^2\text{-}OCH{=}CH_2)$ (figure 15).[16] In the reaction, a bridging hydride adds to the organic substrate and carbon dioxide is released. The vinyloxy bridging ligand has been demonstrated to react with hydrogen chloride to give the cluster $(\mu^2\text{-}H)Os_3(CO)_{10}(\mu^2\text{-}Cl)$ and acetaldehyde (figure 15).[16] An important note about hydride bridged triosmium clusters is that the second bridging hydride is unreactive towards substitution. Thus these clusters do not have the option to exchange the hydride ligand and achieve a difunctional $Os_3(CO)_{10}(\mu^2\text{-}X)_2$ structure.

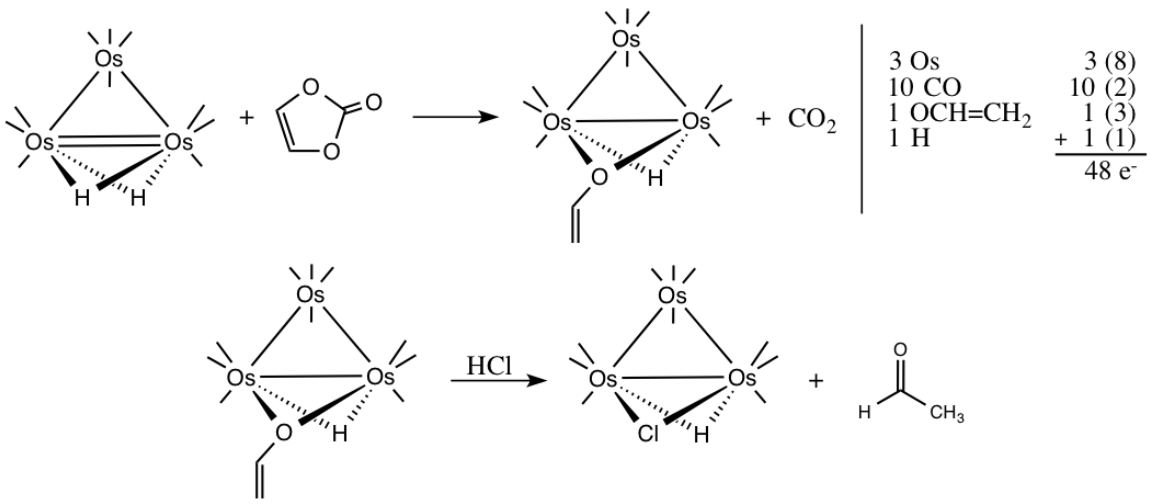

Figure 15 – Scheme of reaction of $(\mu^2\text{-H})Os_3(CO)_{10}$ with 1,3-dioxol-2-one to produce the cluster $(\mu^2\text{-H})Os_3(CO)_{10}(\mu^2\text{-OCH=CH}_2)$ (right) and the electron count of the product (left). Subsequent reaction with hydrogen chloride produces acetaldehyde and the cluster $(\mu^2\text{-H})Os_3(CO)_{10}(\mu^2\text{-Cl})$.

This reaction scheme mimics a catalytic reaction in that the cluster modifies the organic substrate to produce some other free organic product; however, it does not regenerate the active catalyst and so is not truly catalytic.

Terminal ligands may also be introduced to triosmium carbonyl clusters. One example is the reaction of $Os_3(CO)_{12}$ with trimethyl phosphite ($P(OMe)_3$).[12] This reaction affords a mixture of mono-, di-, and trisubstituted phosphite derivatives (figure 16).[12]

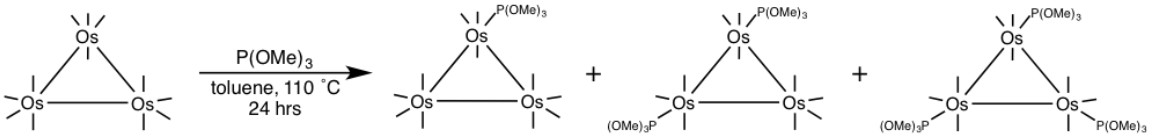

Figure 16 – Scheme of reaction of $Os_3(CO)_{12}$ with trimethyl phosphite.

That this reaction requires such high temperature and extended reaction time owes to the low reactivity of $Os_3(CO)_{12}$. The formation of multiple products is common with such forcing reaction conditions. To readily substitute carbonyl ligands for trimethyl phosphite

is a desired feature of organometallic complexes. This is because a great deal of structural information may be deduced with infrared spectra of the initial and phosphite clusters.

Clusters of the dibridged form $Os_3(CO)_{10}(\mu^2\text{-}X)_2$ with no bridging hydride ligand and without a M–M bond on the bridged edge are yet another structural motif in the chemistry of osmium carbonyl (figure 17).

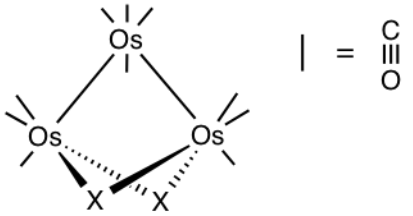

Figure 17 – Generic structure of a dibridged cluster of the form $Os_3(CO)_{10}(\mu^2\text{-}X)_2$.

The absence of a bridging hydride means that the cluster has the option of functionalization at both bridging ligand positions. A review of the literature reveals that this type of cluster is very rare.[9] Of the few reports that mention attempted synthesis of dibridged clusters, only one route obtained this form of cluster as the major product.[12] As such, not much is known about this form of dibridged cluster.

Dibridged clusters were first observed as minor products in the synthesis of $Os_3(CO)_{12}$ by Lewis (figure 18).[5]

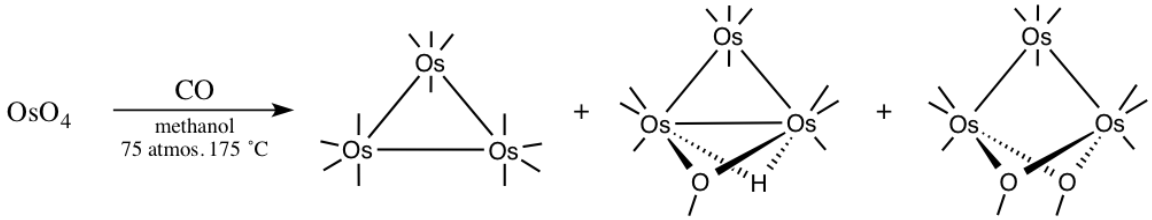

Figure 18 – Scheme of $Os_3(CO)_{12}$ synthesis by Lewis.

Depending on the alcohol used in the reaction, the corresponding alkoxide cluster $Os_3(CO)_{10}(\mu^2\text{-}OR)_2$ is obtained in very low yield (~5%).[5] The primary focus of this

laboratory is dibridged alkoxide clusters of the form $Os_3(CO)_{10}(\mu^2\text{-}OR)_2$. In the past, this laboratory obtained the cluster $Os_3(CO)_{10}(\mu^2\text{-}OEt)_2$ from a supplier who produced large quantities of $Os_3(CO)_{12}$ via Lewis' synthesis in ethanol. In time, the supplier halted production of $Os_3(CO)_{12}$ and this laboratory was in need of a new source of $Os_3(CO)_{10}(\mu^2\text{-}OEt)_2$ for the ongoing studies of dibridged clusters.

After the source of $Os_3(CO)_{10}(\mu^2\text{-}OEt)_2$ went dry this laboratory investigated alternative synthetic routes to obtain the cluster. In the literature, there are several attempted conversions of $Os_3(CO)_{12}$ to $Os_3(CO)_{10}(\mu^2\text{-}OMe)_2$, an analogue of $Os_3(CO)_{10}(\mu^2\text{-}OEt)_2$ with similar reactivity, all of which reported very low yield of the desired product (figure 19).[17,18]

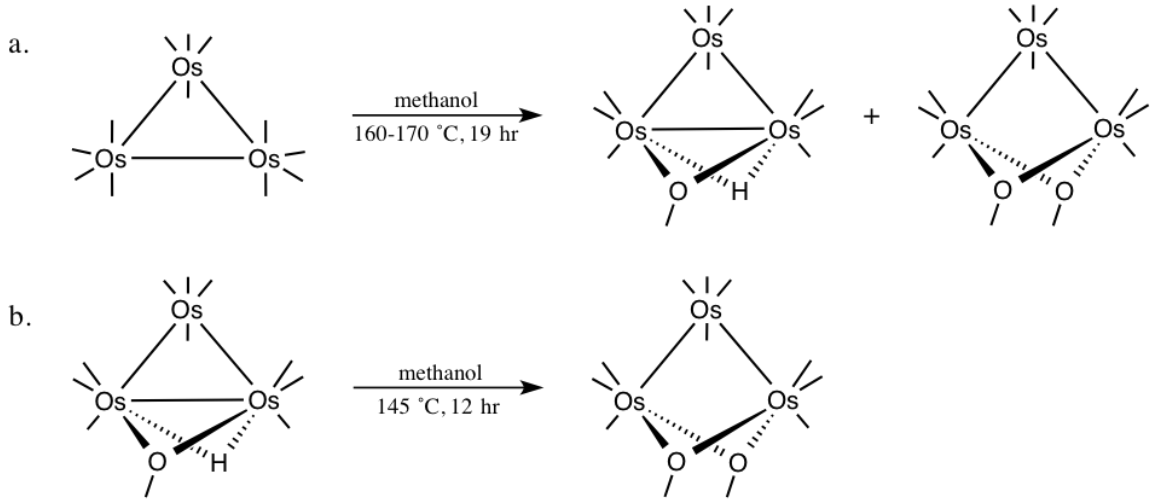

Figure 19 – Scheme of routes to $Os_3(CO)_{10}(\mu^2\text{-}OMe)_2$ in literature. Routes a and b afford the cluster $Os_3(CO)_{10}(\mu^2\text{-}OMe)_2$ in 13% and 19% yield, respectively.[17,18]

Due to the high cost of the cluster $Os_3(CO)_{12}$ these low yield procedures were not practical starting points for the goals of this laboratory. Thus the search for a new synthetic route continued.

While there is no high-yield literature route to $Os_3(CO)_{10}(\mu^2\text{-}OR)_2$, the dihalide cluster analogues $Os_3(CO)_{10}(\mu^2\text{-}X)_2$ are well known.[12] In 1970 Lewis et al. reported on the syntheses of halide cluster derivatives $Os_3(CO)_{12}X_2$ (X = Cl, Br, I) and subsequent conversion to cyclic ten-carbonyl analogues $Os_3(CO)_{10}(\mu^2\text{-}X)_2$ on heating in a hydrocarbon solvent (figure 20).[12]

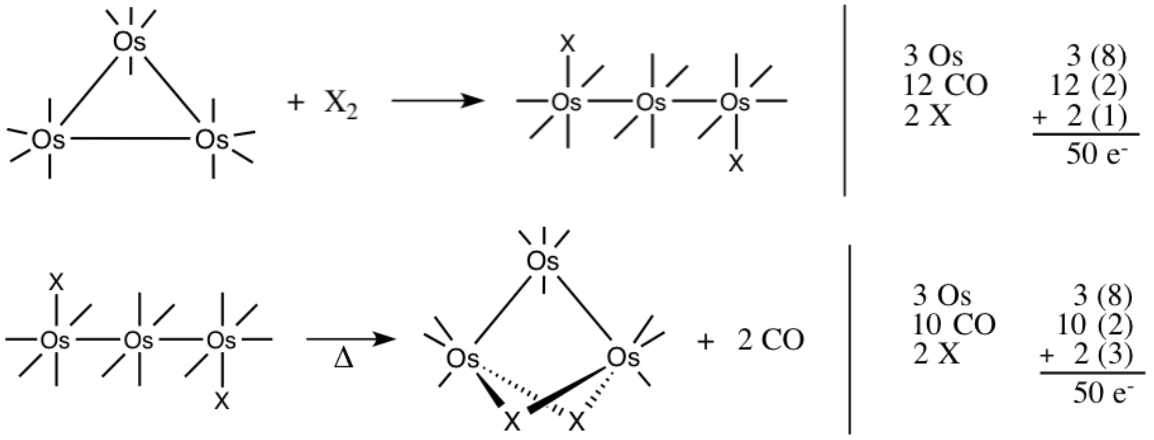

Figure 20 – Synthetic routes to $Os_3(CO)_{12}X_2$ and $Os_3(CO)_{10}(\mu^2\text{-}X)_2$ clusters (left) and electron counts for these two types of clusters (right).

Oxidative addition of halogen X_2 to $Os_3(CO)_{12}$ affords the linear dihalide clusters.[12] In compliance with the 18-electron rule an Os–Os bond is broken. One of the most intriguing features of $Os_3(CO)_{12}X_2$ clusters is that triangular geometry is restored by heating the cluster.[12] The mechanism of cyclization has not yet been established, but one may observe that the nature the halide ligand changes from a terminal 1-electron donor to a bridging 3-electron donor.

A new route to $Os_3(CO)_{10}(\mu^2\text{-}OEt)_2$ was pioneered by Ashish Shah at Drew University in 2010.[19] In this new route, $Os_3(CO)_{12}Cl_2$ is generated via Deeming's procedure[40] and then heated in ethanol under a nitrogen atmosphere to obtain the desired

product, $Os_3(CO)_{10}(\mu^2\text{-}OEt)_2$ in good yield (figure 21). Shah's synthetic route was later optimized by a series of researchers, including this one.[19-22] These results are discussed herein (see Chapter 3).

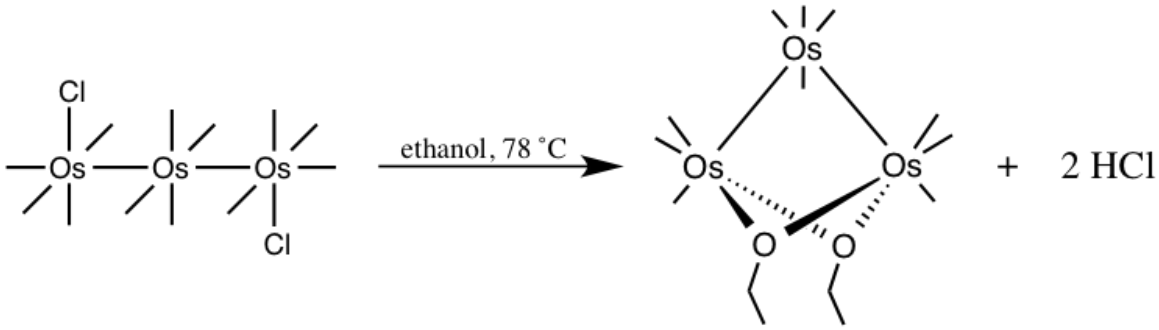

Figure 21 – Scheme of $Os_3(CO)_{10}(\mu^2\text{-}OEt)_2$ synthesis from $Os_3(CO)_{12}Cl_2$ pioneered by Ashish Shah.

This form of dibridged system is studied for the option of functionalization at both bridging ligand positions. These clusters may react at either terminal or bridging ligand positions. A series of researchers at Drew University investigated the reaction kinetics of carbonyl displacement by trimethyl phosphite in dibridged clusters (figure 22).[23,24]

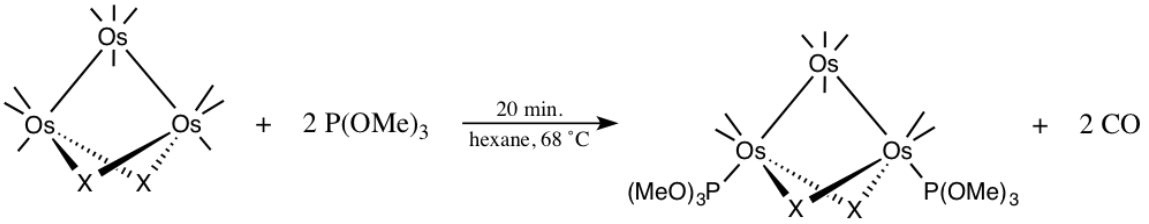

Figure 22 – Substitution of carbon monoxide for trimethylphosphite ligands in various $Os_3(CO)_{10}(\mu^2\text{-}X)_2$ clusters.

Assuming pseudo first order reaction kinetics, Baum and Cavaliere found that the observed activation energy was the same for the three dihalide clusters $Os_3(CO)_{10}(\mu^2\text{-}X)_2$ (X = Cl, Br, I) and on the same order of magnitude as an Os–Os bond.[23,24] This suggests that the

rate-determining step is the breaking of an Os–Os bond. A mechanism for phosphite substitution was thus proposed (figure 23).

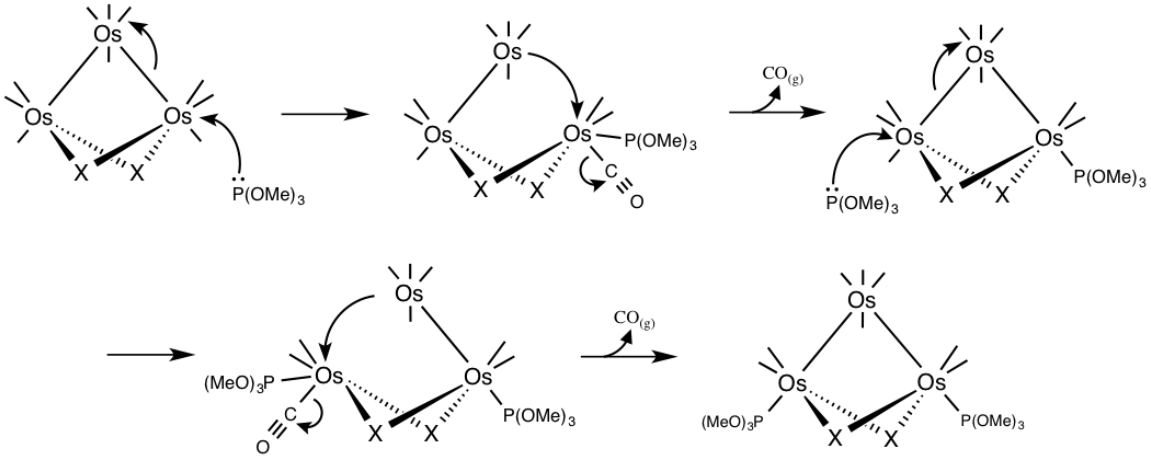

Figure 23 – Proposed mechanism for the displacement of carbon monoxide by trimethyl phosphite in clusters with formula $Os_3(CO)_{10}(\mu^2\text{-}X)_2$.

In 2013, Timothy Barnum found evidence to support this reaction mechanism via computational analysis of the cluster molecular orbitals. Barnum found that the activation energy for each of the three reactions are roughly equivalent on the order of an Os–Os bond.[25] However, slight variation in the rate constants of these reactions (Cl > Br > I) was reported by Baum and Cavaliere.[23,24] This finding was attributed to a steric effect of the halogen on the cluster. Said steric effect would not appear in the activation energy term, but rather in the pre exponential coefficient of the Arrhenius equation. Lastly, they observed that substitution occurs only at the position *trans* to the Os–Os bond, producing a single disubstituted product.[23,24]

Replacement of bridging ligands in dibridged triosmium clusters has been demonstrated by this laboratory. In 2000, Johnathan Babyak studied alkoxide substitution reactions with the cluster $Os_3(CO)_{10}(\mu^2\text{-}OEt)_2$.[26] He found that this cluster reacts with a

variety of different alcohols to give the corresponding disubstituted analogue, $Os_3(CO)_{10}(\mu^2\text{-}OR)_2$ (figure 24).[14,26]

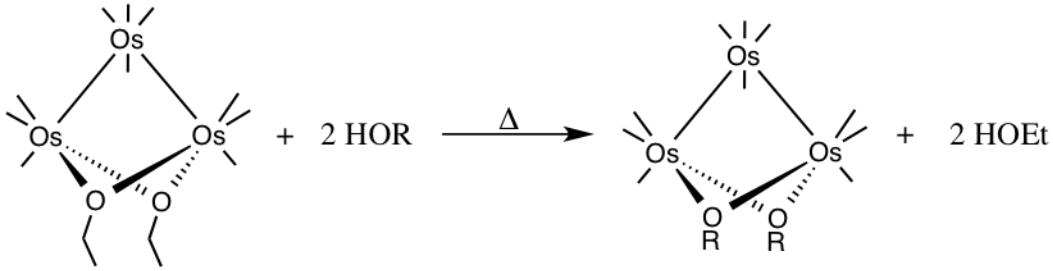

Figure 24 – Bridging ligand substitution of $Os_3(CO)_{10}(\mu^2\text{-}OEt)_2$ with an alcohol, HOR (R = OMe, OEt, O*i*Pr, O*n*Pr, O*i*Bu)

This reaction emphasizes the significance of the $Os_3(CO)_{10}(\mu^2\text{-}OEt)_2$ synthetic route. With access to the cluster $Os_3(CO)_{10}(\mu^2\text{-}OEt)_2$, an entire library of oxyligand derivatives of dibridged triosmium clusters is now possible.

Some ligands have complicating functionality that interacts differently with the cluster. For example, the substituted phenol, mesitol, is cyclometallated on reaction with $Os_3(CO)_{10}(\mu^2\text{-}OEt)_2$ (figure 25).[26] This mesitol ligand is said to be *bidentate* because it is is coordinated twice to the cluster.

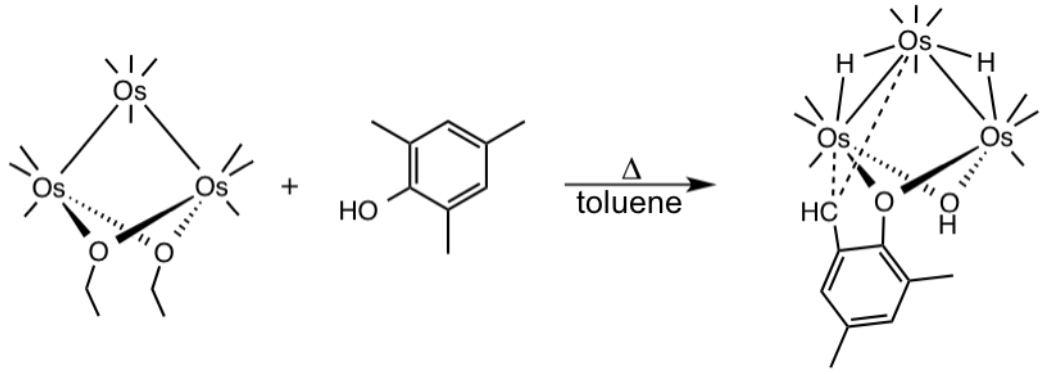

Figure 25 – Reaction of $Os_3(CO)_{10}(\mu^2\text{-}OEt)_2$ with mesitol giving a cyclometallated product.

This result may be attributed to the high temperature and extended reaction time required to achieve alkoxide substitution in $Os_3(CO)_{10}(\mu^2\text{-}OEt)_2$. Cyclometallation of mesitol is not entirely unexpected. Similar cyclometallated products have been reported in the literature as the result of prolonged heating (figure 26).[27]

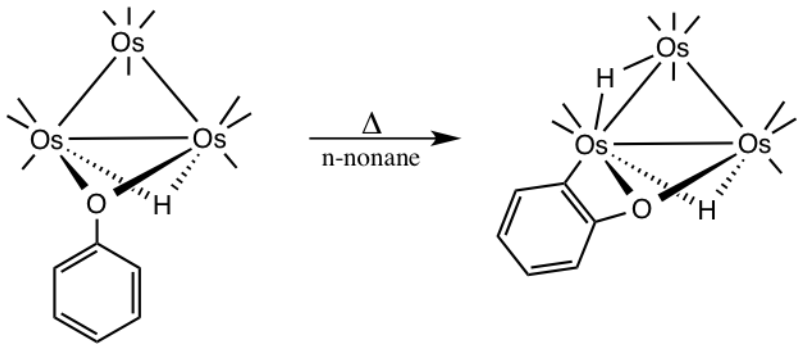

Figure 26 – Thermolysis reaction of $(\mu^2\text{-}H)Os_3(CO)_{10}(\mu^2\text{-}OPh)$ in n-nonane at reflux.

Thus the possibility of cyclometallation places limitations on ligand choice when designing metal cluster systems. Having studied how simple alcohols interact with dibridged clusters, this laboratory has expanded the scope of its investigations to substitution with bifunctional ligands.

Dibridged Systems with Bifunctional Ligands

Metal clusters may offer unique electronic properties due to the presence of metal-metal bonds within a molecular structure. Of particular interest is the potential capacity of a cluster to act as a molecular switch. A molecular switch is a system in which an electron of a cluster may be excited to an excited state where it is transferred to the opposite cluster. Introduction of a bifunctional ligand to a metal cluster offers several new coordination

options, including the option to connect two clusters. A linked cluster system might allow for differential redox potential between the two metal clusters (figure 27).

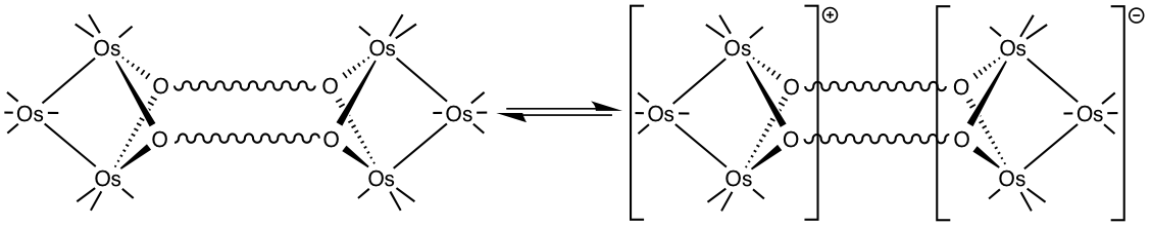

Figure 27 – Model of electron transfer process in a linked cluster system. An unspecified excitation process incites an electron to be transferred from one cluster to the other via the bridging ligands, resulting in a charge separation. The bridging ligand depicted is intended only to serve as an example and is not to be taken as being capable of electron transfer.

With an appropriate bridging ligand and differential redox potential, it may be possible to achieve electron transfer between the two clusters. Bridging ligands capable of participating in an electron transfer process might include delocalized π-systems. Before this laboratory can reach this phase of the project, it is first necessary to investigate how different bifunctional ligands interact with the metal cluster.

There are several examples of clusters with bifunctional ligands in the literature. Leong et al. have reported the synthesis of a number of clusters having the form $(\mu^2\text{-H})Os_3(CO)_{10}(\mu\text{-E}\sim\text{E'H})$ from $(\mu^2\text{-H})Os_3(CO)_{10}(\mu^2\text{-OH})$ or $Os_3(CO)_{10}(NCMe)_2$ (figure 28).[28]

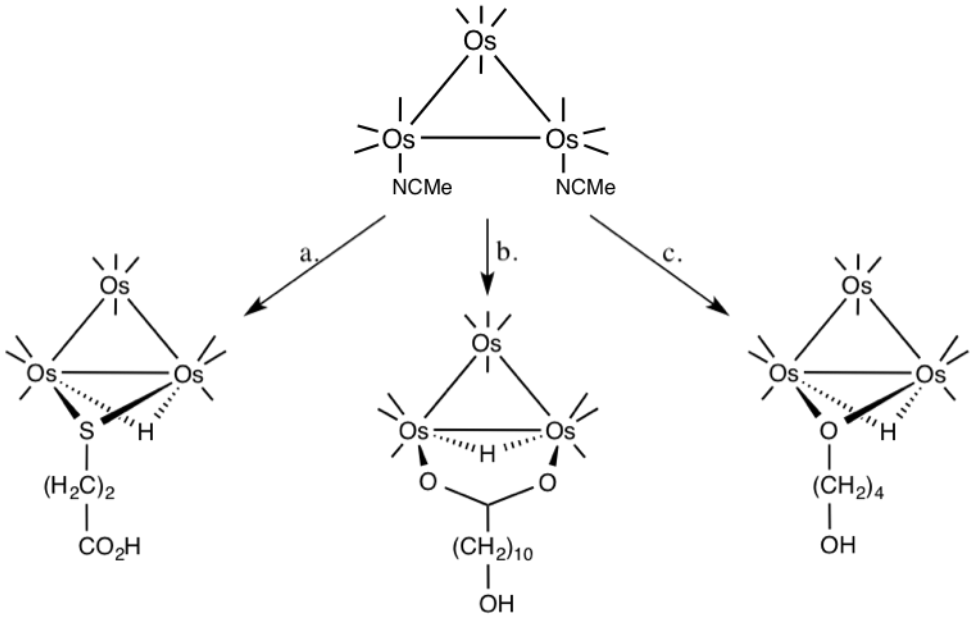

Figure 28 – Scheme of select syntheses of substituted clusters with bifunctional ligands and bridging hydride by Leong et al. demonstrates binding affinity SH > CO_2H > OH. Ligands are as follows: a. $HS(CH_2)_2CO_2H$; b. $HO_2C(CH_2)_{10}OH$; c. $HO(CH_2)_4OH$.

Bifunctional ligands with thiol, alcohol and carboxylate functional groups are reported to have relative binding affinities of SH > COOH > OH.[28] In addition to substituted clusters, low yield of the corresponding linked cluster was also reported in reactions with certain ligands.[28] For example, the cluster $\{(\mu^2\text{-H})Os_3(CO)_{10}\}_2(\mu^2,\mu^2\text{-S}(CH_2)_8S)$ was reported in low yield from the reaction of $(\mu^2\text{-H})Os_3(CO)_{10}(\mu^2\text{-OH})$ with 1,8-octanedithiol (figure 29).[28]

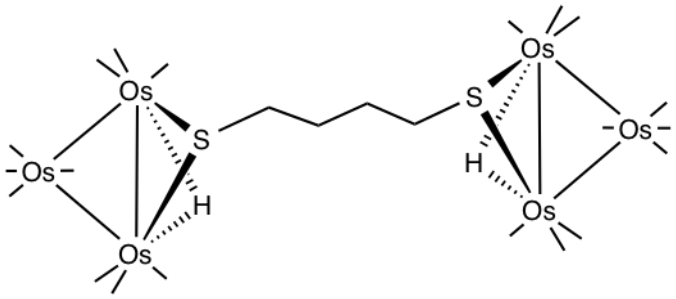

Figure 29 – Structure of a linked cluster via bifunctional ligand, $\{(\mu^2\text{-H})Os_3(CO)_{10}\}_2(\mu^2,\mu^2\text{-S}(CH_2)_4S)$, reported by Leong et al.[28]

In a separate work by the same group, the reactivity of $(\mu^2\text{-H})Os_3(CO)_{10}(\mu^2\text{-OH})$ with various diols was investigated (figure 30).[29] In reactions with diols where the two alcohol groups were inequivalent, the researchers found that coordination at the less hindered site was favored.

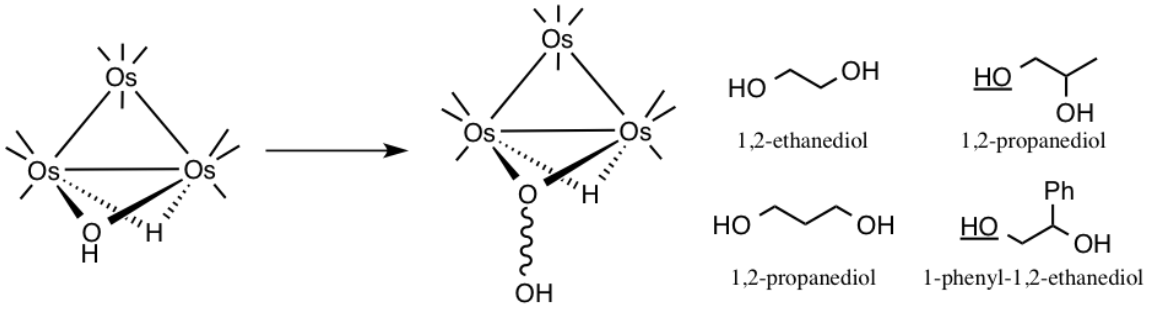

Figure 30 – Reaction of $(\mu^2\text{-H})Os_3(CO)_{10}(\mu^2\text{-OH})$ with a diol HO~OH forms the substituted product. In diols with inequivalent hydroxyl groups the coordinated hydroxyl is underlined.

This research on bifunctional ligands by Leong et al. ties closely into the work that is being done in this laboratory. Researchers of this laboratory have investigated the functionalization of $Os_3(CO)_{10}(\mu^2\text{-OEt})_2$ with various diol ligands.[30,31]

In 2006, Justin Mykietyn of Drew University investigated the functionalization of $Os_3(CO)_{10}(\mu^2\text{-OEt})_2$ with ethylene glycol bridging ligands. He was able to demonstrate that the reaction of $Os_3(CO)_{10}(\mu^2\text{-OEt})_2$ with ethylene glycol produces an unstable octacarbonyl cluster $Os_3(CO)_8(\mu^2\text{-O(CH}_2)_2\text{O})_2$ with two fewer carbonyls (figure 31).[30]

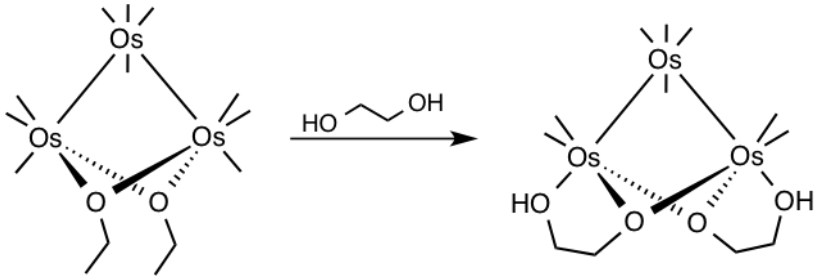

Figure 31 - Scheme of Mykietyn's findings on the reaction of $Os_3(CO)_{10}(\mu^2\text{-}OEt)_2$ with ethylene glycol.

The unstable cluster $Os_3(CO)_8(\mu^2\text{-}O(CH_2)_2OH)_2$ is proposed to contain highly unusual bidentate alkoxide ligands. It readily reacts with carbon monoxide to give the cluster $Os_3(CO)_{10}(\mu^2\text{-}O(CH_2)_2OH)_2$, thereby supporting Mykietyn's proposed structure (figure 32).[30]

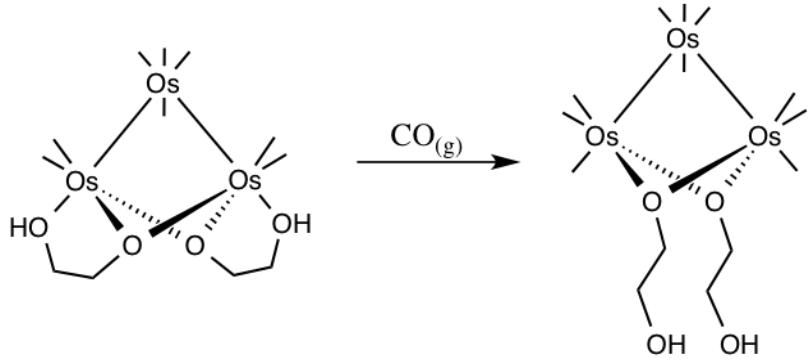

Figure 32 – Scheme of carbonylation of unstable cluster $Os_3(CO)_8(\mu^2\text{-}O(CH_2)_2OH)_2$.

The cluster $Os_3(CO)_8(\mu^2\text{-}O(CH_2)_2OH)_2$ has also been found to naturally decompose to $Os_3(CO)_{10}(\mu^2\text{-}O(CH_2)_2OH)_2$ within hours at room temperature.[30] This natural decomposition is thought to occur via some carbonyl scavenging mechanism between adjacent clusters. Introduction of other bifunctional ligands has been demonstrated by this laboratory.

In 2009, Ann Mularz of Drew University investigated the reaction of $Os_3(CO)_{10}(\mu^2\text{-}OEt)_2$ with 1,6-hexanediol.[31] Mularz successfully generated the disubstituted cluster

$Os_3(CO)_{10}(\mu^2\text{-}O(CH_2)_6OH)_2$. Additionally, she demonstrated that subsequent reaction of this cluster with an equivalent of $Os_3(CO)_{10}(\mu^2\text{-}OEt)_2$ affords a linked cluster system, $\{Os_3(CO)_{10}\}_2(\mu^2,\mu^2\text{-}O(CH_2)_6O)_2$ (figure 33).[31]

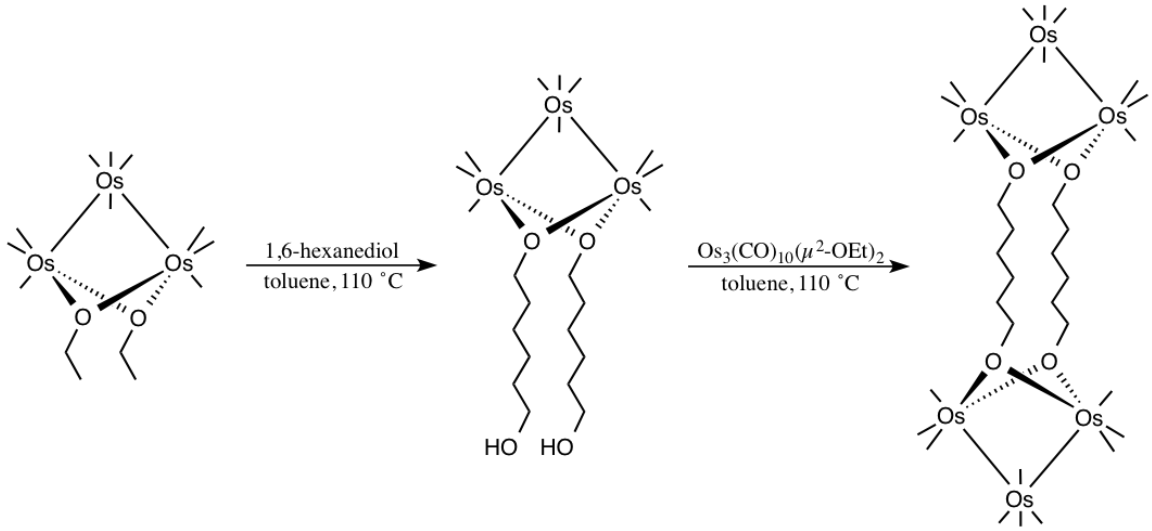

Figure 33 - Stepwise synthesis of the dicluster $\{Os_3(CO)_{10}\}_2(\mu^2,\mu^2\text{-}O(CH_2)_6O)_2$ by Ann Mularz.

This work by Mularz shows that a systematic approach is a viable route to study linked cluster systems. This finding is the basis of current research goals in the Pearsall laboratory. Furthering the development of this pathway to dibridged linked cluster systems may enable the synthetic design of linked clusters having interesting physical properties.

As mentioned at the beginning of this section, the introduction of bifunctional ligands to the cluster opens the option of *several* new coordination modes. In addition to linked cluster systems, bifunctional ligands also allow for other coordinations, including that which was observed in the Mykietyn cluster, $Os_3(CO)_8(\mu^2\text{-}O(CH_2)_2OH)_2$.[30] Other clusters with intramolecularly coordinated bifunctional ligands have been proposed. One of the products reported by Mularz in the synthesis of $Os_3(CO)_{10}(\mu^2\text{-}O(CH_2)_6OH)_2$ is

proposed to have a bidentate 1,6-hexanediol ligand coordinated at each of the bridging ligand positions (figure 34).[31]

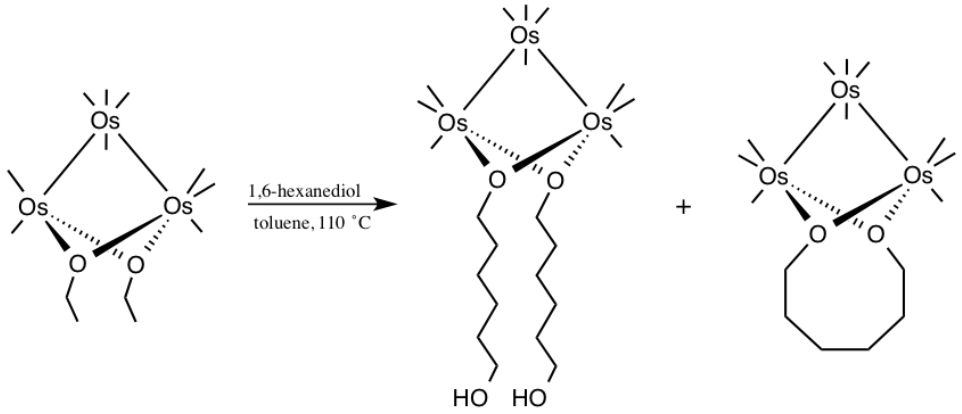

Figure 34 – Reaction of $Os_3(CO)_{10}(\mu^2\text{-}OEt)_2$ with 1,6-hexanediol and proposed products, $Os_3(CO)_{10}(\mu^2\text{-}O(CH_2)_6OH)_2$ (left) and $Os_3(CO)_{10}(\mu^2\text{-}O(CH_2)_6O)$ (right).

Note that this coordination is different from that observed by Mykietyn. Mularz' structure is supported by spectroscopic characterization. This unique form of intramolecularly coordinated ligand has been unambiguously demonstrated by Professor Powell of Abilene Christian University in Texas.[32] Professor Powell investigated the reaction of $Os_3(CO)_{12}$ with carboxylic acids in a microwave reactor (figure 35).

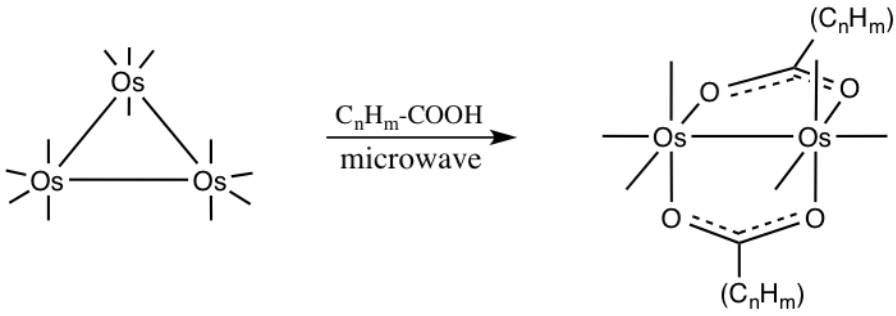

Figure 35 – Scheme of Powell's microwave-assisted reaction of $Os_3(CO)_{12}$ with carboxylic acids.

Among the products, the cluster $Os_2(CO)_6(\mu^2,\mu^2\text{-}OOC(CH_2)_8COOH)$ was isolated. The structure of this cluster was characterized using X-ray diffraction crystallography, and thus

unambiguously determined to have an intramolecularly coordinated dicarboxylic acid ligand.

In 2015, Erika Portero of Drew University investigated the reaction of $Os_3(CO)_{10}(\mu^2\text{-OEt})_2$ with 1,10-decanedicarboxylic acid.[33] Portero found that the reaction afforded different products when conducted in different hydrocarbon solvents. At elevated temperature using heptane solvent, the disubstituted diosmium complex $Os_2(CO)_6(\eta^2,\mu^2\text{-}OOC(CH_2)_{10}COOH)_2$ is obtained. At lower temperature using hexane solvent, however, the looped diosmium complex $Os_2(CO)_6(\eta^2,\mu^2,\mu^2\text{-}OOC(CH_2)_{10}COO)$ is obtained (figure 36).[33]

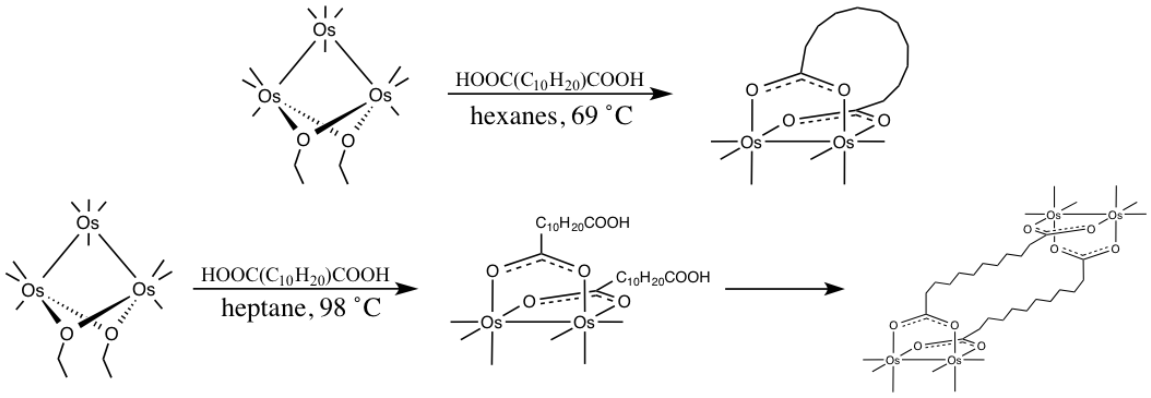

Figure 36 – Schemes of the reaction of $Os_3(CO)_{10}(\mu^2\text{-OEt})_2$ with 1,10-decanedicarboxylic acid in different reaction conditions.

Portero proposed that the difference in product distribution was due to the lower solubility of the dicarboxylic acid at lower temperature. This looped complex is similar to that reported by Powell, but has yet to be confirmed unambiguously.[32,33]

Continuing with this laboratory's investigations on oxyligand functionalization of dibridged triosmium clusters, diol ligands of shorter carbon chain length must be studied. A comprehensive understanding of the interactions of diol ligands with the cluster is

necessary for the design of linked cluster systems. To this end, Mularz' systematic pathway was applied to functionalize $Os_3(CO)_{10}(\mu^2\text{-}OEt)_2$ with 1,5-pentanediol bridging ligands (figure 37). The results of this investigation are detailed herein.

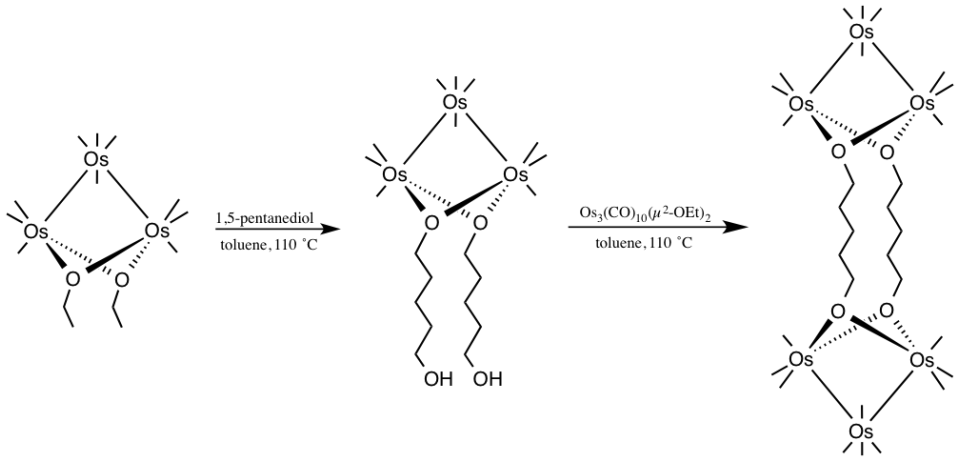

Figure 37 – Scheme of systematic synthesis of clusters linked via 1,5-pentanediol bridging ligands.

Chapter 2 – Methods of Characterization

General Experimental

All reactions were carried out under a nitrogen atmosphere. Solvents used were dried over molecular sieves (4 Å). Reaction mixtures were purified using preparative plate chromatography with UV fluorescent (500 μm) silica gel plates or silica gel column chromatography. Proton NMR spectra were recorded in deuterated chloroform on a Bruker 400 MHz NMR Spectrometer. Infrared spectra were recorded on a Nicolet iS10 FT-Infrared Spectrometer using a liquid cell with sodium chloride plates. The cluster $Os_3(CO)_{12}Cl_2$ was prepared according to the literature procedure.[12] All chemical reagents were purchased from Sigma Aldrich® and used as supplied without further purification.

Thin Layer Chromatography

Chromatography is the separation of components of a mixture by chemical properties determined by intermolecular forces. Both analytical and preparative chromatography are utilized in this research to separate mixtures of osmium clusters by relative polarity. Thin layer chromatography (TLC) is an analytical technique that provides information about the number of components of a mixture and their relative polarities.

In a typical TLC analysis, a solution is spotted at the baseline of the *stationary phase*—a thin layer of silica gel on a plastic chip. The chip is then lowered into a chamber containing a low volume of *mobile phase*—a solvent system designed to be an appropriate mix of polar and nonpolar organic solvents. As the mobile phase *runs* up the TLC chip via capillary action the compounds will interact with both the stationary and mobile phases;

and depending on their affinity for interaction with each phase, will travel a distance up the chip.

The *retention factor* (R_f) is a qualitative measure for a compound's relative affinity for the mobile phase. It is defined as the ratio of distance traveled by a compound to the distance traveled by the solvent (Equation 1).

$$R_f = \frac{distance\ traveled\ by\ analyte}{distance\ traveled\ by\ solvent} \qquad \text{(Equation 1)}$$

The measured R_f value of a compound depends on the composition of the mobile phase, and is characteristic of the compound for the given solvent system. By adjusting the proportions of polar and nonpolar organic solvents in the mobile phase, one can design a method to achieve separation. With this information it is possible to do preparative chromatography to purify the components of a mixture.

The osmium clusters that are studied in this research may be separated using chromatography. Depending on the ligand at the bridging position (and some other factors), the cluster may interact differently with the stationary phase. For example, a hydroxyl group on the bridging ligand will increase interaction with the polar silica gel surface, thereby reducing the R_f value. By monitoring a reaction on TLC, the technique provides rapid detection of unreacted starting material and product formation. It additionally enables the design of solvent systems to purify a mixture of products via preparative chromatography. The solvent system is a mixture of polar solvent – typically ethyl acetate or dichloromethane – and hexanes as the nonpolar component.

Infrared Spectroscopy

Infrared spectroscopy is a technique that provides information about the various vibrational modes that result in a shift in the overall dipole moment of the molecule. In organic chemistry IR is used to detect the presence of different arrangements of atoms (functional groups). This is due to the fact that each vibrational mode for a particular arrangement has a discrete frequency of absorption. For example, the frequency of absorption for a single carbonyl bond stretch of an organic molecule is typically observed as a strong band at $\nu \cong 1700\ cm^{-1}$. The frequency of absorption for a vibrational stretching mode depends on the strength of the bonds; or more rigorously, it is the energy required for excitation to an excited vibrational mode of the molecule. This definition applies to both organic and organometallic systems.

A plethora of information is contained in the infrared spectrum of a metal carbonyl cluster, for which we generally examine C≡O stretching frequencies. For any cluster, by considering the carbonyl ligands as a set of vectors along the bond axes and determining its point group symmetry, it is possible to predict the number of IR-active carbonyl-stretching modes. Osmium carbonyl clusters with the same symmetry will have identical *carbonyl-stretching patterns*; that is, the series of absorptions in the region 2200 – 1600 cm^{-1} will be identical in terms of the frequency difference between absorptions and their relative intensities.

Table 01 – Relationship between symmetry and infrared carbonyl-stretching pattern in triosmium clusters

Formula	Structure	Point Group	Infrared Spectrum
$Os_3(CO)_{10}(\mu^2\text{-}OEt)_2$	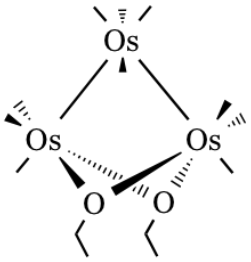	C_{2v}	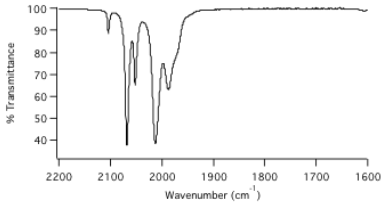 ν (cm^{-1}) = 2104 (w), 2068 (vs), 2051 (m), 2012 (s), 1984 (m)
$Os_3(CO)_{10}(\mu^2\text{-}I)_2$	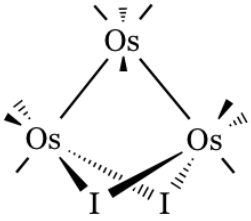	C_{2v}	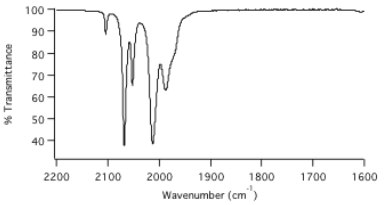 ν (cm^{-1}) = 2111 (w), 2074 (vs), 2058 (m), 2019 (s), 1991 (m)
$Os_3(CO)_{12}I_2$	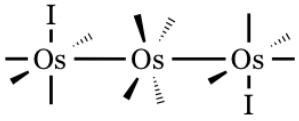	C_{2h}	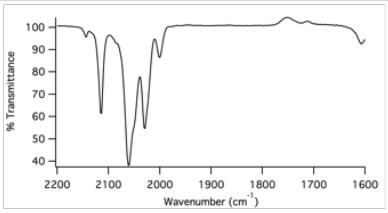 ν (cm^{-1}) = 2144 (w), 2114 (s), 2060 (vs), 2030 (s), 2000 (m)
$Os_3(CO)_{12}$	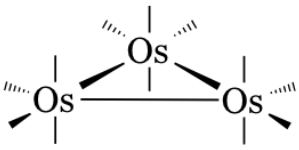	D_{3h}	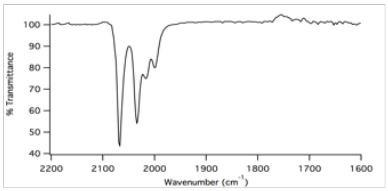 ν (cm^{-1}) = 2067 (vs), 2034 (s), 2017 (m), 2000 (m)

Table 01 depicts the concepts described above by comparing the infrared spectra of four osmium carbonyl clusters. The first two clusters in the figure are $Os_3(CO)_{10}(\mu^2\text{-}OEt)_2$ and $Os_3(CO)_{10}(\mu^2\text{-}I)_2$, respectively, which both have C_{2v} symmetry and identical carbonyl-stretching patterns. These two examples reflect two of the previously mentioned ideas,

that any two clusters of equal carbonyls and symmetry will have an identical carbonyl-stretching pattern; and that the strength of the carbonyl bonds influence the frequency of absorption. The pattern of $Os_3(CO)_{10}(\mu^2\text{-}I)_2$ absorbs at frequencies approximately 7 cm^{-1} higher than that of $Os_3(CO)_{10}(\mu^2\text{-}OEt)_2$, thereby effectively reflecting the electronic natures of bridging iodide and ethoxide ligands.

The next example in Table 01 is the linear cluster $Os_3(CO)_{12}I_2$, which has C_{2h} symmetry. As expected from the above definition, its infrared spectrum differs from that of the previous two examples. The carbonyl-stretching pattern is characteristic of all osmium clusters with C_{2h} symmetry and similar structure.

The last cluster shown in Table 01 is $Os_3(CO)_{12}$, which has D_{3h} symmetry. There is no other osmium carbonyl cluster with similar structure or symmetry, so its infrared spectrum is somewhat unique. It is not entirely unique, however, due to the cluster $Ru_3(CO)_{12}$, which has an identical carbonyl-stretching pattern.[34] The four examples given in Table 01 serve to reinforce the idea that infrared spectroscopy is a powerful technique for the study of transition metal carbonyl clusters.

In addition to the ability to distinguish osmium complexes of different structures and symmetries, infrared spectroscopy may be used to quantify the amount of a pure cluster. The absorbance of light at specific wavelengths is proportional to the concentration of cluster in solution with constant pathlength. This phenomenon is known as the Beer-Lambert law, and it enables measurement of relatively low concentrations of compound in solution (Equation 2).

$$log\frac{I}{I_0} = A = \varepsilon Cb \qquad \text{Equation 2}$$

The variables ε and b in Equation 2 are constants representing the molar absorptivity and pathlength, respectively. Molar absorptivity (ε) has units L^{-1} cm^{-1} and is characteristic for a compound absorbing light of specific wavelength. The lower limit of quantitation for this technique depends on the intensity of the absorption at the specified wavelength. It is of particular utility to this research due to the high intensity carbonyl stretches in osmium carbonyl clusters. This feature provides high molar absorptivity values for carbonyl stretch absorptions, and thus enables low concentration measurements. The molar absorptivity is derived by generating a calibration curve for the pure compound in solution (figure 38).

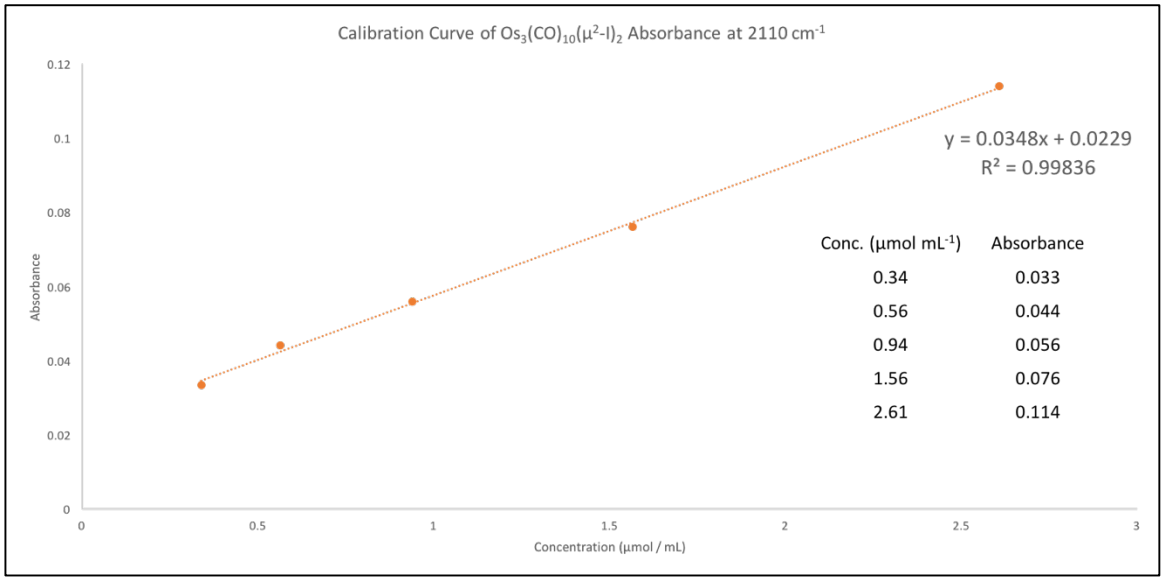

Figure 38 – Calibration curve of $Os_3(CO)_{10}(\mu^2\text{-}I)_2$ absorbance at 2110 cm^{-1}. Molar absorptivity is given by the slope of the trendline equation.

Nuclear Magnetic Resonance Spectroscopy

Proton Nuclear Magnetic Resonance spectroscopy (^{1}H NMR) is a technique that can be used to gain insight into the structure of a compound. The technique relies on the magnetic spin state of a proton and the proton's proximity to other protons on the molecule.

It induces a powerful external magnetic field to force all protons to parallel spin state. The proton then absorbs electromagnetic radiation of specific energy and reemits the radiation to a detector. The specific energy absorbed by the proton is dependent on the energy gap between spin states. This gap is influenced by the electronic environment about the proton and thus the structure of the compound can be determined via ^{1}H NMR output.

The ^{1}H NMR spectral output yields information about the protons of chemical compounds in solution. The most basic piece of information that can be obtained via ^{1}H NMR spectroscopy is the number of chemically unique hydrogens. Chemically unique hydrogens will differ from other hydrogens by chemical shift and/or multiplicity. The chemical shift value describes a proton's proximity to certain functional groups in the molecule. For example, a proton of dichloromethane would have a chemical shift of 5.32 ppm, whereas a proton of a saturated hydrocarbon would have a chemical shift between 0.3–1.8 ppm. The higher chemical shift of dichloromethane is due to the inductive deshielding effect of the two chlorine atoms.

The multiplicity of a chemically unique proton is another property that may help in determining structure. Multiplicity describes the shape of the signal in a ^{1}H NMR spectrum, which is determined by neighboring protons that are chemically unique. For example, in the ^{1}H NMR spectrum of ethanol we would expect to see three signals for the three sets of chemically unique hydrogens (figure 39).

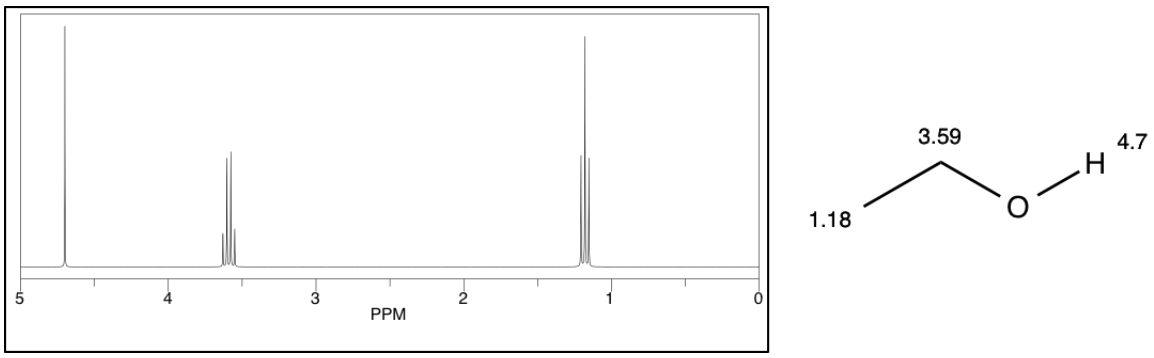

Figure 39 – Calculated ^{1}H NMR spectrum (left) and structure (right) of ethanol. This ^{1}H NMR spectrum was predicted using ChemBioDraw® ver. 14.0.

Signal *'a'* appears as a triplet because it is *coupled to* the two adjacent *'b'* protons. In contrast, signal *'b'* appears as a quartet because it is *coupled to* the three adjacent *'a'* protons. The alcohol proton *'c'* appears as a singlet due to the high electron density about the oxygen, which *blocks* it from coupling to any protons across the C-O bond.

Integration is another feature of an NMR signal that can be useful when determining structure. It measures the area under a proton signal, which is proportional to the number of protons of that type. As a reference, the area under one proton signal is integrated and set to 1.00. All other proton signal integrations are proportional to the reference integration. For example, if the area under signal *'a'* is integrated first, then the value 1.00 corresponds to 3 protons. Integration of signal *'b'* would then be expected to have the value 0.67 because it is 2/3 of the protons associated with signal *'a'*. By combining the three properties of ^{1}H NMR signals it may be possible to propose a structure for the compound.

In this research ^{1}H NMR is used to gain information about protons about the cluster. It is very useful for determining if there is a bridging hydride in the structure. Bridging hydrides typically result in a signal between -10 – -20 ppm, a very highly shielded region unlike that found in typical organic compounds.[38] In addition to bridging hydrides, other

cluster coordinated ligands produce a unique chemical shift. For example, bridging ethoxide ligands (and other bridging alkoxides) produce a signal at 4.4 ppm, while this signal in free ethanol appears around 3.6 ppm. Thus ^{1}H NMR spectroscopy offers crucial information on the nature of a ligand-cluster interaction.

Chapter 3 – Synthetic Routes to $Os_3(CO)_{10}(\mu^2\text{-}OEt)_2$

The development of new synthetic routes to alkoxy substituted clusters of the type $Os_3(CO)_{10}(\mu\text{-}OR)_2$ (R = H, Me, Et) has been of great interest to the Pearsall laboratory for many years. Ashish Shah was one of the first researchers of this laboratory to successfully synthesize $Os_3(CO)_{10}(\mu^2\text{-}OEt)_2$ from the $Os_3(CO)_{12}$ derivative, $Os_3(CO)_{12}Cl_2$ (figure 40).[19]

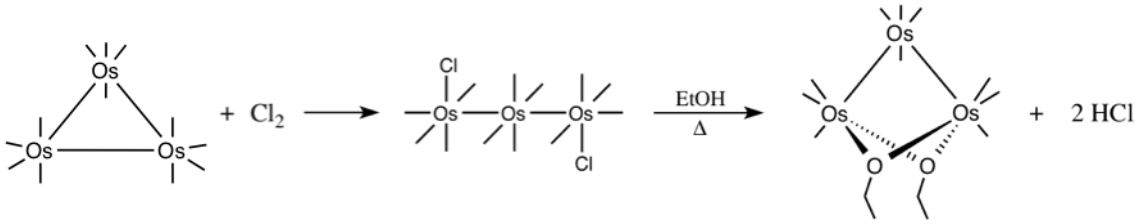

Figure 40 – The original synthetic pathway to $Os_3(CO)_{10}(\mu^2\text{-}OEt)_2$ via chlorinated cluster intermediate $Os_3(CO)_{12}Cl_2$ with ethanol that was pioneered by Ashish Shah.[19]

This discovery was an important milestone for this research as it enabled in-house synthesis of the crucial starting material to the study of dibridged triosmium clusters. Moderate yield of $Os_3(CO)_{10}(\mu^2\text{-}OEt)_2$ was first reported, but this pathway was later optimized by a series of researchers, including this one.

Alternative pathways via other halide cluster intermediates have also been investigated. Reaction of the ten-carbonyl analogue, $Os_3(CO)_{10}(\mu^2\text{-}Cl)_2$, with ethanol has been studied as a potential alternative route to $Os_3(CO)_{10}(\mu^2\text{-}OEt)_2$ (figure 41).

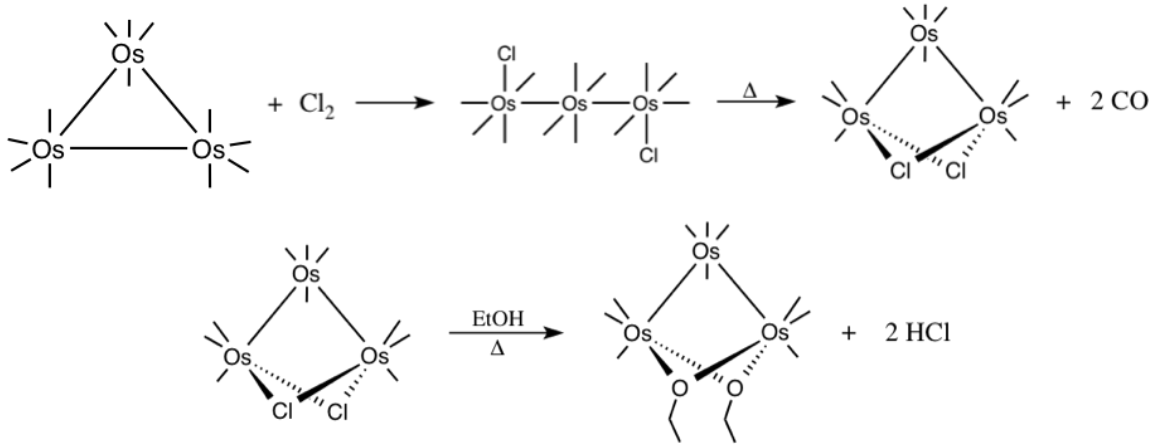

Figure 41 – Scheme of the $Os_3(CO)_{10}(\mu^2\text{-}Cl)_2$ pathway to $Os_3(CO)_{10}(\mu^2\text{-}OEt)_2$ synthesis starting with $Os_3(CO)_{12}$.

This approach does not provide any advantage over direct reaction with $Os_3(CO)_{12}Cl_2$ because overall yield is reduced with the additional cyclization step. For some time, the original $Os_3(CO)_{12}Cl_2$ pathway served as a satisfactory route to the study of $Os_3(CO)_{10}(\mu^2\text{-}OEt)_2$; that is, until the root cause of low yield was realized. It was suspected that that low yields via these two dichloride intermediate pathways were attributed to a competing reaction between $Os_3(CO)_{10}(\mu^2\text{-}OEt)_2$ and hydrogen chloride byproduct (figure 42).[35]

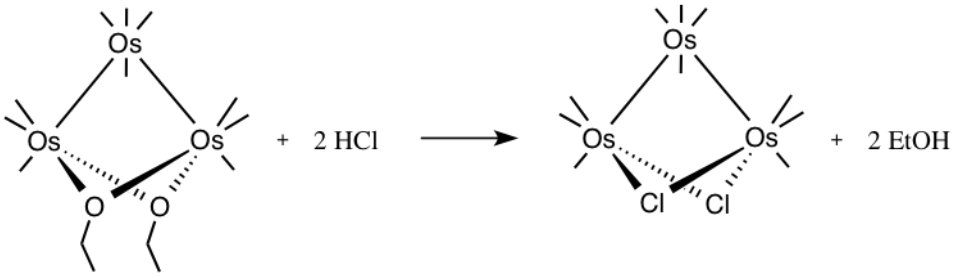

Figure 42 – Reverse reaction of $Os_3(CO)_{10}(\mu^2\text{-}OEt)_2$ with hydrogen chloride affords the ten-carbonyl chloride analogue, $Os_3(CO)_{10}(\mu^2\text{-}Cl)_2$.

This competing reaction dilemma was overcome with the addition of a solid base, alumina, to the reaction mixture to remove hydrogen chloride as it forms (figure 43).[35]

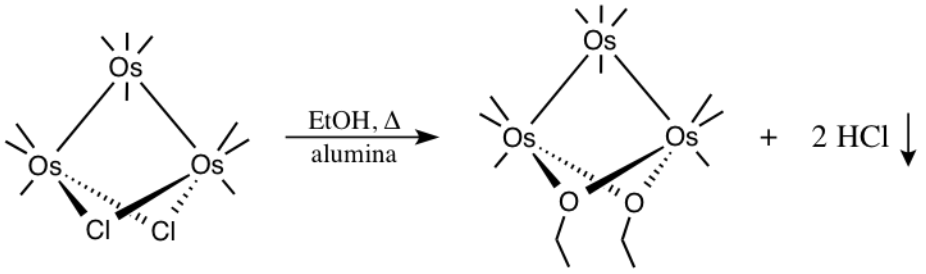

Figure 43 – Scheme of the modified reaction of $Os_3(CO)_{10}(\mu^2\text{-}Cl)_2$ in ethanol with alumina.

With the presence of alumina, higher yields were be achieved in the $Os_3(CO)_{10}(\mu^2\text{-}Cl)_2$ pathway.[35] In this work the use of alumina in the $Os_3(CO)_{12}Cl_2$ pathway has been investigated. Results are discussed herein.

To avoid the use of chlorine gas in the generation of the intermediate cluster $Os_3(CO)_{12}Cl_2$, analogous reactions using bromide and iodide cluster intermediates have been attempted in the presence of alumina. The results of these investigations are discussed herein.

Several researchers in this laboratory have reported a byproduct in the reaction of $Os_3(CO)_{12}Cl_2$ with ethanol. This product, referred to as ω, was first proposed to be a conformational isomer of $Os_3(CO)_{10}(\mu^2\text{-}OEt)_2$ on the basis of its identical TLC behavior (figure 44).

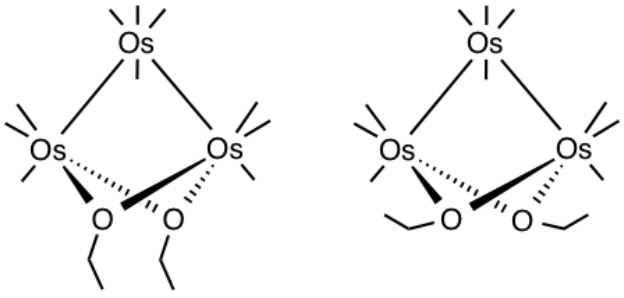

Figure 44 – Structure of $Os_3(CO)_{10}(\mu^2\text{-}OEt)_2$ (left) and the originally proposed structure of ω as a conformational isomer of $Os_3(CO)_{10}(\mu^2\text{-}OEt)_2$ (right).

Due to their identical TLC behaviors, mixtures of ω and $Os_3(CO)_{10}(\mu^2\text{-}OEt)_2$ cannot be separated via chromatography. As such, all spectroscopic data of the ω cluster is cluttered with $Os_3(CO)_{10}(\mu^2\text{-}OEt)_2$ signals. Despite this, a spectroscopic profile of ω has been reported. It has a ten-carbonyl IR stretching pattern with higher frequency than that of $Os_3(CO)_{10}(\mu^2\text{-}OEt)_2$. A carbonyl stretch at 2076 cm^{-1} is the common indicator for the presence of ω in solution. In ^1H NMR spectra containing ω, it has the same two signals as $Os_3(CO)_{10}(\mu^2\text{-}OEt)_2$, but with both the quartet (-O–$\underline{CH_2}$–CH_3) and triplet (-O–CH_2–$\underline{CH_3}$) signals of the ω coordinated ethoxide shifted upfield by ~0.10 ppm to 4.32 ppm (figure 45).

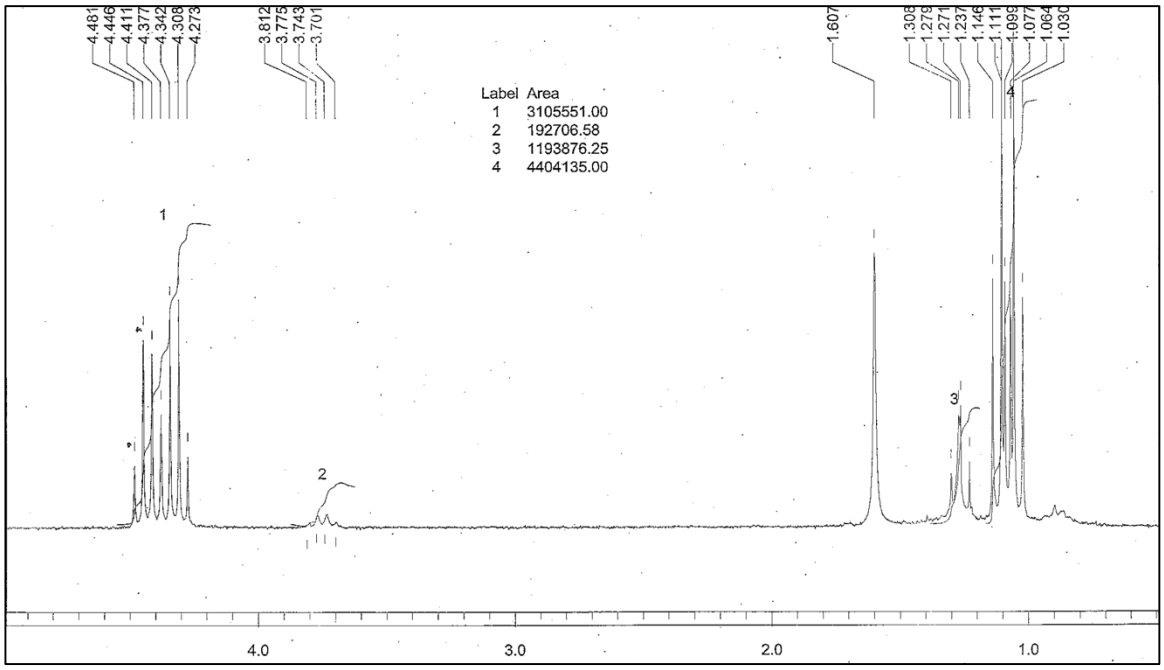

Figure 45 – ^1H NMR spectrum of a mixture of $Os_3(CO)_{10}(\mu^2\text{-}OEt)_2$ with ω impurity. The spectrum shows two signals at 4.43 (q) and 4.32 (q) ppm corresponding to the bridging ethoxide ligands (-O–$\underline{CH_2}$–CH_3) of $Os_3(CO)_{10}(\mu^2\text{-}OEt)_2$ and ω, respectively. Spectrum recorded by Lynn Schmit after extensive purification.[36]

Frequency and chemical shift differences in the IR and ^{1}H NMR spectra of ω suggest that it is not simply a conformational isomer of $Os_3(CO)_{10}(\mu^2\text{-}OEt)_2$. The true structure of ω has been serendipitously discovered by this researcher. Results of this finding are discussed herein.

3.1 – Experimental

Reaction of $Os_3(CO)_{12}Cl_2$ with ethanol

$Os_3Cl_2(CO)_{12}$ (300 mg, 307 μmol) was dissolved in 300 mL 200-proof ethanol and heated at reflux under N_2 atmosphere for 25 hours. Reaction was monitored by IR periodically. The reaction mixture was removed from heat and cooled to room temperature. The product was purified via fractional crystallization at -20 ˚C. Approximately 105 mg (112 μmol) of the desired product $Os_3(CO)_{10}(\mu^2\text{-}OEt)_2$ was isolated (35% yield). A series of other clusters were obtained over the course of the crystallization including $Os_3(CO)_{12}$, $Os_3(CO)_{12}Cl_2$, ω, and an unidentified product referred to as 'product X'.

Reaction of $Os_3(CO)_{12}Cl_2$ with ethanol and alumina

To a mixture of $Os_3(CO)_{12}Cl_2$ (20 mg, 20 μmol) and alumina (210 mg, 2.06 μmol) was added 20 ml. of 200-proof ethanol. The reaction mixture was heated at reflux under N_2 atmosphere for 14 hours and monitored by IR periodically. The reaction mixture was vacuum filtered on a Buchner funnel lined with celite. Fractional crystallization from ethanol at -20 ˚C afforded yellow crystals. IR of the impure product was obtained in

dichloromethane (IR-1). Approximately 15.5 mg (16.5 μmol) of the desired product $Os_3(CO)_{10}(\mu^2\text{-}OEt)_2$ was obtained (79% yield).

Conversion of ω to $Os_3(CO)_{10}(\mu^2\text{-}OEt)_2$

An initial IR spectrum was recorded of the mixture of $Os_3(CO)_{10}(\mu^2\text{-}OEt)_2$ (~38mg, 40 μmol by calibration curve (2103 cm^{-1}) and the impurity known as ω in 15-ml. dichloromethane solution (IR-2). This mixture was reconstituted in 35-ml. of 200-proof ethanol and one *scoop* of alumina was added. The reaction mixture was heated at reflux under an N_2 atmosphere for 10 hours and monitored by IR periodically. The resulting solution was suction filtered and ethanol solvent was evaporated on a rotary evaporator. The yellow product was reconstituted in 40-ml. of dichloromethane, at which point a brown precipitate was observed. The solution was decanted and brown precipitate was discarded. IR spectrum of the yellow dichloromethane solution was recorded (IR-3). Approximately 50 μmol of pure $Os_3(CO)_{10}(\mu^2\text{-}OEt)_2$ was obtained, which represents conversion of 10 μmol of ω in the mixture to $Os_3(CO)_{10}(\mu^2\text{-}OEt)_2$.

Synthesis of $Os_3(CO)_{12}I_2$

To a 250-ml. round-bottomed flask was added osmium carbonyl (100 mg, 110 μmol) and 50-ml. of anhydrous dichloromethane. A solution of iodine (30.8 mg, 121 μmol) in 20 ml. of dichloromethane was added dropwise to the reaction mixture. The pink reaction mixture was allowed to stir under N_2 atmosphere for 3 hours, at which point its infrared spectrum showed the desired product and no peaks corresponding to unreacted

starting material. Dichloromethane was removed via rotary evaporator affording an orange powder. The crude product was rinsed with approximately 1 ml. of dichloromethane, giving a dark-red solution and a bright-yellow solid. A bit of the solid was dissolved in 1 ml. of dichloromethane and its infrared spectrum was acquired, revealing a very clean $Os_3(CO)_{12}I_2$ carbonyl-stretching pattern. Additional product recovery was attempted on the dark-red dichloromethane solution, but these efforts proved unsuccessful. Approximately 75.5 mg (65 μmol) of the desired product $Os_3(CO)_{12}I_2$ was isolated (59% yield).

Reaction of $Os_3(CO)_{12}I_2$ with ethanol and alumina

$Os_3(CO)_{12}I_2$ (17.7 mg, 15.3 μmol) was dissolved in 18 ml. of absolute ethanol. To the solution was added ~100 mg of alumina and heated at reflux (78 ˚C) under N_2 atmosphere for 40 hours. The reaction was monitored periodically using IR. Alumina was suction filtered off from the solution over a layer of celite. Ethanol solvent volume was reduced on the rotary evaporator and the solution was cooled at -20 ˚C for fractional crystallization. Fractional crystallization was repeated to a final volume of ~0.5 ml. at which point no crystals were obtained and the experiment was discontinued. The reaction did not afford the desired product $Os_3(CO)_{10}(\mu^2\text{-OEt})_2$.

Reaction of $Os_3(CO)_{10}(\mu^2\text{-I})_2$ with ethanol and alumina

$Os_3(CO)_{10}(\mu^2\text{-I})_2$ (16.5 mg, 14.9 μmol) was dissolved in 16-ml. of absolute ethanol. To the reaction mixture was added ~150 mg of alumina. The solution was heated to a

gentle reflux under N_2 atmosphere and was monitored periodically using IR and TLC. After 345-minutes the reaction mixture was removed from heat and the alumina was removed via vacuum filtration. Ethanol solvent was removed with a rotary evaporator. On reconstituting the mixture in dichloromethane a red solid was observed. The solution was decanted and the infrared spectrum was obtained. The solution was chromatographed on a silica gel column eluting with 25-ml. of 10% dichloromethane / hexanes. Approximately 13.2 mg (14.0 μmol) of the desired product, $Os_3(CO)_{10}(\mu^2\text{-}OEt)_2$ was isolated (93% yield).

3.2 – Results & Discussion

In recent years the Pearsall laboratory has discovered a high-yield synthetic route to $Os_3(CO)_{10}(\mu^2\text{-}OEt)_2$ via halogenated cluster intermediates (figure 46).[19-22] This work follows up with the further development of this new synthetic route.

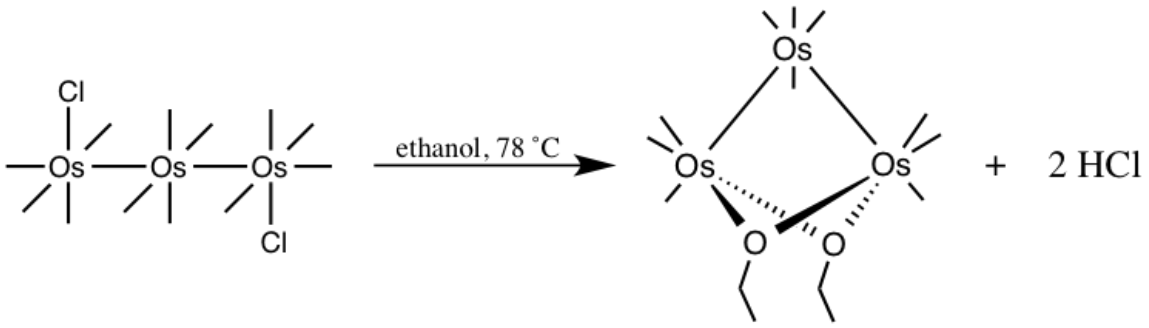

Figure 46 – Generic scheme of synthesis of $Os_3(CO)_{10}(\mu^2\text{-}OEt)_2$ via halogenated cluster intermediates.

Direct reaction of $Os_3(CO)_{12}Cl_2$ and ethanol affords the desired product $Os_3(CO)_{10}(\mu^2\text{-}OEt)_2$ in low yield (35%). When alumina was added to the reaction mixture yield was improved significantly (79%). The use of less hazardous halogens bromine and iodine in the intermediate halogen cluster was investigated by a series of researchers to eliminate the

risk of exposure to, and use of, gaseous chlorine.[21,22] Yield data from these investigations in the presence of alumina has been compiled in Table 02.

Table 02 – Summary of $Os_3(CO)_{10}(\mu^2\text{-}OEt)_2$ isolated yield via halogen intermediate in the presence of alumina.

Synthetic Route (w/ alumina)	Yield of 12-carbonyl dihalide	Yield of 10-carbonyl dihalide	Yield of bisethoxide	Overall yield	Reference(s)
$Os_3(CO)_{12}Cl_2$	>95%		79%	75%	RS
$Os_3(CO)_{12}Br_2$	N/A		48%	N/A	*22*
$Os_3(CO)_{12}I_2$	59%		0%	0%	RS
$Os_3(CO)_{10}(\mu^2\text{-}Cl)_2$	>95%	93%	57%	50%	*21, 40*
$Os_3(CO)_{10}(\mu^2\text{-}Br)_2$	N/A	82%	59%	N/A	*10, 22, 37, 40*
$Os_3(CO)_{10}(\mu^2\text{-}I)_2$	59%[40]	25%[10]	94%	14%	RS, *10, 40*

As this data suggests, the most efficient synthetic route to $Os_3(CO)_{10}(\mu^2\text{-}OEt)_2$ is via the $Os_3(CO)_{12}Cl_2$ cluster intermediate. Although $Os_3(CO)_{10}(\mu^2\text{-}I)_2$ represents an appealing pathway, the overall yield from $Os_3(CO)_{12}$ is quite low. This is due to the formation of a diosmium complex byproduct in the synthesis of $Os_3(CO)_{10}(\mu^2\text{-}I)_2$ (figure 47).[12]

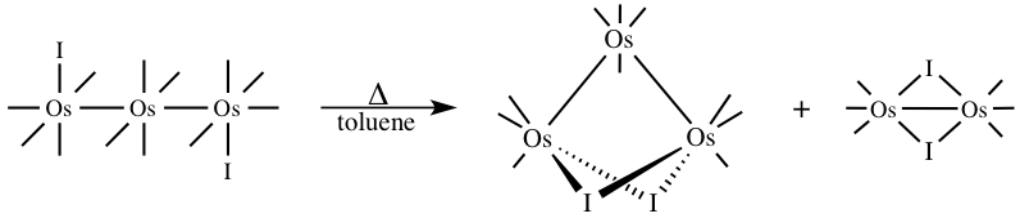

Figure 47 – Scheme of thermolysis reaction of $Os_3(CO)_{12}I_2$ in toluene forming $Os_3(CO)_{10}(\mu^2\text{-}I)_2$ and $Os_2(CO)_6I_2$.

The diosmium byproduct $Os_2(CO)_6I_2$ accounts for approximately 50% of the yield in this synthetic step and poses a significant loss of yield to the synthesis of $Os_3(CO)_{10}(\mu^2\text{-}OEt)_2$. Thus the $Os_3(CO)_{12}Cl_2$ pathway remains the superior route with respect to overall yield. Even though the $Os_3(CO)_{10}(\mu^2\text{-}I)_2$ route did not prove superior to $Os_3(CO)_{10}(\mu^2\text{-}OEt)_2$ synthesis, the fact that the synthetic step from $Os_3(CO)_{10}(\mu^2\text{-}I)_2$ to $Os_3(CO)_{10}(\mu^2\text{-}OEt)_2$ afforded near quantitative yield and in shorter time is noteworthy. That the reaction of

$Os_3(CO)_{10}(\mu^2\text{-}I)_2$ with ethanol in the presence of alumina produces the cluster $Os_3(CO)_{10}(\mu^2\text{-}OEt)_2$ in shorter time than with any other halogenated cluster intermediate suggests that the bridging iodide ligand activates the cluster towards substitution.

The formation of an inseparable byproduct in the $Os_3(CO)_{12}Cl_2$ pathway, ω, was also investigated. This pathway often produces significant amounts of ω, an undesirable byproduct that was previously suspected to be a conformational isomer of $Os_3(CO)_{10}(\mu^2\text{-}OEt)_2$ (figure 48).

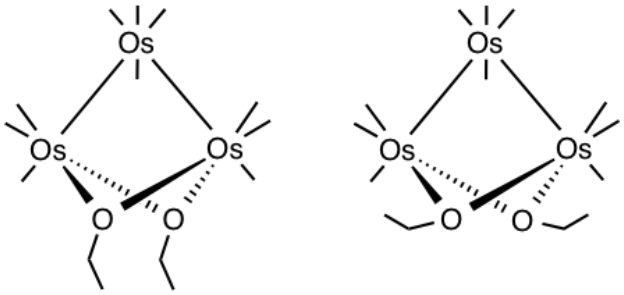

Figure 48 – Initially proposed structures of α- and ω-$Os_3(CO)_{10}(\mu^2\text{-}OEt)_2$ as conformational isomers.

In this work we propose a different structure for ω as the monosubstituted intermediate cluster, $Os_3(CO)_{10}(\mu^2\text{-}Cl)(\mu^2\text{-}OEt)$ (figure 49).

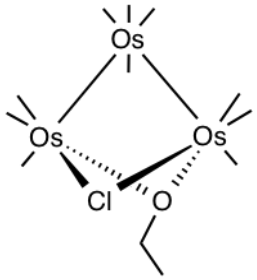

Figure 49 – Newly proposed structure of ω as the chloro-ethoxy- cluster $Os_3(CO)_{10}(\mu^2\text{-}Cl)(\mu^2\text{-}OEt)$.

This product is generally obtained along with $Os_3(CO)_{10}(\mu^2\text{-}OEt)_2$ in varying amounts as a mixture during the fractional crystallization process. In this work, conversion of a mixture

of ω and $Os_3(CO)_{10}(\mu^2\text{-}OEt)_2$ to pure $Os_3(CO)_{10}(\mu^2\text{-}OEt)_2$ was achieved by heating in ethanol in the presence of alumina. An additional 10 μmol of pure $Os_3(CO)_{10}(\mu^2\text{-}OEt)_2$ was generated by this reaction, thereby supporting the proposed intermediate structure of ω. This experiment demonstrates that higher yield of pure $Os_3(CO)_{10}(\mu^2\text{-}OEt)_2$ may be obtained simply by extending the reflux duration in the $Os_3(CO)_{12}Cl_2$ pathway in the presence of alumina.

The spectroscopic profile of the ω impurity does not support it being a conformational isomer of $Os_3(CO)_{10}(\mu^2\text{-}OEt)_2$. Instead, we propose that it is the monosubstituted intermediate, $Os_3(CO)_{10}(\mu^2\text{-}Cl)(\mu^2\text{-}OEt)_2$. Infrared spectra with ω present show that it has a higher frequency ten-carbonyl pattern than does $Os_3(CO)_{10}(\mu^2\text{-}OEt)_2$ (figure 50).

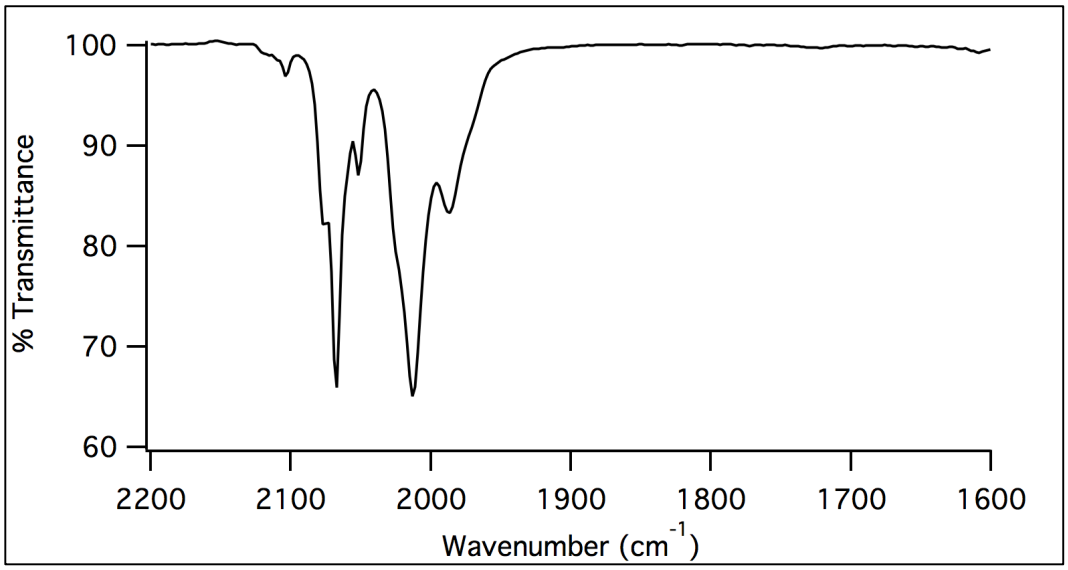

Figure 50 – Infrared spectrum of a mixture of $Os_3(CO)_{10}(\mu^2\text{-}OEt)_2$ and ω.

In this spectrum, the frequency of the ω stretch at 2076 cm^{-1} corresponds to the 2068 cm^{-1} band of the $Os_3(CO)_{10}(\mu^2\text{-}OEt)_2$ ten-carbonyl pattern. A simple conformation change is not

expected to shift the carbonyl stretching frequency by 8 cm^{-1}. Conspicuously, the frequency of this ω carbonyl stretching band falls between that of the corresponding bands in the clusters $Os_3(CO)_{10}(\mu^2\text{-}OEt)_2$ (2068 cm^{-1}) and $Os_3(CO)_{10}(\mu^2\text{-}Cl)_2$ (2085 cm^{-1}) (figure 51).

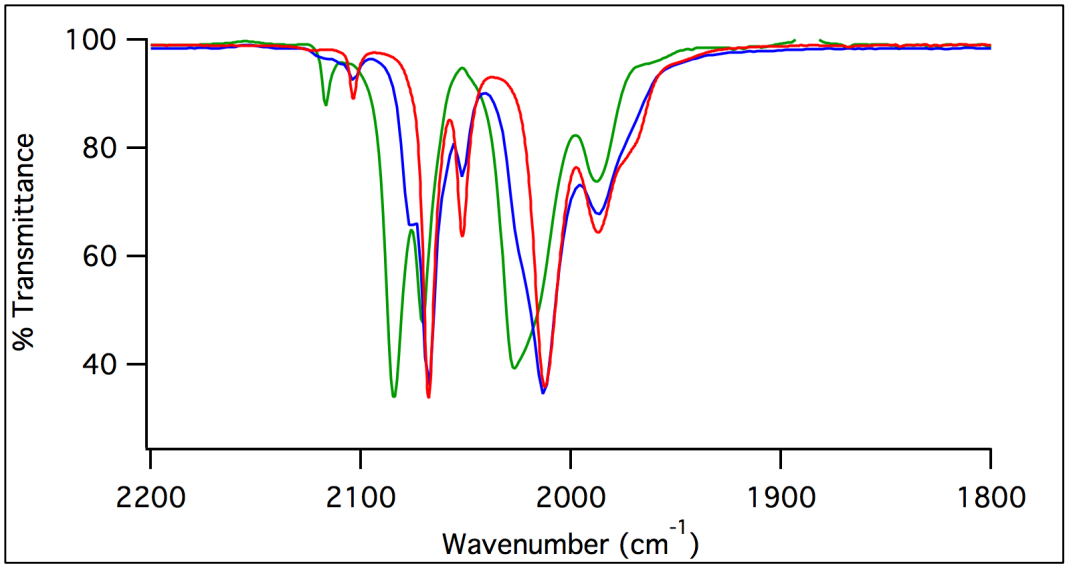

Figure 51 – Infrared spectra overlay of $Os_3(CO)_{10}(\mu^2\text{-}Cl)_2$ (green), $Os_3(CO)_{10}(\mu^2\text{-}OEt)_2$ (red), and an impure $Os_3(CO)_{10}(\mu^2\text{-}OEt)_2$ sample with ω impurity (blue). Spectrum shows that a carbonyl stretch in the ω ten-carbonyl pattern has frequency 2076 cm^{-1}, which happens to be between the corresponding stretch in spectra of $Os_3(CO)_{10}(\mu^2\text{-}Cl)_2$ and $Os_3(CO)_{10}(\mu^2\text{-}OEt)_2$.

A comparison of the ten-carbonyl stretching patterns of $Os_3(CO)_{10}(\mu^2\text{-}OEt)_2$ and $Os_3(CO)_{10}(\mu^2\text{-}Cl)_2$ suggests that bridging chloride ligands strengthen the C≡O bonds by decreasing back-donation to the CO π* orbital. The intermediacy of the ω peak frequency of 2076 cm^{-1} is thus consistent with the proposed ω structure $Os_3(CO)_{10}(\mu^2\text{-}Cl)(\mu^2\text{-}OEt)$.

In the ^1H NMR spectrum of a mixture of $Os_3(CO)_{10}(\mu^2\text{-}OEt)_2$ with ω impurity it is clear that the coordinated ethoxide signal (–O–$\underline{CH_2}$–CH_3) of ω (4.32 ppm) is more shielded than that of $Os_3(CO)_{10}(\mu^2\text{-}OEt)_2$ (4.42 ppm) (figure 52).[36]

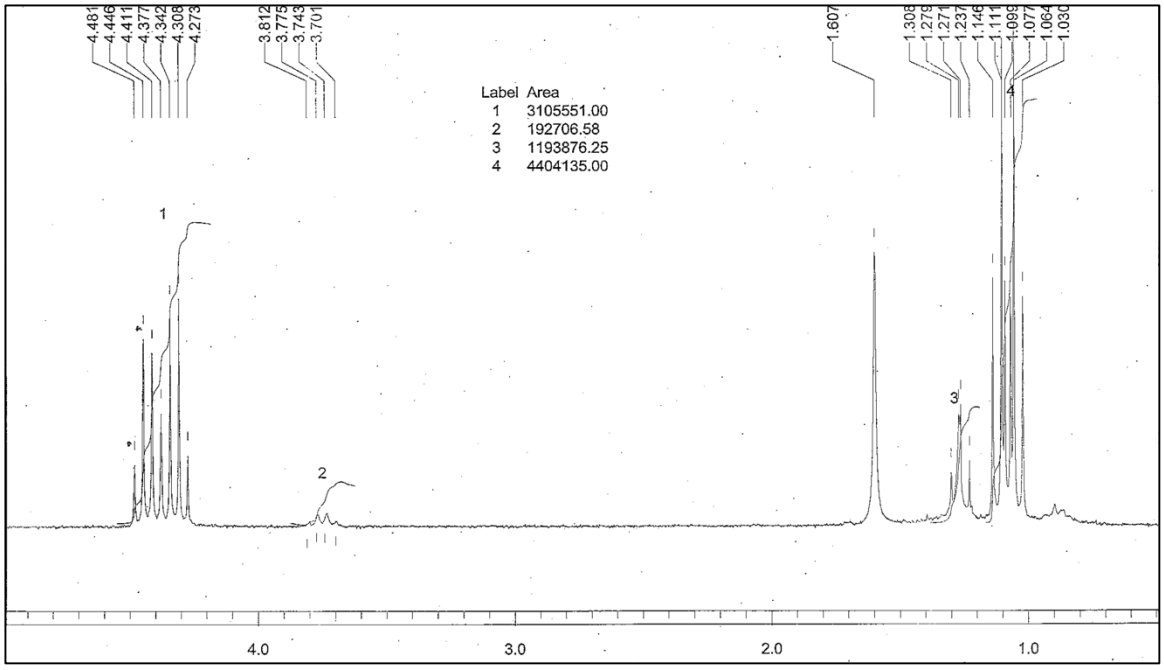

Figure 52 – ^{1}H NMR spectrum of a mixture of $Os_3(CO)_{10}(\mu^2\text{-}OEt)_2$ with ω impurity. The spectrum shows two signals at 4.43 (q) and 4.32 (q) ppm corresponding to the bridging ethoxide ligands (–O–$\underline{CH_2}$–CH_3) of $Os_3(CO)_{10}(\mu^2\text{-}OEt)_2$ and ω, respectively. Spectrum recorded by Lynn Schmit after extensive purification.[36]

This is consistent with the ω ethoxide being near to a less electronegative group. A bridging chloride (EN_{Cl} 3.16) is thus consistent with the observation that ω has a more shielded ethoxide signal than bridging alkoxide (EN_O 3.44). Therefore, the proposed structure of ω as $Os_3(CO)_{10}(\mu^2\text{-}Cl)(\mu^2\text{-}OEt)$ is consistent with its spectroscopic profile.

An ω derivative has been isolated by this researcher in the reaction of $Os_3(CO)_{10}(\mu^2\text{-}OEt)_2$ with 1,5-pentanediol where starting $Os_3(CO)_{10}(\mu^2\text{-}OEt)_2$ was apparently contaminated with ω (figure 53).

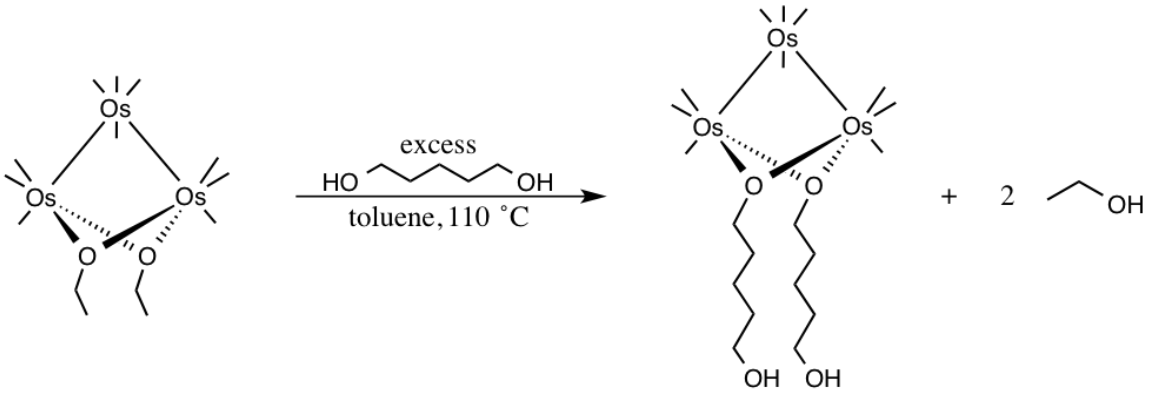

Figure 53 – Scheme of reaction of $Os_3(CO)_{10}(\mu^2\text{-}OEt)_2$ with 1,5-pentanediol.

In this experiment, the ω cluster was functionalized with 1,5-pentanediol, thereby giving it unique TLC behavior. This substituted cluster was thus purified with chromatography and its infrared and ^{1}H NMR spectra were recorded (IR-4, NMR-1). The IR spectrum of this substituted cluster is consistent with the ten-carbonyl pattern of ω (figure 54).

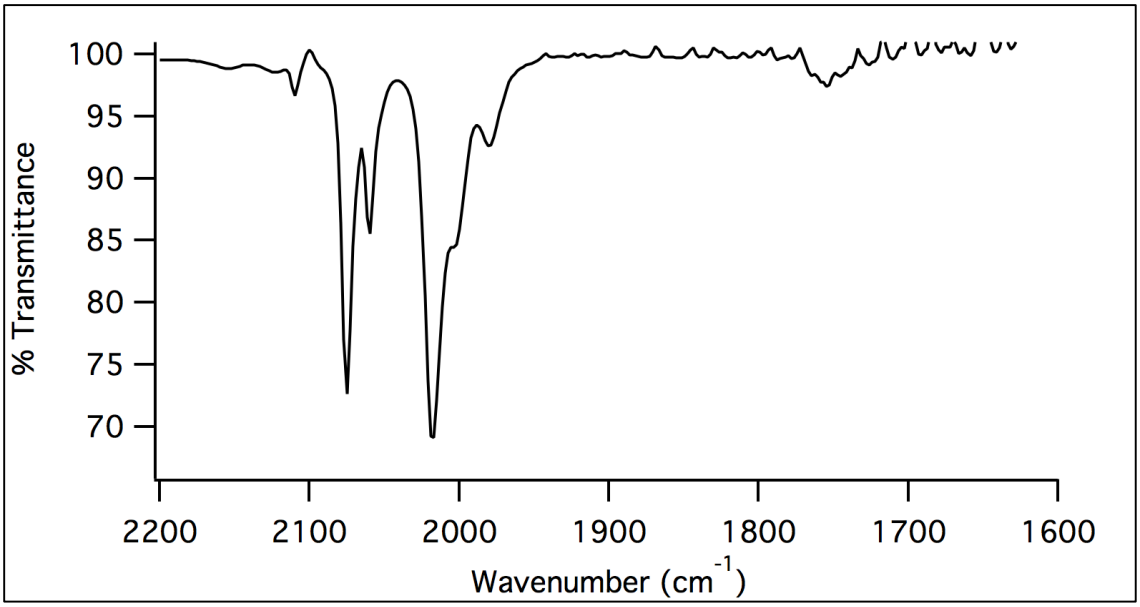

Figure 54 – Infrared spectrum of the 1,5-pentanediol functionalized ω derivative proposed to be the cluster $Os_3(CO)_{10}(\mu^2\text{-}Cl)(\mu^2\text{-}O(CH_2)_5OH)$; ν (cm^{-1}) = 2109 (w), 2076 (s), 2059 (m), 2117 (vs), 2005 (m), 1980 (w).

As mentioned above, the higher frequency ten-carbonyl pattern is consistent with the presence of a bridging chloride. The chemical shift of proton signals in the ^{1}H NMR spectrum are also consistent with the spectroscopic profile of ω (figure 55).

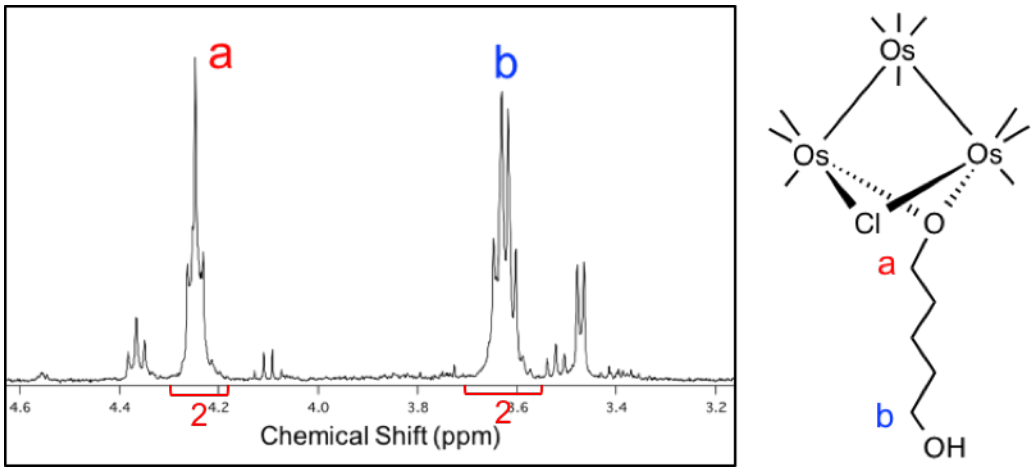

Figure 55 – Proton NMR spectrum (left) of 1,5-pentanediol functionalized ω derivative obtained as a minor product in the synthesis of $Os_3(CO)_{10}(\mu^2\text{-}O(CH_2)_5OH)_2$. Proposed structure (right) is the cluster $Os_3(CO)_{10}(\mu^2\text{-}Cl)(\mu^2\text{-}O(CH_2)_5OH)$.

The structure of this substituted ω derivative was concluded to be $Os_3(CO)_{10}(\mu^2\text{-}Cl)(\mu^2\text{-}O(CH_2)_5OH)$ on the basis of its similar spectroscopic character to ω and its relatively polar TLC behavior. This finding supports the proposed structure of ω as $Os_3(CO)_{10}(\mu^2\text{-}Cl)(\mu^2\text{-}OEt)$ because on reaction with 1,5-pentanediol substitution of the ethoxide ligand is expected to occur readily. This ω derivative is further discussed in Chapter 4.

Chapter 4 – Alkoxide Substitution with Straight-Chain Diols

Functionalization of dibridged cluster with bifunctional ligands is important to the design of linked cluster systems. The cluster $Os_3(CO)_{10}(\mu^2\text{-}OEt)_2$ is an excellent starting material to the study of dibridged systems due to the reactivity of bridging ethoxide ligands. Its bridging ethoxide ligands are readily substituted for another 3-electron donor by heating in the presence of the desired ligand. Ligand exchange of bridging ligand has been demonstrated by Mykietyn and Mularz with ethylene glycol and 1,6-hexanediol, respectively. The expected bridging-pendant coordination mode was eventually realized, however, both of these researchers reported complicating coordination modes with introduction of the bifunctional ligand (figure 56).[30,31]

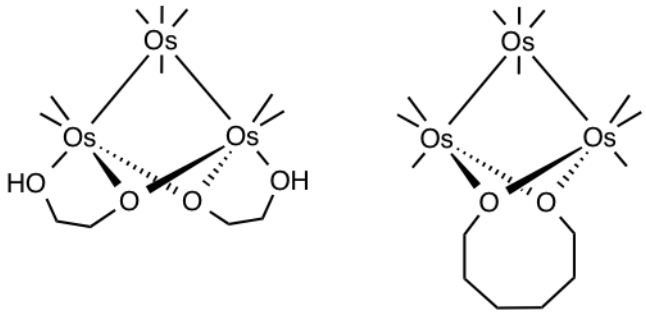

Figure 56 – Mykietyn *loop* (left) is an ethylene glycol functionalized cluster with bidentate coordinated diol. The bidentate nature of this ligand is unique because the ligand coordinates differently to the cluster at each alcohol. Mularz *ring* (right) is a 1,6-hexanediol functionalized cluster with bidentate coordinated diol. This ligand is unique because it is coordination at both bridging positions.

These new coordination modes in reactions with ethylene glycol are *very* different to that proposed with 1,6-hexanediol.[30,31] It is unknown whether these coordination modes are unique to these ligands or if there is a range of ligand chain length that would also engage. For this reason, one should never assume that a ligand will undergo simple substitution. A comprehensive investigation must be conducted on the interactions of each possible ligand.

A systematic study of bifunctional ligand interactions would reveal what types of ligand satisfy these unique coordination modes. In this chapter we continue investigations on the effect of chain length on the interactions between $Os_3(CO)_{10}(\mu^2\text{-}OEt)_2$ and organic diols. To this end, the reaction of 1,5-pentanediol with $Os_3(CO)_{10}(\mu^2\text{-}OEt)_2$ was studied (figure 57).

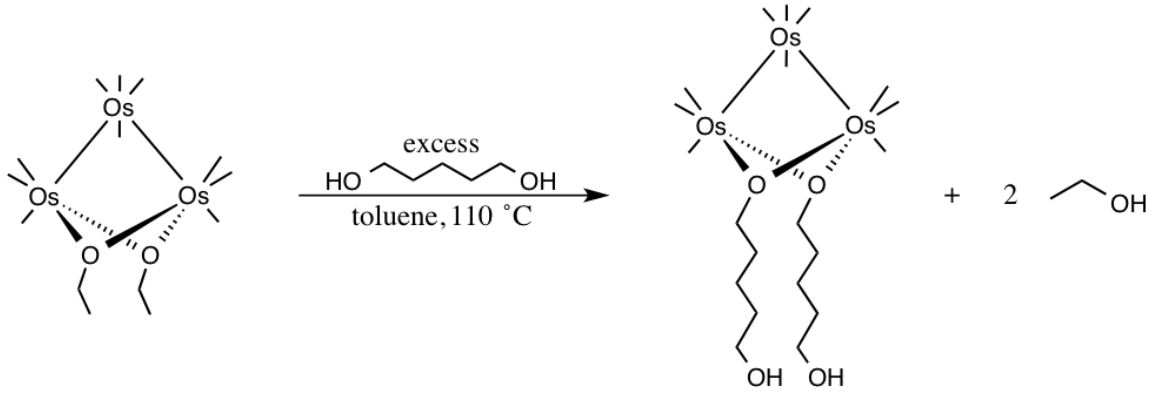

Figure 57 – Scheme of reaction of $Os_3(CO)_{10}(\mu^2\text{-}OEt)_2$ with 1,5-pentanediol.

This work had previously been attempted by Estephanie Rivero, who discovered that in contrast to substitutions with 1,2-ethanediol and 1,6-hexanediol, this reaction was very unpredictable and apparently sensitive to reaction conditions.[37] This work builds on these unusual results and her work will be referred to throughout.

4.1 – Experimental

This experimental section represents a distillation of many reaction attempts over a period of several months. In all, 10 attempts were made. All yields were determined using the molar absorptivity of $Os_3(CO)_{10}(\mu^2\text{-}OEt)_2$ (figure 58). Starting $Os_3(CO)_{10}(\mu^2\text{-}OEt)_2$ was obtained as described in Chapter 3.

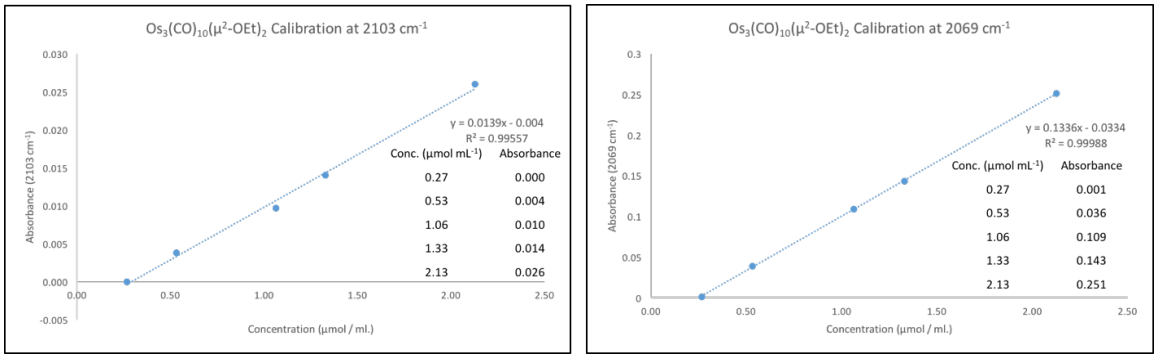

Figure 58 – Calibration curves of $Os_3(CO)_{10}(\mu^2\text{-}OEt)_2$ absorbance at 2103 (left) and 2069 cm^{-1} (right).

Reaction of $Os_3(CO)_{10}(\mu^2\text{-}OEt)_2$ with 1,5-pentanediol (20 minutes)

$Os_3(CO)_{10}(\mu^2\text{-}OEt)_2$ (23 mg, 24 μmol) was dissolved in 23 ml. of toluene. A 92-fold excess of 1,5-pentanediol (0.23 ml., 2.2 mmol) was added to the reaction mixture and heated at reflux under N_2 atmosphere for 20-minutes. Reaction progress was monitored by IR and on TLC in 50% ethyl acetate/hexanes solvent system. After 20-minutes at reflux the reaction mixture was cooled to room temperature. The toluene layer was retrieved by pipet decant and then cooled at -20 ˚C in the freezer. The chilled toluene layer was removed from a colorless precipitate by pipet decant. An infrared spectrum was recorded for the colorless precipitate in dichloromethane and confirmed the presence of 1,5-pentanediol with no carbonyl-stretches (IR-5). No further analysis of colorless precipitate was done.

On TLC in dichloromethane solvent system three spots are observed: A (R_f 0.71), B (R_f 0.27) and C (R_f 0.04). Products were separated by passing the mixture through a silica column with dichloromethane, followed by ethyl acetate to collect the most polar product. The solvents were removed from each of the products, and re-dissolved in chloroform-d. Infrared spectra were obtained for each product revealing that each has an identical ten-carbonyl pattern (IR-6, IR-4, IR-7). Component A was determined to be unreacted starting material $Os_3(CO)_{10}(\mu^2\text{-}OEt)_2$ by TLC reference and its infrared spectrum. Proton NMR spectra were obtained for components B (NMR-1) and C (NMR-2).

Reaction of $Os_3(CO)_{10}(\mu^2\text{-}OEt)_2$ with 1,5-pentanediol (60 minutes)

To a 100-ml. round-bottomed flask was added $Os_3(CO)_{10}(\mu^2\text{-}OEt)_2$ (44.8 mg, 47.5 μmol) and 45-ml. of toluene. A 90-fold excess of 1,5-pentanediol (0.45 ml., 4.3 mmol) was added to the solution. The reaction mixture was heated at reflux (110 ˚C) under a nitrogen atmosphere. The reaction was monitored on TLC in a 20% ethyl acetate / hexanes solvent system for 60 minutes, at which point the starting material spot (R_f 0.60) was undetected and two product spots had appeared: B (R_f 0.20, weak) and C (R_f 0.02, intense). Solvent was removed and the crude product was dissolved in 30-ml. of dichloromethane. Excess 1,5-pentanediol was extracted with a total of seven 10-ml. portions of Millipore water and the organic phase was dried over anhydrous calcium chloride pellets. The crude product mixture was purified on a 6-inch silica gel column. Polarity of the ethyl acetate / hexanes mobile phase was increased over time from 20% to 100% to achieve good separation. The desired product C was identified as $Os_3(CO)_{10}(\mu^2\text{-}O(CH_2)_5OH)_2$ and was obtained in good

yield (49%). This product was characterized by TLC and by infrared and proton NMR spectroscopies (IR-8, NMR-3).

Extended reaction of $Os_3(CO)_{10}(\mu^2\text{-}OEt)_2$ with 1,5-pentanediol in toluene (20 hours)

To a 25-ml. round-bottomed flask was added $Os_3(CO)_{10}(\mu^2\text{-}OEt)_2$ (10 mg, 10 μmol) and 10-ml. of toluene. A ninety-fold excess of 1,5-pentanediol (0.10 ml., 0.95 mmol) was added to the yellow solution. The reaction mixture was heated to reflux under a nitrogen atmosphere for 20-hours. An infrared spectrum was recorded after 19-hours, revealing a strong $H_4Os_4(CO)_{12}$ pattern as the only product (IR-9). Reaction mixture was removed from heat and cooled to ambient temperature after 20-hours at reflux, at which point an insoluble dark-brown precipitate was observed on the walls of the flask. Infrared spectrum of this precipitate showed the presence of 1,5-pentanediol and no carbonyls. The pale yellow toluene solution was decanted to a clean flask and cooled at -20 ˚C to remove insoluble materials and excess 1,5-penanediol. From the cool solution a white precipitate with infrared spectrum consistent with $H_4Os_4(CO)_{12}$ and 1,5-pentanediol was removed. The solution was concentrated on rotary evaporator for spectroscopic characterization. On TLC in 50% ethyl acetate / hexanes solvent system two product spots were observed at R_f 0.42 and R_f 0.57. Infrared spectrum of this solution was recorded, revealing a very weak ten-carbonyl pattern in addition to a significant 1726 cm^{-1} band, owing to tiny yield of these products (IR-10). A proton NMR spectrum of the crude product was recorded and revealed it to be very complex with peaks which might correspond to the proposed organic ester product (NMR-4).

4.2 – Results & Discussion

The reaction of $Os_3(CO)_{10}(\mu^2\text{-}OEt)_2$ with 1,5-pentanediol affords a variety of different products with varied reaction time. Reflux duration was varied to study the sequence of product formation and to find the optimal reaction time to generate the substituted cluster $Os_3(CO)_{10}(\mu^2\text{-}O(CH_2)_5OH)_2$. Preliminary spectroscopic analysis suggests sequential substitution of ethoxide ligands for 1,5-pentanediol. Moderate yield of the disubstituted product, $Os_3(CO)_{10}(\mu^2\text{-}O(CH_2)_5OH)_2$ is obtained within one hour at reflux. Additionally, reactions with extended reaction times (> 20 hours) were studied to examine the thermal stability of cluster products. Quantitative conversion to a singular form of cluster buildup, $H_4Os_4(CO)_{12}$ was observed with extended reaction time.

Reaction of $Os_3(CO)_{10}(\mu^2\text{-}OEt)_2$ with 1,5-pentanediol in toluene (20-60 minutes)

In reactions of shorter reflux duration, the stepwise formation of the disubstituted diol cluster $Os_3(CO)_{10}(\mu^2\text{-}O(CH_2)_5OH)_2$ is observed. An intermediate product is present on TLC in 50% ethyl acetate / hexanes solvent system within the first 10 minutes at reflux (figure 59).

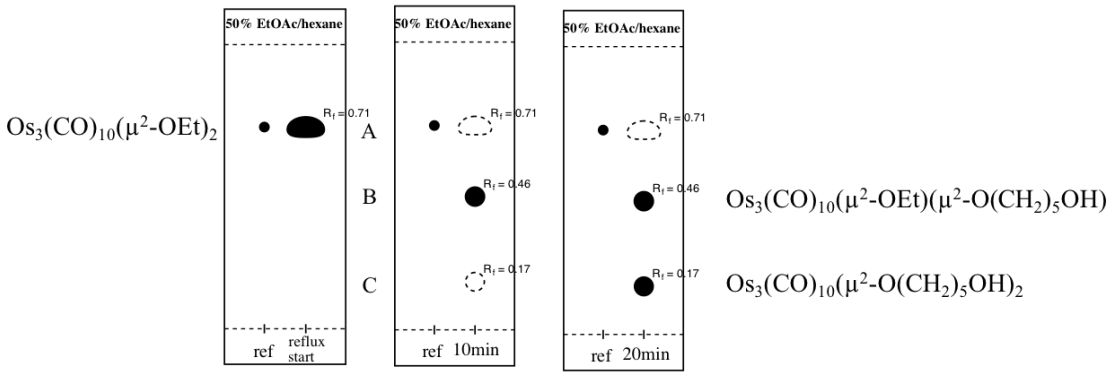

Figure 59 – TLC progression of the 20-minute reaction of $Os_3(CO)_{10}(\mu^2\text{-}OEt)_2$ with 1,5-pentanediol. This progression shows the sequential formation of two products in the first 20-minutes at reflux. On extending the reflux duration to 60-minutes, the product B spot (R_f 0.46) fades away as product C (R_f 0.17) intensifies.

In addition to unreacted starting material, two products are observed on TLC in 50% ethyl acetate / hexanes: products B (R_f 0.46) and C (R_f 0.17), which form sequentially.

Preliminary spectroscopic analysis of product C indicates that it is the disubstituted cluster $Os_3(CO)_{10}(\mu^2\text{-}O(CH_2)_5OH)_2$. To shorten a potentially redundant discussion, product C will be characterized using data from the 60-minute reaction, which afforded a very clean product. The associated product C data from this 20-minute reaction is provided in the appendix (IR-7, NMR-2). On the basis of its relatively polar TLC behavior and its spectroscopic profile, the structure of product C has been proposed to be the desired product, $Os_3(CO)_{10}(\mu^2\text{-}O(CH_2)_5OH)_2$. This product has an infrared spectrum with a clean ten-carbonyl stretching pattern with frequency consistent with it being of the formula $Os_3(CO)_{10}(\mu^2\text{-}OR)_2$ (figure 60) (IR-8).

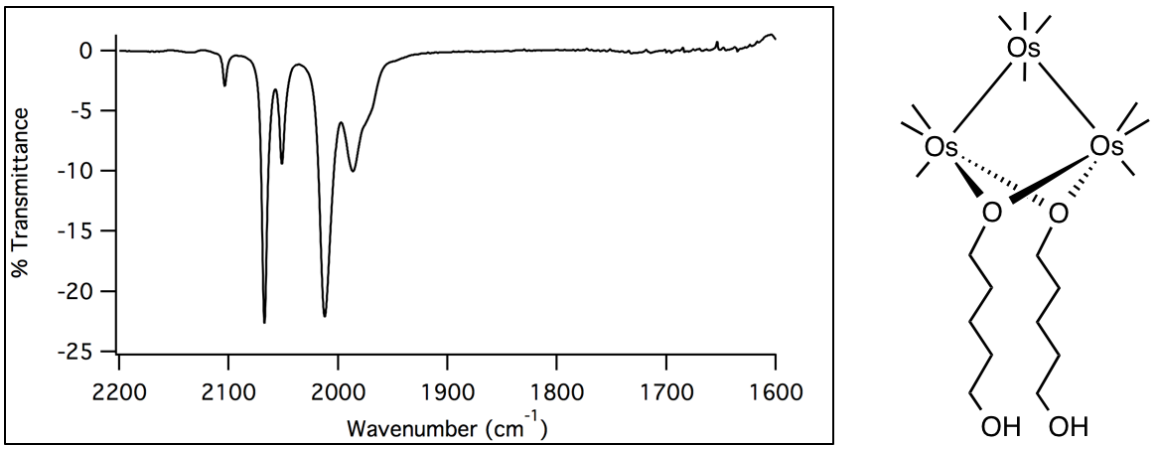

Figure 60 – Infrared spectrum of product C from the 60-minute reaction of $Os_3(CO)_{10}(\mu^2\text{-}OEt)_2$ with 1,5-pentanediol. Structure of product C is proposed to be the disubstituted cluster $Os_3(CO)_{10}(\mu^2\text{-}O(CH_2)_5OH)_2$.
ν (cm^{-1}) = 2104 (w), 2067 (s), 2051 (m), 2012 (s), 1987 (m)

The ^{1}H NMR spectrum of product C is also consistent with the proposed structure (figure 61) (NMR-3).

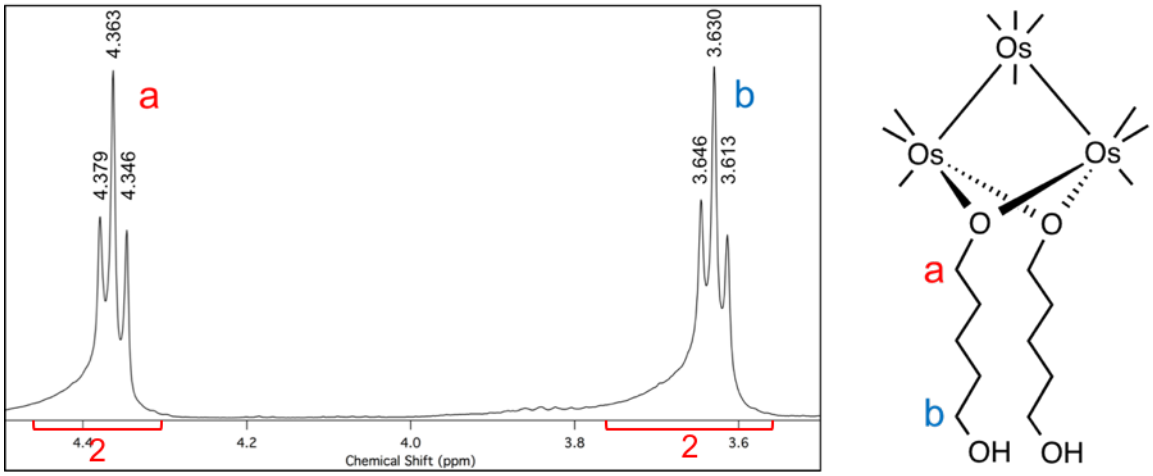

Figure 61 – ^{1}H NMR spectrum (left) and proposed structure (right) of product C from the 60-minute reaction of $Os_3(CO)_{10}(\mu^2\text{-}OEt)_2$ with 1,5-pentanediol.

Peaks were assigned to protons on the proposed structure on the basis of chemical shift values associated with methylene adjacent to bridging coordinated oxygen (~4.45 – 4.35 ppm) and that of free 1,5-pentanediol (3.74 ppm). Two triplet signals at 4.63 and 3.63 ppm

are consistent with the proposed structure of product C. The signal at 4.63 ppm is likely the methylene adjacent to a coordinated oxygen (–O–$\underline{CH_2}$–CH_2–), labeled 'a' on the structure. The signal at 3.63 ppm corresponds to the methylene protons adjacent to the pendant hydroxyl (–CH_2–$\underline{CH_2}$–OH), labeled 'b' on the structure. On the basis of this spectroscopic analysis and relative polarity on TLC, we conclude that the structure of product C is $Os_3(CO)_{10}(\mu^2\text{-}O(CH_2)_5OH)_2$.

We proposed product B to be the monosubstituted intermediate cluster $Os_3(CO)_{10}(\mu^2\text{-}OEt)(\mu^2\text{-}O(CH_2)_5OH)$ on the basis of its spectroscopic profile, in addition to its relatively nonpolar behavior and the sequence in which products B and C formed on TLC. The infrared spectrum of product B has a major ten-carbonyl stretching pattern with frequency consistent with it being of the formula $Os_3(CO)_{10}(\mu^2\text{-}OR)_2$ (figure 62) (IR-4).

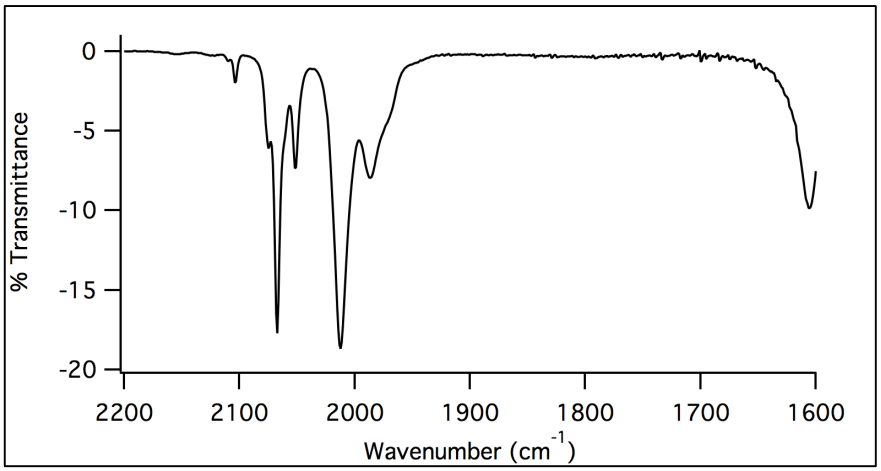

Figure 62 – Infrared spectrum of product B from the 20-minute reaction of $Os_3(CO)_{10}(\mu^2\text{-}OEt)_2$ with 1,5-pentanediol $\nu(cm^{-1})$ = 2104 (w), 2067(s), 2051(m), 2012(s), 1983(m). Structure of product B is proposed to be the monosubstituted cluster $Os_3(CO)_{10}(\mu^2\text{-}OEt)(\mu^2\text{-}O(CH_2)_5OH)$.

The ^{1}H NMR spectrum of product B also supports the proposed structure as the monosubstituted cluster $Os_3(CO)_{10}(\mu^2\text{-}OEt)(\mu^2\text{-}O(CH_2)_5OH)$ (figure 63) (NMR-1).

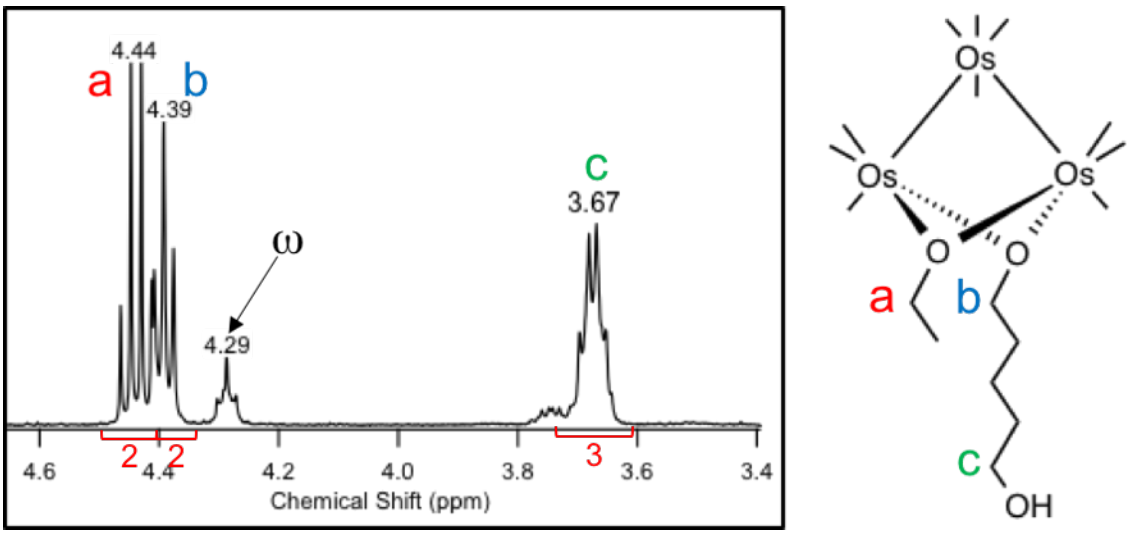

Figure 63 – ^{1}H NMR spectrum (left) and proposed structure (right) of product B, $Os_3(CO)_{10}(\mu^2\text{-}OEt)(\mu^2\text{-}O(CH_2)_5OH)$, in the reaction of $Os_3(CO)_{10}(\mu^2\text{-}OEt)_2$ with 1,5-pentanediol. NMR signals have been assigned to protons on the proposed structure. The signal at 4.29 ppm is an ω impurity.

In the ^{1}H NMR spectrum of product B, signals at chemical shifts of 4.44 (q) and 4.39 (t) ppm have equivalent integrations. These chemical shift values are consistent with the methylene protons adjacent to a bridging coordinated oxygen (–O–$\underline{CH_2}$–). Splitting patterns of these signals suggests that the quartet at 4.44 ppm is a bridging ethoxide (–O–$\underline{CH_2}$–CH_3), and the triplet signal at 4.39 ppm is is the methylene protons adjacent to the coordinated oxygen to a longer alkoxide chain (–O–$\underline{CH_2}$–CH_2–). Equivalent integrations of these two signals indicates that these two signals correspond to different bridging oxyligands of the same cluster product. Thus the proposed structure of product B is consistent with these two signals. The double-triplet signal 3.67 ppm is characteristic of methylene protons adjacent the pendant alcohol group (–CH_2–$\underline{CH_2}$–OH). Integration of this signal does not coincide with that of the corresponding triplet signal at 4.39 ppm, however, which may indicate the presence of residual 1,5-pentanediol.

As discussed in Chapter 3, a 1,5-pentanediol functionalized ω derivative was isolated in this study of bridging ligand substitution. Due to the difficulty of separating mixtures of ω and $Os_3(CO)_{10}(\mu^2\text{-}OEt)_2$, ω-type products were sporadically observed in subsequent reactions of $Os_3(CO)_{10}(\mu^2\text{-}OEt)_2$ with 1,5-pentanediol, and in retrospect proved to be a complicating factor in the initial work of Estephanie Rivero.[37] In her attempts to identify products of the reaction of $Os_3(CO)_{10}(\mu^2\text{-}OEt)_2$ with 1,5-pentanediol, Rivero observed a triplet at 4.29 ppm in addition to the product triplet at 4.40 ppm.[37] Rivero had attributed this signal to a conformational isomer of the disubstituted product $Os_3(CO)_{10}(\mu^2\text{-}O(CH_2)_5OH)_2$ on the basis of its similar spectroscopic profile to that of ω. This ω derivative responsible for the 4.29 ppm signal has been isolated and characterized in one synthesis by this author (IR-11, NMR-5). The infrared spectrum of the purified product has a clean ten-carbonyl stretching pattern consistent with that of the ω impurity in the synthesis of $Os_3(CO)_{10}(\mu^2\text{-}OEt)_2$ (figure 64).

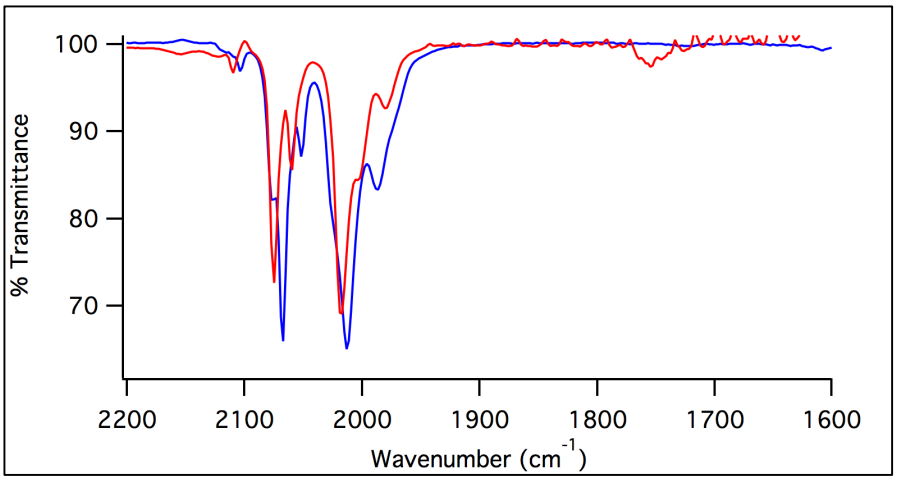

Figure 64 – Overlay comparison of the infrared carbonyl stretching pattern of ω-contaminated $Os_3(CO)_{10}(\mu^2\text{-}OEt)_2$ (blue) and the functionalized ω derivative proposed to be the cluster $Os_3(CO)_{10}(\mu^2\text{-}Cl)(\mu^2\text{-}O(CH_2)_5OH)$ (red). This comparison shows how the full ten-carbonyl pattern of an ω cluster is seen underneath the broad shoulders of $Os_3(CO)_{10}(\mu^2\text{-}OEt)_2$ carbonyl stretches in a mixture.

As was discussed in Chapter 3, a higher frequency ten-carbonyl stretching pattern indicates the presence of a bridging chloride ligand. By the above infrared spectra comparison it is evident that even though an infrared spectrum of pure ω has not been obtained, its ten-carbonyl pattern and C_{2v} point group symmetry are supported by the impure spectrum. The ^{1}H NMR spectrum of this product shows a triplet signal at 4.29 ppm (figure 65).

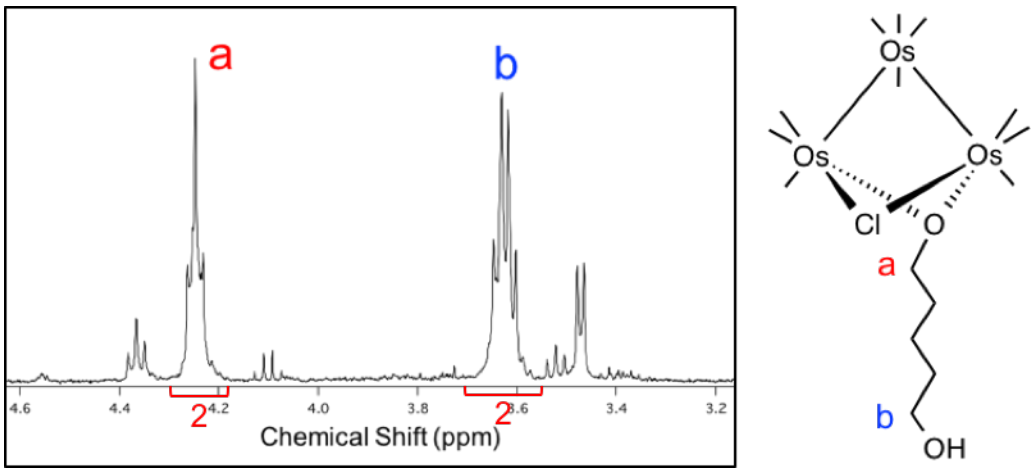

Figure 65 – Proton NMR spectrum of 1,5-pentanediol functionalized ω derivative obtained as a minor product in the synthesis of $Os_3(CO)_{10}(\mu^2\text{-}O(CH_2)_5OH)_2$. Proposed structure is the cluster $Os_3(CO)_{10}(\mu^2\text{-}Cl)(\mu^2\text{-}O(CH_2)_5OH)$.

This triplet signal has an upfield chemical shift consistent with that of ω and a bridging chloride ligand. That it has triplet splitting would suggest that the cluster is functionalized with 1,5-pentanediol bridging ligands. This would additionally explain the relatively polar behavior of this cluster on TLC. On the basis of its spectroscopic profile and the newly proposed structure of ω, we propose that this product is the cluster $Os_3(CO)_{10}(\mu^2\text{-}Cl)(\mu^2\text{-}O(CH_2)_5OH)$.

The appearance of an ω derivative in the alkoxide substitution reaction with 1,5-pentanediol suggests that starting $Os_3(CO)_{10}(\mu^2\text{-}OEt)_2$ was contaminated with the ω cluster,

$Os_3(CO)_{10}(\mu^2\text{-Cl})(\mu^2\text{-OEt})$. On reaction with 1,5-pentanediol this cluster might exchange bridging ethoxide to afford this product, $Os_3(CO)_{10}(\mu^2\text{-Cl})(\mu^2\text{-O(CH}_2)_5\text{OH})$. Persistence of bridging chloride through alkoxide substitution is consistent with observations of varied reflux duration. In the ^{1}H NMR spectrum of product B from the 20 minute reaction of $Os_3(CO)_{10}(\mu^2\text{-OEt})_2$ with 1,5-pentanediol, signals of both $Os_3(CO)_{10}(\mu^2\text{-OEt})(\mu^2\text{-O(CH}_2)_5\text{OH})$ and $Os_3(CO)_{10}(\mu^2\text{-Cl})(\mu^2\text{-O(CH}_2)_5\text{OH})$ are observed (figure 66).

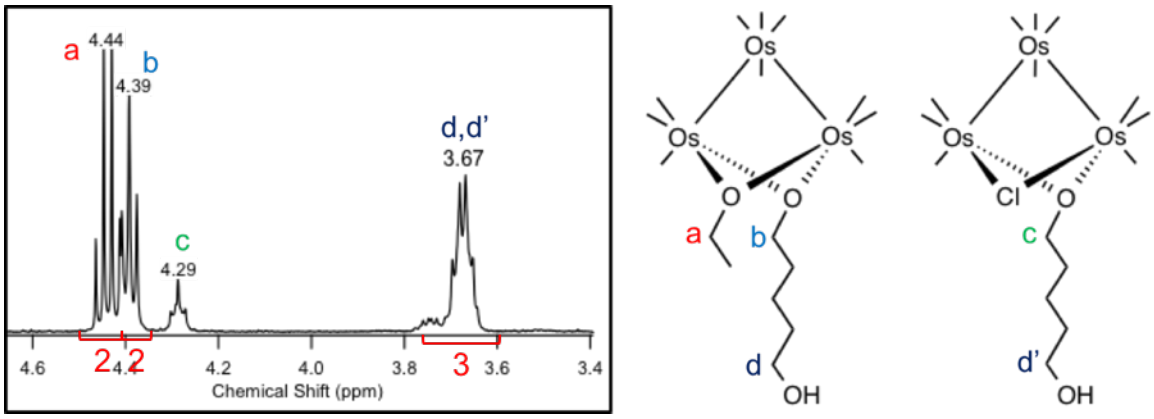

Figure 66 – ^{1}H NMR spectrum and proposed structures of product B, $Os_3(CO)_{10}(\mu^2\text{-OEt})(\mu^2\text{-O(CH}_2)_5\text{OH})$ (left), and ω derivative, $Os_3(CO)_{10}(\mu^2\text{-Cl})(\mu^2\text{-O(CH}_2)_5\text{OH})$ (right) from the 20-minute reaction of $Os_3(CO)_{10}(\mu^2\text{-OEt})_2$ with 1,5-pentanediol.

These two products cannot be purified with chromatography. This is consistent with the observation that bridging chloride and ethoxide ligands cannot be differentiated with TLC. On extending the reflux period to 40 minutes, $Os_3(CO)_{10}(\mu^2\text{-Cl})(\mu^2\text{-O(CH}_2)_5\text{OH})$ appears independent of $Os_3(CO)_{10}(\mu^2\text{-OEt})(\mu^2\text{-O(CH}_2)_5\text{OH})$ in the infrared and ^{1}H NMR spectra (IR-11, NMR-5). This result demonstrates that bridging chloride is less readily substituted than is bridging ethoxide. Therefore, $Os_3(CO)_{10}(\mu^2\text{-Cl})(\mu^2\text{-OEt})$ contaminated starting material would explain the seemingly sporadic appearance of this ω derivative in the product distribution.

Extended reflux periods (> 20 hours)

The reaction of $Os_3(CO)_{10}(\mu^2\text{-}OEt)_2$ with 1,5-pentanediol in toluene with extended reflux period (> 20 hours) was conducted to probe the thermal stability of the substituted cluster products. Prolonged reflux duration afforded quantitative yield of the cluster $H_4Os_4(CO)_{12}$.[14] This singular form of cluster buildup was observed in the infrared spectrum of the reaction mixture after 19 hours at reflux (figure 67) (IR-9).

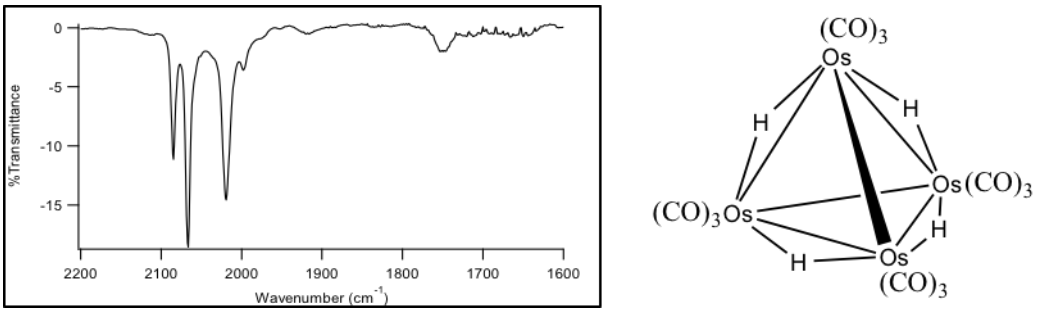

Figure 67 – Reaction mixture infrared spectrum from the reaction of $Os_3(CO)_{10}(\mu^2\text{-}OEt)_2$ with 1,5-pentanediol in toluene at 19-hours reflux (left) and the structure of $H_4Os_4(CO)_{12}$ (right). This spectrum shows a major carbonyl-stretching pattern consistent with the literature infrared spectrum of the cluster $H_4Os_4(CO)_{12}$: $\nu(cm^{-1})$ = 2085(m), 2067(vs), 2019(s), 1998(w).[14] An unrelated product peak is also observed at 1750 cm^{-1}.

When cooled at -20 ˚C, majority of the $H_4Os_4(CO)_{12}$ and residual 1,5-pentanediol precipitated out of the reaction mixture. An infrared spectrum of this precipitate was recorded and the cluster was identified to be $H_4Os_4(CO)_{12}$ by comparison with literature data (IR-10).[14] Minor cluster products still remaining in the toluene solution were characterized with IR and ^1H NMR spectroscopies. Very weak intensity of the carbonyl stretching bands in the infrared spectrum owes to very low yield of this minor products.

The band at 1750 cm^{-1} in the reaction mixture infrared spectrum is suspected to be an organic ester. This peak appears to form in conjunction with $H_4Os_4(CO)_{12}$, so it may be that formation of an organic ester is the result of some redox process between the cluster

and ligand. In the ^{1}H NMR spectrum of the reaction mixture there is evidence for the presence of this organic ester (NMR-4). A quartet at 3.74 ppm adjoined to a triplet at 1.26 ppm with integration values of 2 and 3, respectively, suggest that a free ethyl ester is present in solution (figure 68).

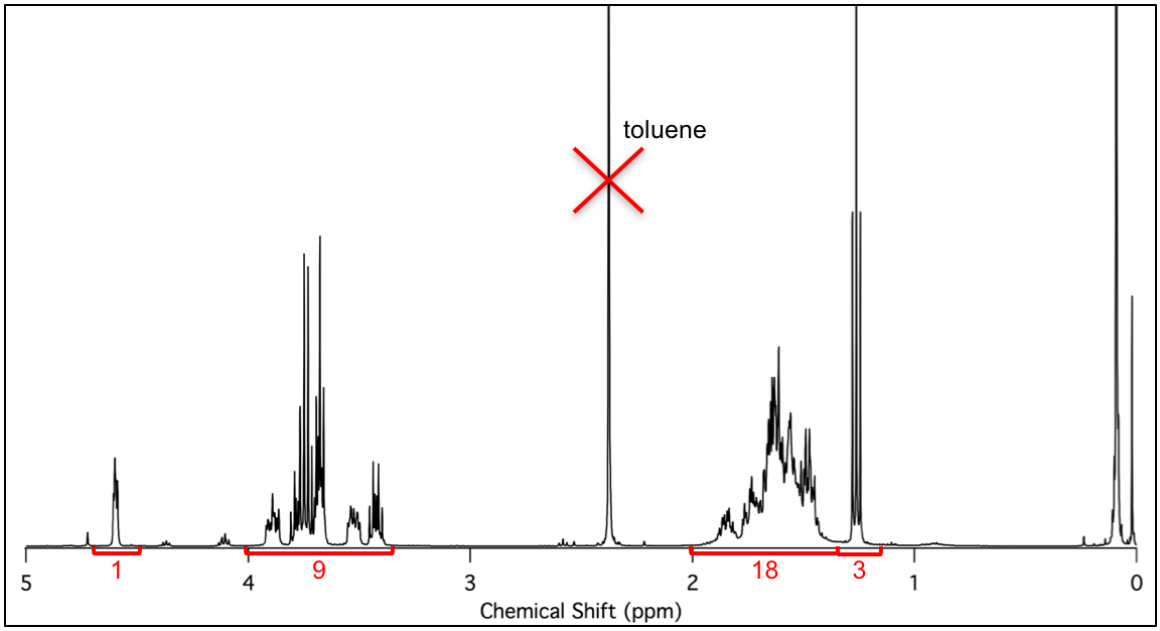

Figure 68 - ^{1}H NMR spectrum of the product from 20-hour reaction of $Os_3(CO)_{10}(\mu^2\text{-}OEt)_2$ with 1,5-pentanediol after -20 ˚C extraction of $H_4Os_4(CO)_{12}$ and 1,5-pentanediol. A quartet at 3.74 ppm (left) and triplet 1.26 ppm (right) correspond to a free ethyl ester in solution.

One might suspect that these integration values are mere coincidence and that this quartet signal at 3.74 ppm is due to residual 1,5-pentanediol from the reaction. This suspicion is answered with the observation that the ^{1}H NMR spectrum of pure 1,5-pentanediol has a double triplet signal with significantly different chemical shift (figure 69).

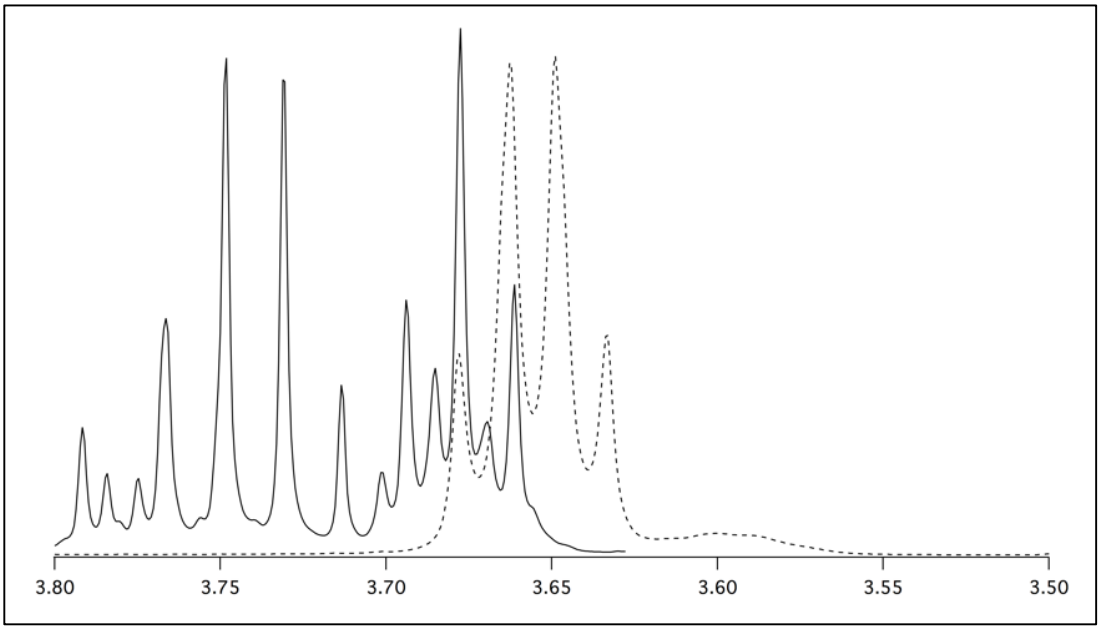

Figure 69 - ^{1}H NMR spectra overlay with product from 20-hours reflux after 1,5-pentanediol extraction (solid line) and reference NMR of 1,5-pentanediol reagent (dashed line).

Based on this ^{1}H NMR analysis, a simple reaction scheme may be proposed (figure 70).

$$4\ Os_3(CO)_{10}(\mu^2\text{-OEt})_2 \xrightarrow{\text{1,5-pentanediol}} 3\ H_4Os_4(CO)_{12} + \text{"}C_xH_yO_zCOOCH_2CH_3\text{"}$$

Figure 70 – Simple scheme for the formation of $H_4Os_4(CO)_{12}$ and the proposed organic ester product.

Further analysis would be necessary for full characterization of this ester product. This would require purification and/or a mass spectrum of the ester to solve its structure. Currently this laboratory is not equipped with an LCMS capable of separating mixtures of heavy metals and small organic molecules. It is unknown as to whether the formation of $H_4Os_4(CO)_{12}$ and the proposed organic ester product depends on the presence of excess 1,5-pentanediol in solution. It is thus necessary to conduct the pyrolysis reaction of $Os_3(CO)_{10}(\mu^2\text{-}O(CH_2)_5OH)_2$ in the absence of free 1,5-pentanediol. By doing so, it might be possible to identify a mechanism for the ligand transformations observed.

Significance of the singular form of cluster buildup, $H_4Os_4(CO)_{12}$

The generation of a solitary form of cluster buildup, $H_4Os_4(CO)_{12}$ in the reaction of $Os_3(CO)_{10}(\mu^2\text{-}OEt)_2$ with 1,5-pentanediol is a remarkably unique finding, which suggests that there is a very specific redox mechanism that might be investigated. Dr. Mary-Ann Pearsall conducted reactions of $Os_3(CO)_{10}(\mu^2\text{-}OEt)_2$ with simple alcohols and found the reactions to product several forms of cluster buildup.[14] The pyrolysis of $Os_3(CO)_{10}(\mu^2\text{-}OEt)_2$ in isobutanol affords at least five osmium cluster decomposition/buildup products, as well as the main $Os_3(CO)_{10}(\mu^2\text{-}OBu^i)_2$ product (figure 71).[14]

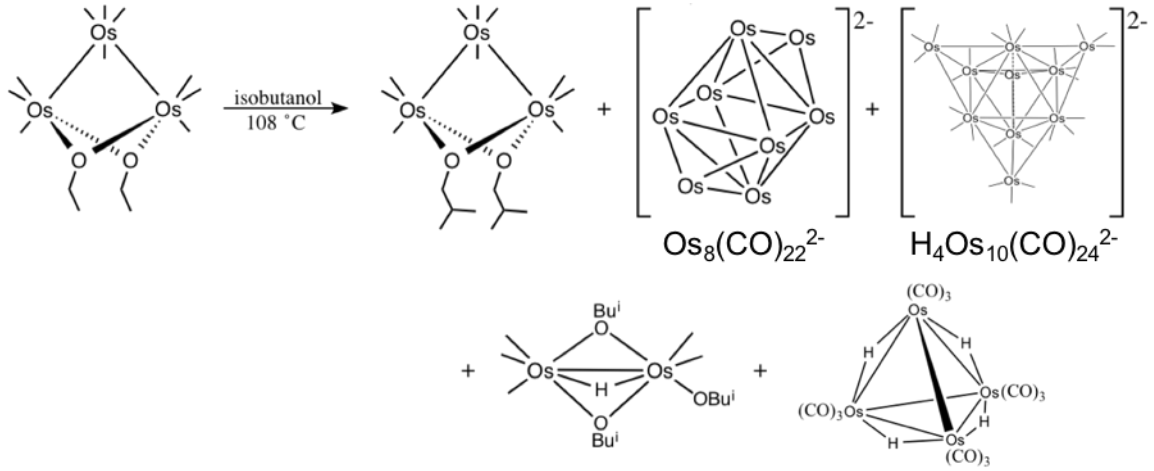

Figure 71 – Reaction scheme for the pyrolysis of $Os_3(CO)_{10}(\mu^2\text{-}OEt)_2$ in isobutanol.

Among the cluster buildup products $H_4Os_4(CO)_{12}$ was identified as a product of the reaction. This result is typical of reactions involving triosmium decacarbonyl clusters. Thus it is noteworthy that thermal treatment of the reaction of $Os_3(CO)_{10}(\mu^2\text{-}OEt)_2$ with 1,5-pentanediol produces a solitary form of cluster buildup.

Chapter 5 – Attempted Synthesis of a Linked Cluster

This laboratory seeks to investigate the fundamental concept of linking two dibridged triosmium decacarbonyl clusters via bifunctional bridging ligands. To further develop the systematic route to linked cluster synthesis by Mularz, a cluster has been functionalized with 1,5-pentanediol bridging ligands. This cluster has pendant hydroxyl functionality, which may have the capacity to link a second triosmium cluster – thereby generating a linked cluster system (figure 72).

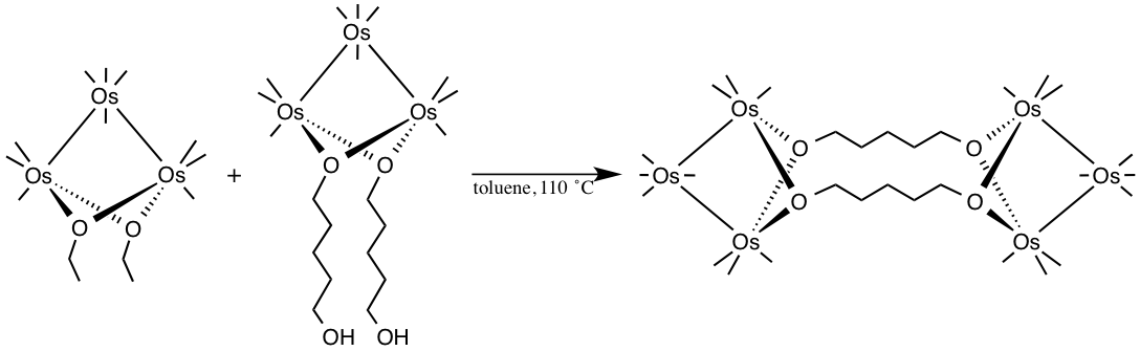

Figure 72 – Scheme of the reaction of $Os_3(CO)_{10}(\mu^2\text{-}OEt)_2$ with $Os_3(CO)_{10}(\mu^2\text{-}O(CH_2)_5OH)_2$ to form the linked cluster $\{Os_3(CO)_{10}\}_2(\mu^2,\mu^2\text{-}O(CH_2)_5O)_2$.

In this chapter the attempted synthesis of a linked cluster system with 1,5-pentanediol bridging ligands will be discussed.

5.1 – Experimental

Reaction of $Os_3(CO)_{10}(\mu^2\text{-}O(CH_2)_5OH)_2$ with $Os_3(CO)_{10}(\mu^2\text{-}OEt)_2$ in toluene

The clusters $Os_3(CO)_{10}(\mu^2\text{-}O(CH_2)_5OH)_2$ and $Os_3(CO)_{10}(\mu^2\text{-}OEt)_2$ were prepared via procedures described above. To a 100-ml. round-bottomed flask was added $Os_3(CO)_{10}(\mu^2\text{-}OEt)_2$ (20 mg, 21 μmol), $Os_3(CO)_{10}(\mu^2\text{-}O(CH_2)_5OH)_2$ (22 mg, 21 μmol) and 40-ml. of toluene. The reaction mixture was heated to reflux (110 ˚C) under a $N_2(g)$ atmosphere for 100 minutes, by which point the color had changed from a pale yellow to a light orange. Reaction progress was monitored by IR and TLC. After 100 minutes the reaction mixture was removed from heat to cool at ambient temperature. On TLC in 40% dichloromethane / hexanes three spots are observed: $R_f = 0.52$ (starting material), 0.34 (vis. yellow), and baseline material (vis. brown). The crude product mixture was purified by preparative plate chromatography with 40% dichloromethane / hexanes solvent system. One band was collected (R_f 0.34) and extracted from silica gel with ethyl acetate followed by dichloromethane. An infrared spectrum of this product in dichloromethane revealed that at least two clusters were present (IR-12). On TLC in 40% ethyl acetate / hexanes solvent system two spots were observed: R_f 0.49 and R_f 0.65. These products were further purified by preparative plate chromatography with 30% ethyl acetate / hexanes solvent system. Two bands were collected and labeled products 1 and 2. On TLC in 30% ethyl acetate / hexanes solvent system products 1 and 2 appeared singular with spots at R_f 0.46 and 0.64, respectively. Products 1 and 2 were characterized by IR (IR-13, IR-14) and ^{1}H NMR (NMR-6, NMR-7). Crystallization of product 1 in dichloromethane / hexanes solution (1 ml. : 1 ml.) via slow evaporation to dryness at ambient temperature afforded red-orange

crystals. Crystallization of product 2 has been attempted but no diffraction quality crystals have yet been obtained.

5.2 – Results & Discussion

Preliminary spectroscopic analysis of product 1 suggests that it may have structure similar to the looped cluster from Mykietyn's ethylene glycol work.[30] With this suspicion, the structure $Os_3(CO)_8(\mu^2\text{-}O(CH_2)_5O)_2$ has been proposed for product 1. The infrared spectrum is similar to the eight-carbonyl pattern of Mykietyn's loop structure (figure 72) (IR-13).

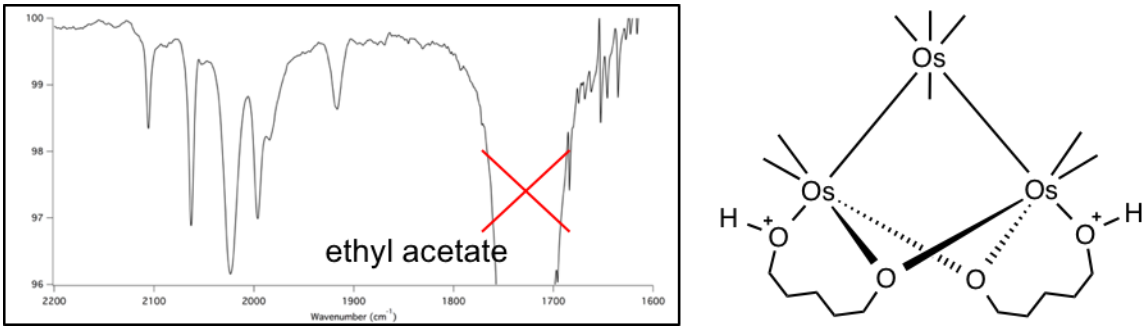

Figure 72 – Infrared spectrum and the initially proposed structure of product 1 from the reaction of $Os_3(CO)_{10}(\mu^2\text{-}OEt)_2$ with $Os_3(CO)_{10}(\mu^2\text{-}O(CH_2)_5OH)_2$. υ ($cm^{-1}$) = 2105 (m), 2062 (s), 2023 (vs), 1999 (s), 1984 (m), 1916 (m)

This carbonyl stretching pattern indicates that the product must be of the formula $Os_3(CO)_8X_2$, but is not unambiguous as to the exact nature of the bridging ligand(s). While both the infrared spectrum and TLC retention characteristics of product 1 are compelling evidence for the structure proposed in figure 72, the ^1H NMR spectrum of product 1 is very complicated and has some inconsistencies with this proposed structure (figure 73) (NMR-6).

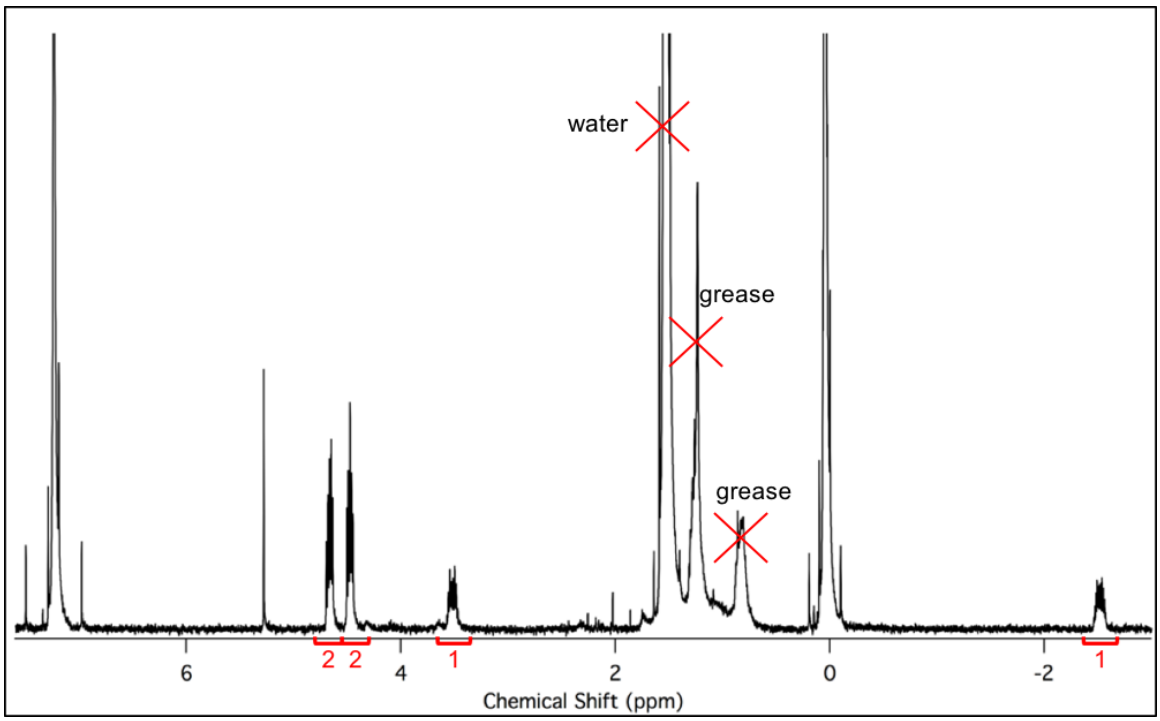

Figure 73 – ^{1}H NMR spectrum of product 1 from the reaction of $Os_3(CO)_{10}(\mu^2\text{-}OEt)_2$ with $Os_3(CO)_{10}(\mu^2\text{-}O(CH_2)_5OH)_2$.

This spectrum has at least five sets of proton signals associated with the product. Signals corresponding to intermediate methylene protons on the carbon chain are present in the spectrum between 1.0 – 1.7 ppm, but are heavily obscured by intense water and grease peaks. There are two signals with chemical shifts that are consistent with the methylene protons adjacent to bridging oxygen at 4.66 and 4.47 ppm. These signals have equivalent integration values of two protons each. The complex splitting patterns of these signals supports a rigid loop-type structure (figure 74).

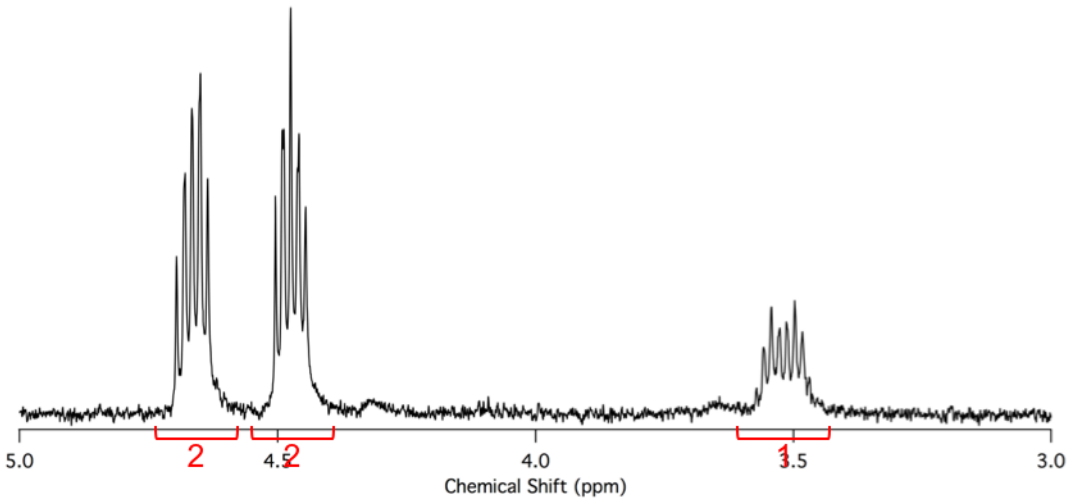

Figure 74 – ^{1}H NMR spectrum of product 1 from the reaction of $Os_3(CO)_{10}(\mu^2\text{-}OEt)_2$ with $Os_3(CO)_{10}(\mu^2,\mu^2\text{-}O(CH_2)_5OH)_2$ in toluene. Detail of multiplet signals at 4.66, 4.47 and 3.51 ppm.

Another signal at 3.51 ppm has a similarly complex splitting pattern. Its chemical shift is in the region generally associated with methylene protons adjacent to a pendant hydroxyl group (–CH_2–$C\underline{H_2}$–OH); however, the presence of such a pendant hydroxyl is not possible due to the relatively nonpolar behavior on TLC. Oddly, this signal has a relative integration accounting for only one proton(s). A very unusual fourth signal is seen at -2.52 ppm, which has a very complex splitting pattern and which integrates to one proton(s) (figure 75).

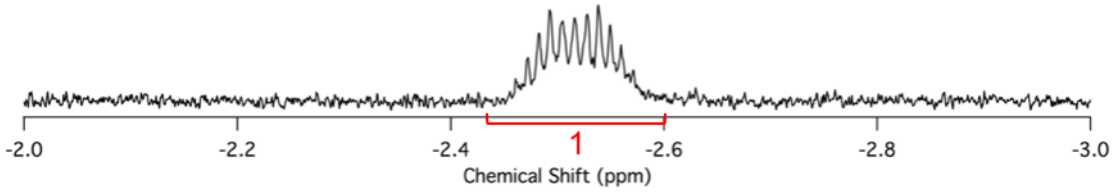

Figure 75 – ^{1}H NMR spectrum of product 1 from the reaction of $Os_3(CO)_{10}(\mu^2\text{-}OEt)_2$ with $Os_3(CO)_{10}(\mu^2,\mu^2\text{-}O(CH_2)_5OH)_2$ in toluene. Detail of the multiplet signal at -2.52 ppm.

Such a highly shielded proton is not expected of the initially proposed structure of product 1 as depicted in figure 72. A review of the literature reveals that this proton does not correspond to terminal or bridging hydride, which generally appear between -10 – -20 ppm.[38] Considering the initially proposed structure, this signal was presumed to be the hydroxyl proton (–CH_2–O(H)–Os), which may have been consistent with respect to the chemical shift observed. However, this interpretation is inconsistent with the complex splitting pattern of this signal and also that a proton is missing at the pendant methylene position (–CH_2–CH_2–OH) with chemical shift 3.51 ppm (figure 76).

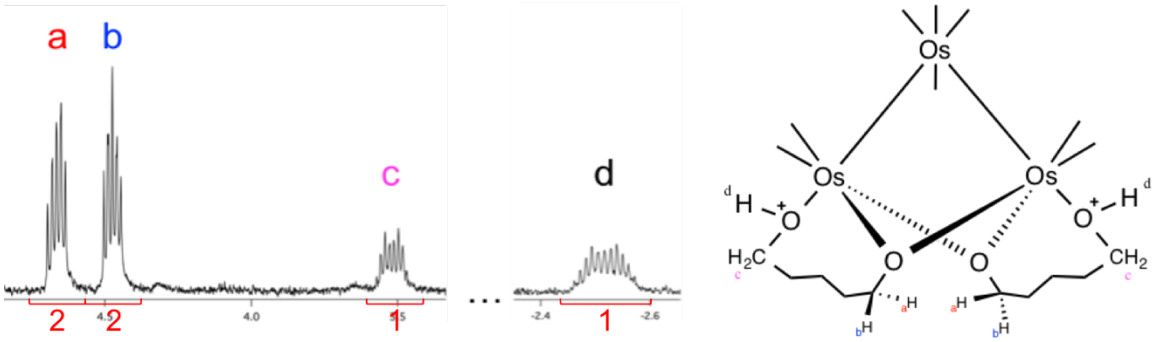

Figure 76 – ^{1}H NMR spectrum and the initially proposed Mykietyn *loop* type structure of product 1 from the reaction of $Os_3(CO)_{10}(\mu^2\text{-}OEt)_2$ with $Os_3(CO)_{10}(\mu^2\text{-}O(CH_2)_5OH)_2$ in toluene.

For these inconsistencies with the initially proposed structure of product 1, we hypothesized that perhaps the signal at -2.52 ppm represents an *agostic* proton. An agostic proton is one which engages in a three-center-two-electron bonding interaction between a carbon and a transition metal center.[39] According to the literature, agostic protons may have chemical shift ranging -5.0 – 8.0 ppm.[39] This would be consistent with that the of the observed signal at -2.52 ppm. Thus a structure with an agostic proton between oxygen and osmium (–O–H–Os) was proposed (figure 77).

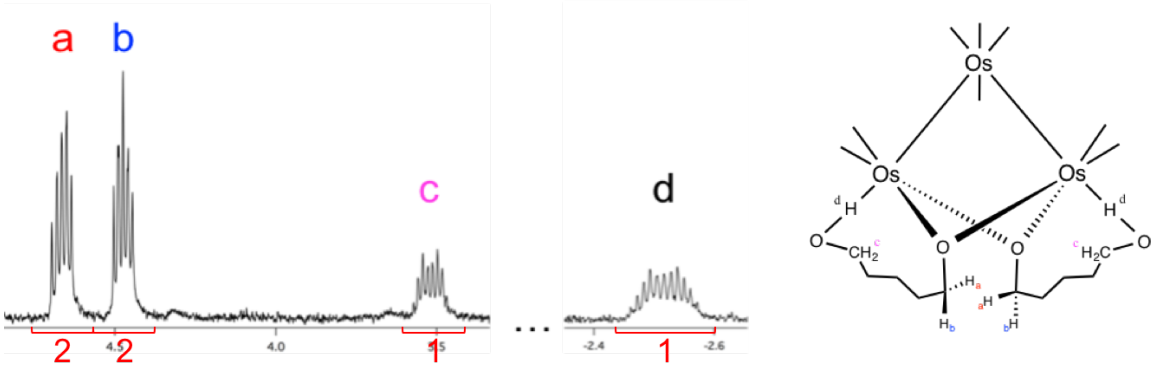

Figure 77 – ^{1}H NMR spectrum and proposed *loop* structure #2 of product 1 from the reaction of $Os_3(CO)_{10}(\mu^2\text{-}OEt)_2$ with $Os_3(CO)_{10}(\mu^2\text{-}O(CH_2)_5OH)_2$ in toluene.

While consistent with the observed chemical shifts for all signals in the ^{1}H NMR spectrum, this structure is inconsistent with respect to the complex splitting pattern of the -2.52 ppm signal. Also, integration of the 3.51 ppm signal accounts for only one of two expected protons. A third structure has been proposed for this product as having an agostic proton from the carbon chain (–C–H–Os) (figure 78).

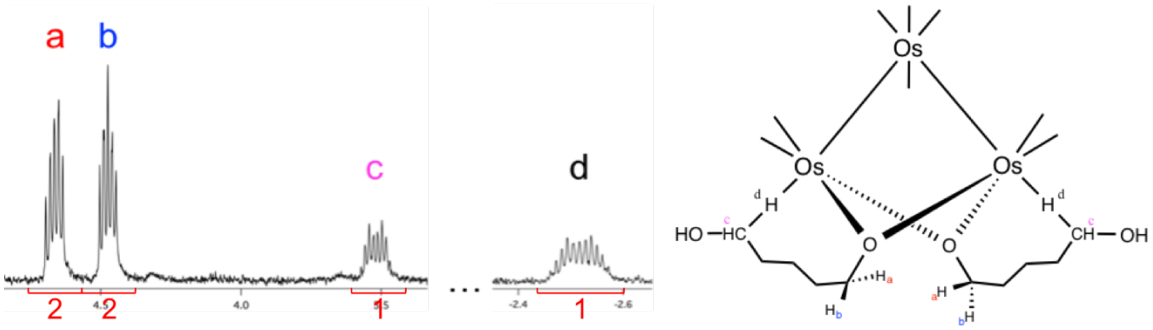

Figure 78 – ^{1}H NMR spectrum and proposed *loop* structure #3 of product 1 from the reaction of $Os_3(CO)_{10}(\mu^2\text{-}OEt)_2$ with $Os_3(CO)_{10}(\mu^2\text{-}O(CH_2)_5OH)_2$ in toluene.

This structure is also inconsistent with the integration values observed in the ^{1}H NMR spectrum. It better satisfies the splitting patterns of hydrogen signals. Since this methylene carbon adjacent to the pendant hydroxyl is chiral, as many as four diastereomers might be present in solution. Thus the complex splitting patterns observed in the ^{1}H NMR spectrum may be due to the presence of multiple enantiomers of proposed structure #3. While now consistent with the observed splitting patterns, structure #3 does not match the peak integrations.

Finally, *loop* structure #4 was proposed on the basis of mismatched integrations and diastereomeric splitting patterns (figure 79).

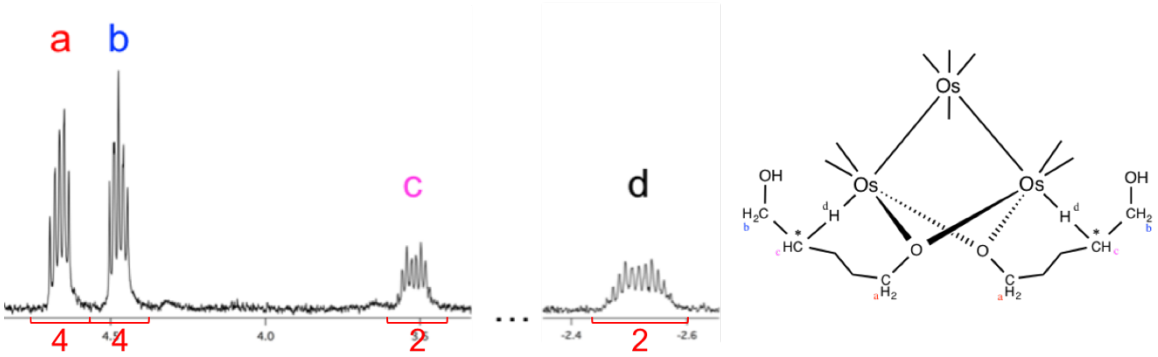

Figure 79 – ^{1}H NMR spectrum and proposed *loop* structure #4 of product 1 from the reaction of $Os_3(CO)_{10}(\mu^2\text{-}OEt)_2$ with $Os_3(CO)_{10}(\mu^2\text{-}O(CH_2)_5OH)_2$ in toluene.

Structure #4 matches both the observed NMR integrations and the complex splitting patterns by the presence of multiple diastereomers in solution. Protons assigned labels b and c were assigned solely based on relative integrations. Their chemical shifts are not backed by any literature values due to the rarity of transition metal complexes with agostic protons. In particular, peak b (4.47 ppm) is far downfield of where a methylene adjacent to a pendant hydroxyl is expected to appear (~3.6 ppm). Since there is very little information about agostic interactions and its effect on the chemical shift of neighboring functionality, these proton assignments were made solely on the basis of relative integration. Structure #4 best matches the spectroscopic profile of product 1.

Preliminary spectroscopic analysis of product 2 reveals that it is similar to that reported by Mularz on the linked cluster $\{Os_3(CO)_{10}\}_2(\mu^2,\mu^2\text{-}O(CH_2)_6O)_2$.[31] Product 2 has been characterized and proposed to be the target linked cluster $\{Os_3(CO)_{10}\}_2(\mu\text{-}O(CH_2)_5O)_2$. The infrared spectrum of product 2 is consistent with a ten-carbonyl stretching pattern with an additional peak at υ = 1991 cm^{-1} (figure 80).

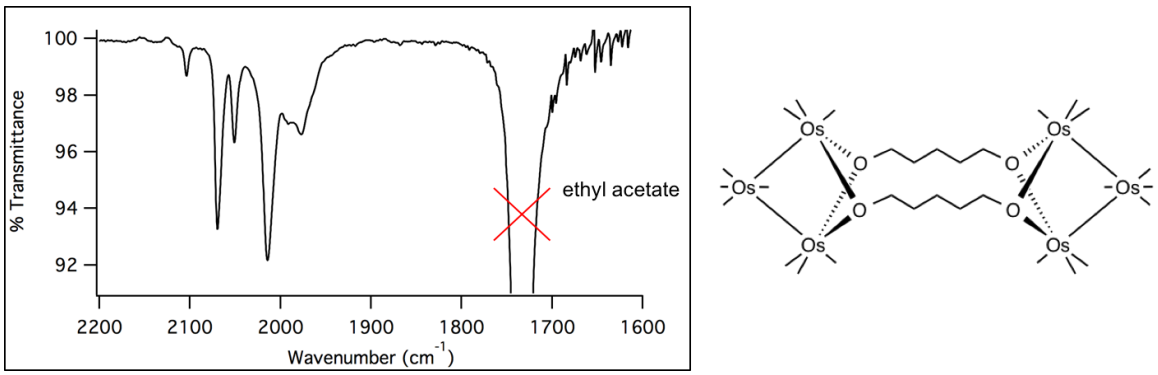

Figure 80 – Infrared spectrum and proposed structure of product 2 from the reaction of $Os_3(CO)_{10}(\mu^2\text{-}OEt)_2$ and $Os_3(CO)_{10}(\mu^2\text{-}O(CH_2)_5OH)_2$. Proposed structure of product 2 is the linked cluster $\{Os_3(CO)_{10}\}_2(\mu 2,\mu 2\text{-}O(CH_2)_5O)_2$. ν (cm^{-1}) = 2103 (w), 2069 (s), 2051 (m), 2014 (vs), 1991 (m), 1976 (m).

Product 2 has an elegantly simple ^{1}H NMR spectrum that is consistent with the proposed linked structure (figure 81).

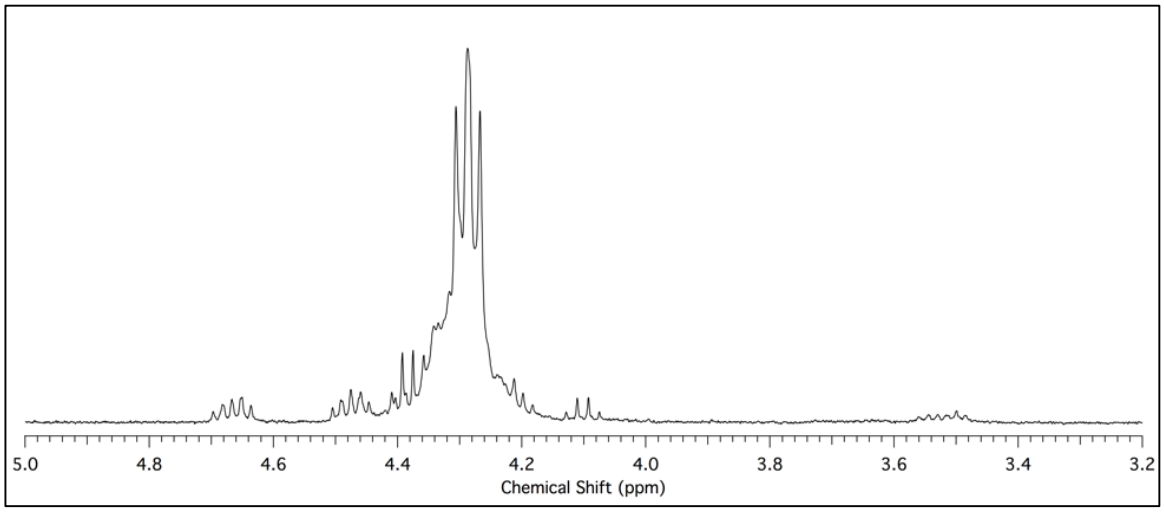

Figure 81 – ^{1}H NMR spectrum of product 2 from the reaction of $Os_3(CO)_{10}(\mu^2\text{-}OEt)_2$ with $Os_3(CO)_{10}(\mu^2\text{-}O(CH_2)_5OH)_2$. Structure of this product is proposed to be the linked cluster $\{Os_3(CO)_{10}\}_2(\mu^2,\mu^2\text{-}O(CH_2)_5O)_2$.

A lone signal is observed downfield at $\partial = 4.287$ ppm with a splitting pattern that resembles a doublet of doublets (dd). This chemical shift is consistent with protons of a carbon adjacent to a bridging coordinated oxygen. The apparent splitting pattern presents the issue

of whether it is two overlapping doublet signals having similar chemical shifts, or a single signal with dd multiplicity. If we interpret this signal has a single signal with dd multiplicity then the data fully supports what would be expected of the spectroscopic profile of the linked cluster $\{Os_3(CO)_{10}\}_2(\mu^2,\mu^2\text{-}O(CH_2)_5O)_2$.

Chapter 5 – Conclusion

With the goal of furthering the development of a new synthetic route to linked triosmium carbonyl clusters the interaction of the cluster $Os_3(CO)_{10}(\mu^2\text{-}OEt)_2$ with 1,5-pentanediol was thoroughly investigated. The results of these investigations are summarized in Figure 80 below. The linked cluster $\{Os_3(CO)_{10}\}_2(\mu^2,\mu^2\text{-}O(CH_2)_5O)_2$ has been achieved via reaction of $Os_3(CO)_{10}(\mu^2\text{-}OEt)_2$ with $Os_3(CO)_{10}(\mu^2\text{-}O(CH_2)_5OH)_2$ in refluxing toluene for 100 minutes. A short-lived intermediate to the formation of $Os_3(CO)_{10}(\mu^2\text{-}O(CH_2)_5OH)_2$ was identified as the monosubstituted cluster $Os_3(CO)_{10}(\mu^2\text{-}OEt)(\mu^2\text{-}O(CH_2)_5OH)$.

On extending the reflux period to 20 hours a singular form of cluster buildup $H_4Os_4(CO)_{12}$ is observed. This cluster appears to form in conjunction with an organic ester moiety, but this has not yet been confirmed. Intermediates leading up to this thermodynamic sink have not yet been identified. It is suspected that one of the products from the reaction to form the linked cluster $\{Os_3(CO)_{10}\}_2(\mu^2,\mu^2\text{-}O(CH_2)_5O)_2$ is an intermediate leading to the formation of $H_4Os_4(CO)_{12}$. The structure of this product is undetermined, but is likely to have some form of agostic proton. To test if this product is an intermediate to $H_4Os_4(CO)_{12}$, it is necessary to conduct the pyrolysis reaction of $Os_3(CO)_{10}(\mu^2\text{-}O(CH_2)_5OH)_2$ in the absence of free 1,5-pentanediol. If our suspicion is true, then this reaction will first afford the unidentified intermediate and then $H_4Os_4(CO)_{12}$ on extension of the reflux period.

Proposed structure #4 for product 1 from the reaction of $Os_3(CO)_{10}(\mu^2\text{-}OEt)_2$ with $Os_3(CO)_{10}(\mu^2\text{-}O(CH_2)_5OH)_2$ may serve as the intermediate to hydride transfer from ligand

to cluster in the formation of $H_4Os_4(CO)_{12}$. If this is in fact an intermediate leading to the thermodynamic product $H_4Os_4(CO)_{12}$, then it might be possible to derive a mechanism for the ligand-cluster transformation. This would contribute to our understanding of what organic transformations may be facilitated by a triosmium cluster – an area in which there is little understanding throughout the field. Therefore, the next step in these investigations of 1,5-pentanediol substituted clusters is to conduct the pyrolysis reaction mentioned above and, in doing so, attempt to characterize any cluster intermediates leading to $H_4Os_4(CO)_{12}$.

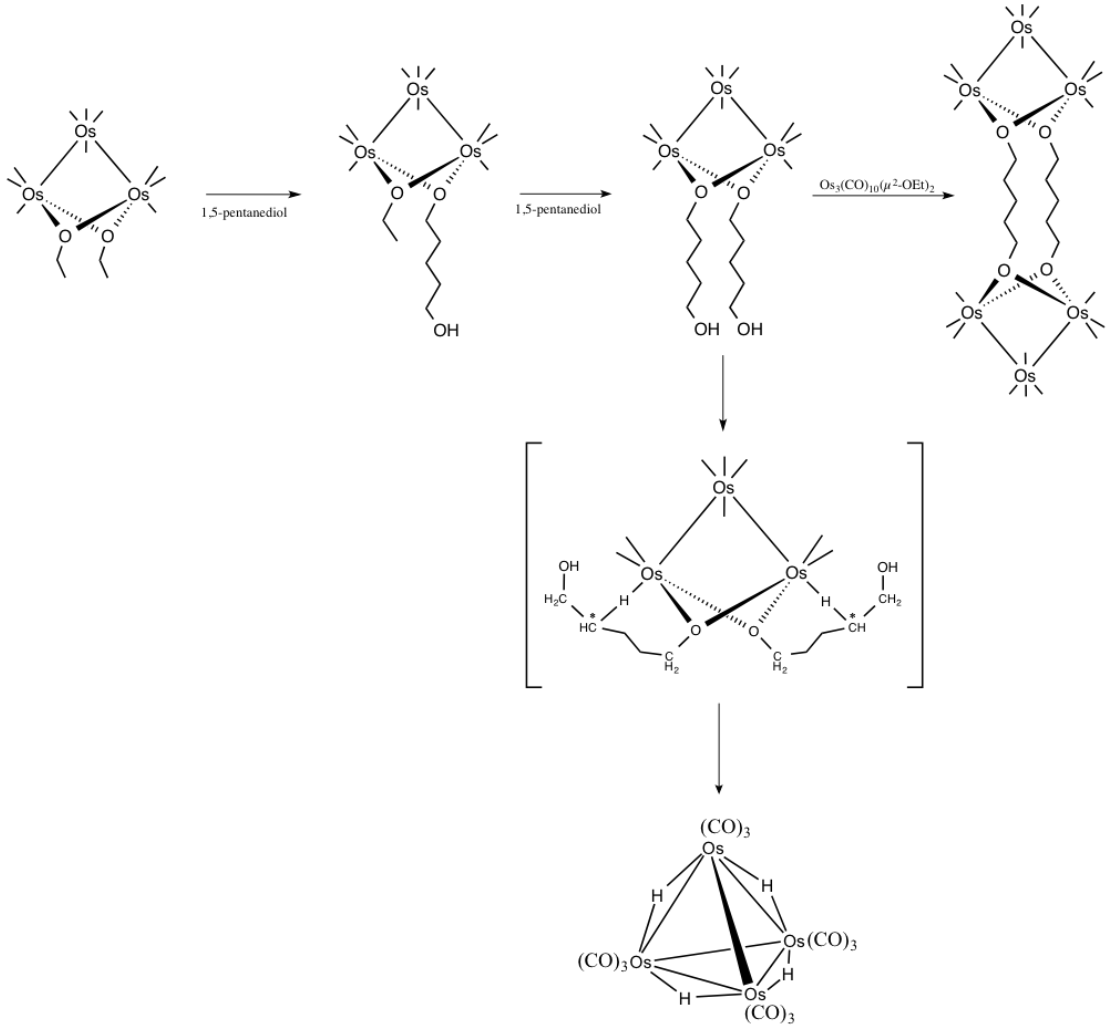

Figure 82 – Summary of findings on the interactions of 1,5-pentanediol with the cluster $Os_3(CO)_{10}(\mu^2\text{-}OEt)_2$. The structure of the cluster shown in brackets has not yet been determined.

7. Works Cited

[1] Cotton, F. A.; Wilkinson, G., Advanced Inorganic Chemistry. 5th ed.; Wiley: 1988.

[2] Miessler, G. L.; Tarr, D. A. Inorganic Chemistry. 4th ed.; Pearson Prentice Hall: 2011.

[3] Kampmeier, J. A. *J. Org. Chem.*, **1980**, *45*, 315.

[4] Kleiderer, E. C.; Kornfeld, E. C. Raney-Nickel as an Organic Oxidation-Reduction Catalyst. *J. Org. Chem.*, **1948**, *13*, 455.

[5] Johnson, B. F. G.; Lewis, J.; Kilty, P.A. *Chem. Comm.* **1968**, 180.

[6] Bradford, C. W.; Nyholm, R. S. *Chem. Comm.* **1967**, 384.

[7] Deeming, A. J. *Triosmium Clusters. Advances in Organometallic Chemistry*. **1986**, *26*, 1-96.

[8] Johnson, B.F.G.; Lewis, J.; Pippard, D.A. *J. Chem. Soc. Dalton Trans.* **1981,** 407.

[9] Burgess, K. Reactions of Triosmium Clusters with Organic Compounds. *Polyhedron*, **1984**, *3*, 1175.

[10] Lewis, J.; Johnson, B. F. G.; Deeming, A. J. Chemistry of Polynuclear Compounds. Part XVIII. Some Reactions of Dodecacarbonyltriosmium and some Related Derivatives. *J. Chem. Soc. (A)*, **1970**, 897.

[11] Cabeza, J. A.; Martínez-García, M. A.; Riera, V.; García-Granda, S.; Ardura, D. Triosmium carbonyl complexes containing bridging ligands derived from *ortho*-functionalized anilines. *J. Organomet. Chem.*, **1996**, *525*, 133.

[12] Johnson, B.F.G.; Lewis, J.; Pippard, D.A. *J. Chem. Soc. Dalton Trans.* **1981,** 407.

[13] Braga, D.; Lewis, J.; Johnson, B. F. G.; McPartin, M.; Nelson, W. J. H.; Vargas, M. D. Synthesis and x-ray analysis of the tetrahydrido dianion $[H_4Os_{10}(CO)_{24}]^{2-}$, the first noncarbido decaosmium cluster. *J. Chem. Soc., Chem. Commun.* **1983**, 241.

[14] Pearsall, Mary-Ann. Synthesis and reactivity of some osmium carbonyl clusters. PhD. Dissertation, Cambridge University, 1984.

[15] Knox, S. A. R.; Koepke, J. W.; Andrews, M. A.; Kaesz, H. D. *J. Am. Chem. Soc.* **1975**, *97*, 3942.

[16] Arce, A. J.; Deeming, A. J.; Donovan-Mtunzi, S.; Kabir, S. E. *J. Chem. Soc. Dalton Trans.* **1985,** 2479.

[17] Azam, K. A.; Deeming, A. J.; Kimber, R. E.; Shukla, P. R. *J. Chem. Soc. Dalton Trans.*, **1976**, 1853.

[18] Walter, T. H.; Frauenhoff, G. R.; Shapley, J. R.; Oldfield, E. *Inorg. Chem.*, **1991**, *30*, 4732.

[19] Shah, Ashish.; Crotty, Joe. Unpublished Results. Drew University, Madison, NJ, 2010.

[20] Patel, Runi. Unpublished Results. Drew University, Madison, NJ, 2011.

[21] Reuger, Catherine. Unpublished Results. Drew University, Madison, NJ, 2016.

[22] Marak, Katherine. Unpublished Results. Drew University, Madison, NJ, 2016.

[23] Baum, B. E. An investigation of the kinetics of the disubstitution reaction of triosmium complexes of type $Os_3(CO)_{10}(\mu^2\text{-}X)_2$ (X = Cl, Br, I, OMe, OEt, O*i*Pr, O*t*Bu, OPh) with trimethyl phosphite. Honors Thesis. Drew University, Madison NJ, 2004.

[24] Cavaliere, V. Kinetics of Osmium Carbonyl Clusters. Unpublished Results. Drew University, Madison, NJ, 2006.

[25] Barnum, T. J. Synthesis and theoretical analysis of dibridged triosmium carbonyl clusters. Honors Thesis. Drew University, Madison, NJ, 2013.

[26] Babyak, J. Studies of the substitution of bridging alkoxy ligands in triosmium carbonyl clusters and their effects on reactivity. Honors Thesis. Drew University, Madison, NJ, 2000.

[27] K.A. Azam, A.J. Deeming, R.E. Kimber and P.R. Shukla. Metallation of hydroxyl-aryl and –alkyl Compounds by Reaction with Dodecacarbonyl-*triangulo*-triosmium. *J. Chem. Soc. Dalton Trans.* **1976**, 1853-1858.

[28] Leong, W. K.; Chunxiang, L. The reaction of triosmium and –ruthenium clusters with bifunctional ligands. *J. Organomet. Chem.* **2008**, *693*, 1292.

[29] Lum, M.W.; Leong, W.K. Chemical transformations on diol anchored to a triosmium cluster. *J. Chem. Soc. Dalton Trans.* **2001**, 2476-2481.

[30] Mykietyn, Justin. Triosmium carbonyl clusters and their reactions with ethylene glycol. Honors Thesis, Drew University, Madison, NJ, 2006.

[31] Mularz, Ann. Reactions of Triosmium Clusters with 1,6-hexanediol. Honors Thesis. Drew University, Madison, NJ, 2009.

[32] Pyper, K. J.; Jung, J. Y.; Newton, B. S.; Nesterov, V. N.; Powell, G. L. Reactions of $Os_3(CO)_{12}$ with Carboxylic Acids in a Microwave Reactor; Synthesis of $Os_2(benzoate)_2(CO)_6$, a Dinuclear Osmium(I) Compound with Aromatic Carboxylate Ligands. *J. Organomet. Chem.* **2013**, *723*, 103.

[33] Portero, Erika. Organometallic Chemistry: Bisethoxide and Dicarboxylic acids Reactions to Form Linked Systems. Unpublished Results, Drew University, Madison, NJ, 2014.

[34] Bruce, M. I.; Stone, F. G. A. Low-pressure synthesis of $Ru_3(CO)_{12}$. *Chem. Commun.*, **1966**, 684.

[35] Pearsall, Mary-Ann. Personal Communication. Drew University, Madison, NJ, 2014.

[36] Schmit, Lynn. Unpublished Results. Drew University, Madison, NJ, 2012.

[37] Rivero, Estephanie. Unpublished Results. Drew University, Madison, NJ, 2014.

[38] Frauenhoff, G. R. Oxyligand derivatives of triosmium dodecacarbonyl. *Coord. Chem. Rev.*, **1992**, *121*, 131.

[39] Barquera-Lozada, J. E.; Obenhuber, A.; Hauf, C.; Scherer, W. On the Chemical Shifts of Agostic Protons. *J. Phys. Chem. A*, **2013**, *117*, 4304.

[40] Johnson, B.F.G.; Lewis, J.; Kilty, P. A. *J. Chem. Soc. (A)*, **1968**, 2859.

8. Spectral Appendix

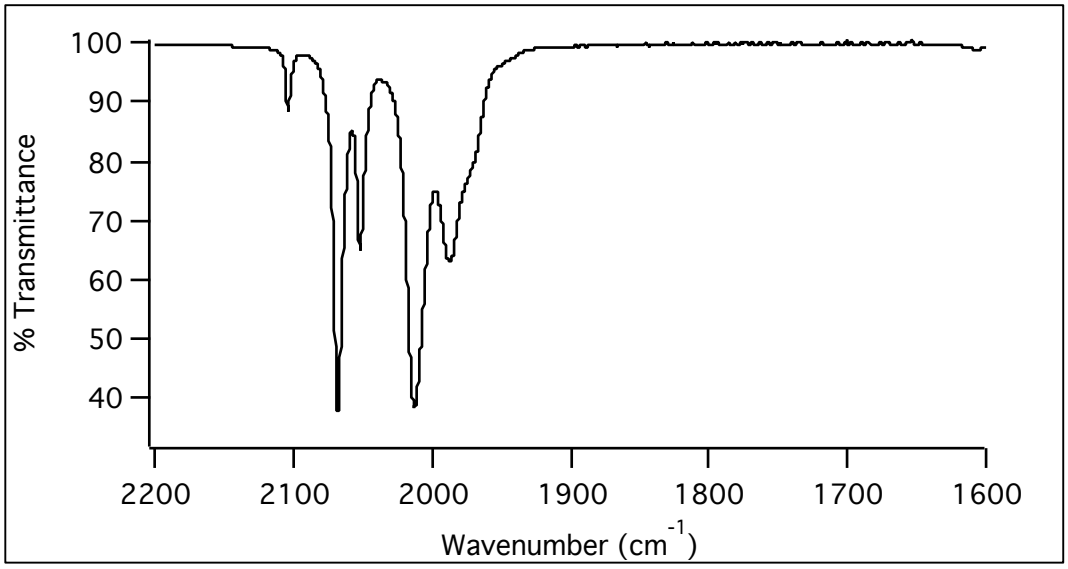

IR-1 – Infrared spectrum of pure $Os_3(CO)_{10}(\mu^2\text{-}OEt)_2$ obtained from the reaction of $Os_3(CO)_{12}Cl_2$ with ethanol in the presence of alumina.

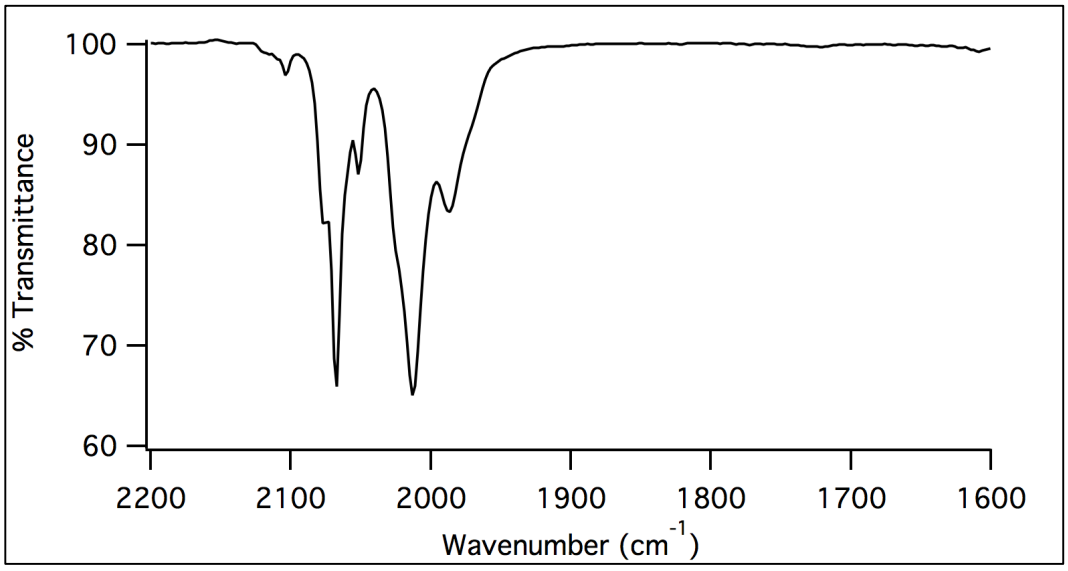

IR-2 – Infrared spectrum of $Os_3(CO)_{10}(\mu^2\text{-}OEt)_2$ containing ω impurity.

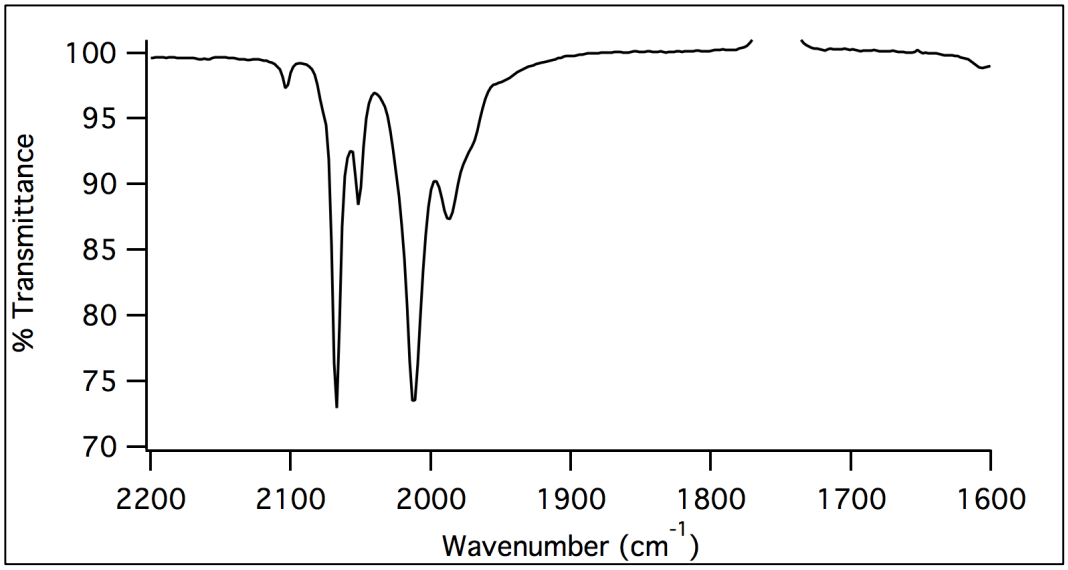

IR-3 – Infrared spectrum of $Os_3(CO)_{10}(\mu^2\text{-}OEt)_2$ obtained after partially converting a mixture of $Os_3(CO)_{10}(\mu^2\text{-}OEt)_2$ and ω to pure $Os_3(CO)_{10}(\mu^2\text{-}OEt)_2$.

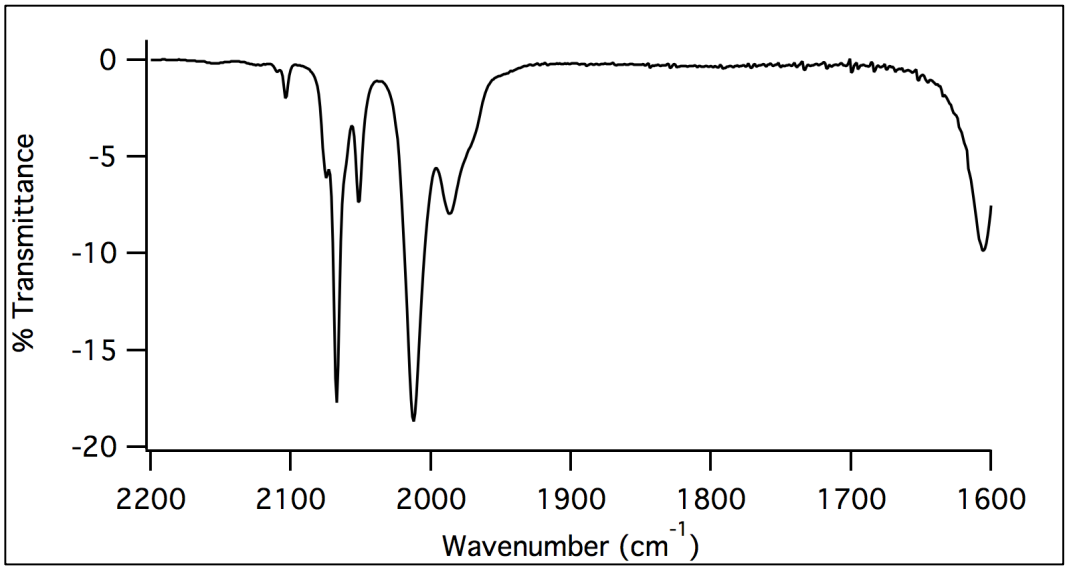

IR-4 – Infrared spectrum of product B from the 20-minute reaction of $Os_3(CO)_{10}(\mu^2\text{-}OEt)_2$ with 1,5-pentanediol. Structure is proposed to be the monosubstituted cluster $Os_3(CO)_{10}(\mu^2\text{-}OEt)(\mu^2\text{-}O(CH_2)_5OH)$.

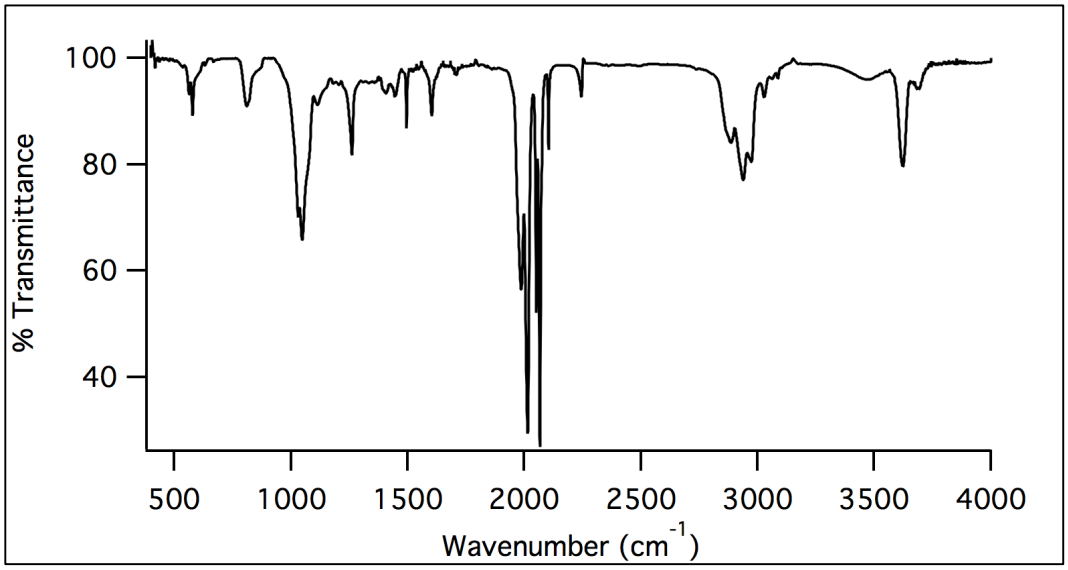

IR-5 – Infrared spectrum of the colorless precipitate obtained from cooling reaction mixture at -20 ˚C in the 20-minute reaction of $Os_3(CO)_{10}(\mu^2\text{-}OEt)_2$ with 1,5-pentanediol. Spectrum is characteristic of 1,5-pentanediol.

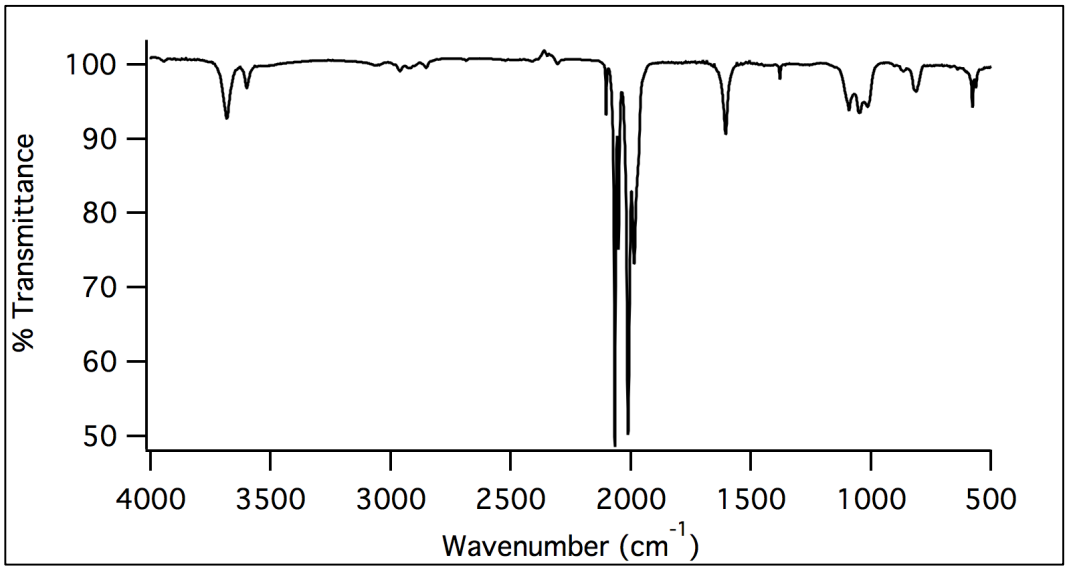

IR-6 – Infrared spectrum of compound A from the 20-minute reaction of $Os_3(CO)_{10}(\mu^2\text{-}OEt)_2$ with 1,5-pentanediol. This compound was deduced to be unreacted starting material.

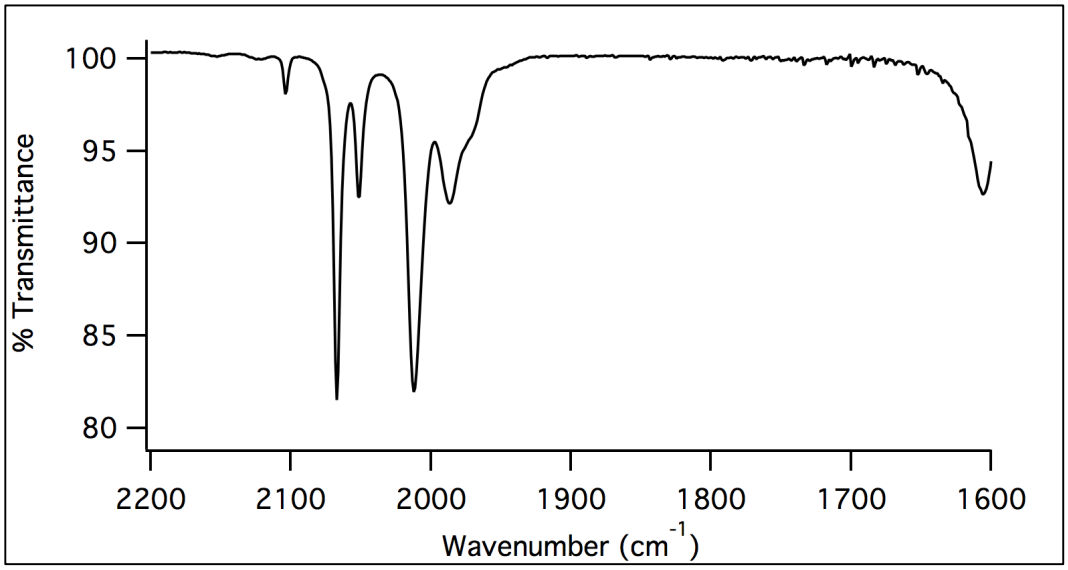

IR-7 – Infrared spectrum of product C from the 20-minute reaction of $Os_3(CO)_{10}(\mu^2\text{-}OEt)_2$ with 1,5-pentanediol. Structure is proposed to be the disubstituted cluster $Os_3(CO)_{10}(\mu^2\text{-}O(CH_2)_5OH)_2$.

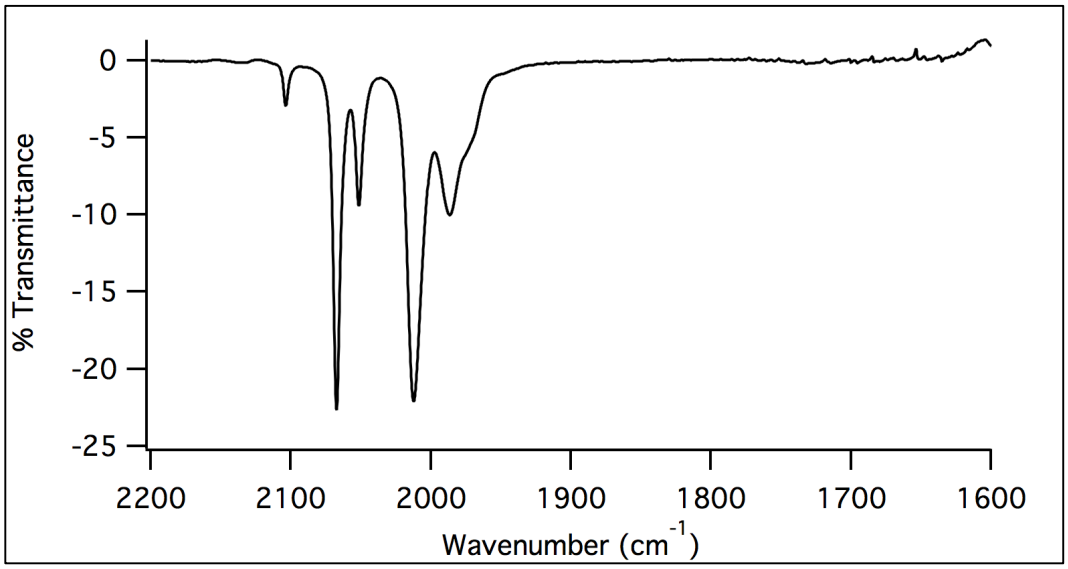

IR-8 – Infrared spectrum of product C from the 60-minute reaction of $Os_3(CO)_{10}(\mu^2\text{-}OEt)_2$ with 1,5-pentanediol. Structure is proposed to be the disubstituted cluster $Os_3(CO)_{10}(\mu^2\text{-}O(CH_2)_5OH)_2$.

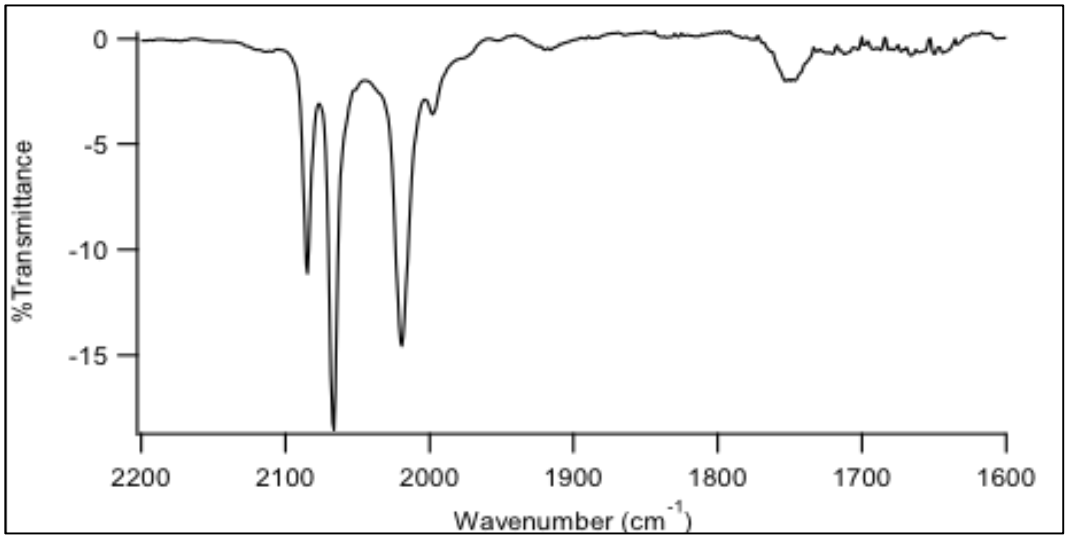

IR-9 – Infrared spectrum of the reaction mixture of the 20-hour reaction of $Os_3(CO)_{10}(\mu^2\text{-}OEt)_2$ with 1,5-pentanediol after 19-hours at reflux in toluene. Spectrum shows the dominant carbonyl stretching pattern to be characteristic of the cluster $H_4Os_4(CO)_{12}$.

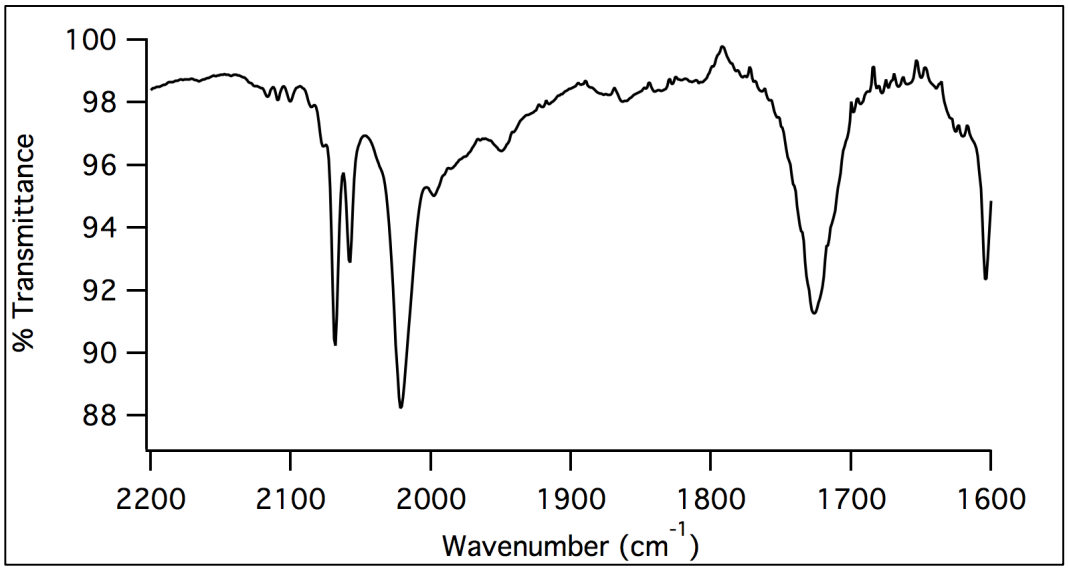

IR-10 – Infrared spectrum of the toluene solution from the 20-hour reaction of $Os_3(CO)_{10}(\mu^2\text{-}OEt)_2$ with 1,5-pentanediol after cooling at -20 ˚C. Spectrum shows minor cluster carbonyl stretching bands at very low intensity.

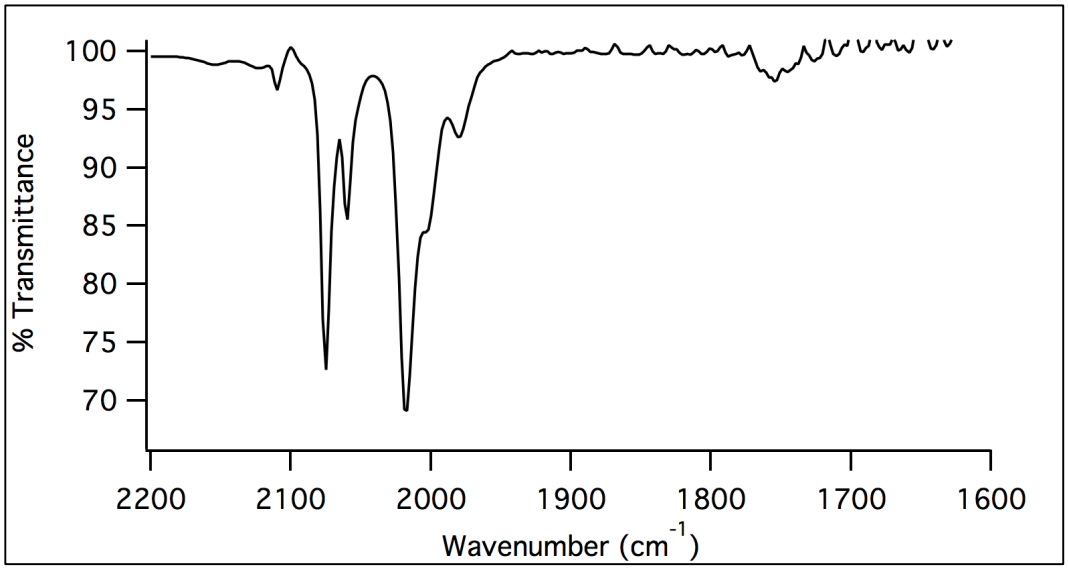

IR-11 – Infrared spectrum of product B from a 40-minute reaction of $Os_3(CO)_{10}(\mu^2\text{-}OEt)_2$ with 1,5-pentanediol. Structure is proposed to be the cluster $Os_3(CO)_{10}(\mu^2\text{-}Cl)(\mu^2\text{-}O(CH_2)_5OH)$.

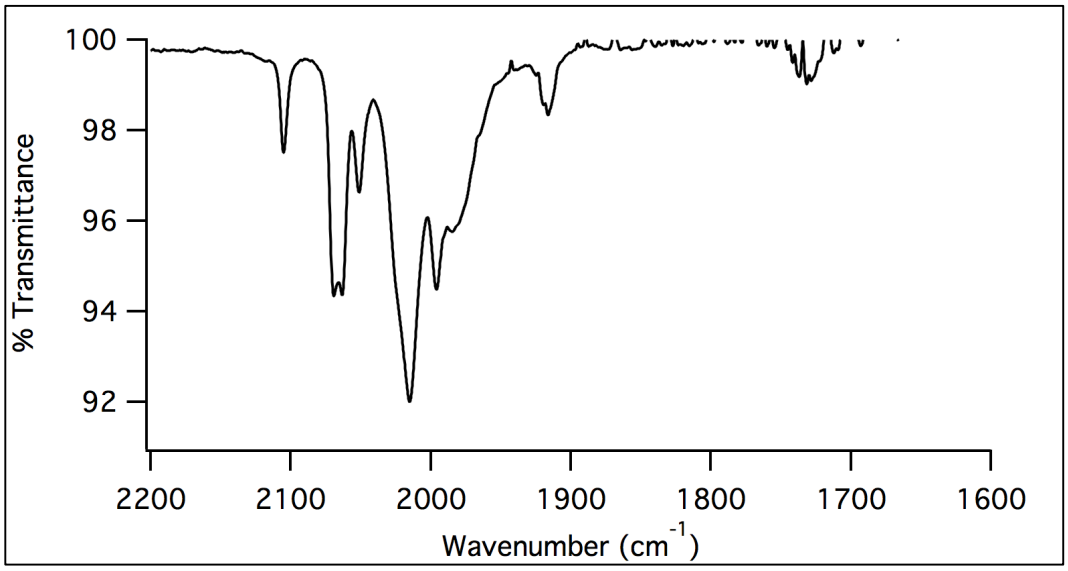

IR-12 – Infrared spectrum of a band collected after preparative plate separation of the crude product from the reaction of $Os_3(CO)_{10}(\mu^2\text{-}OEt)_2$ with $Os_3(CO)_{10}(\mu^2\text{-}O(CH_2)_5OH)_2$. Spectrum shows that at least two clusters are present in solution.

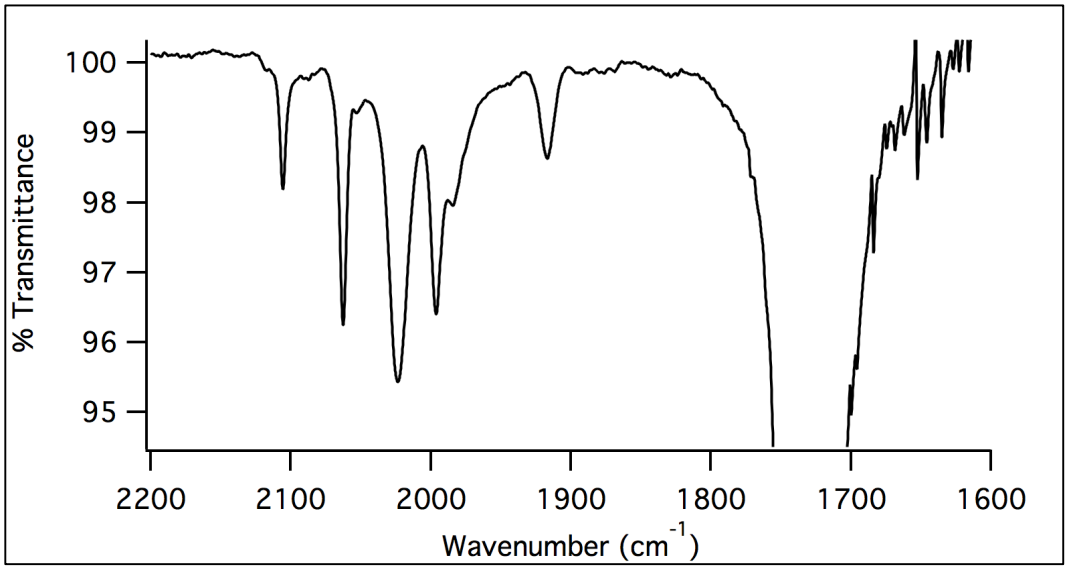

IR-13 – Infrared spectrum of product 1 from the 100-minute reaction of $Os_3(CO)_{10}(\mu^2\text{-}OEt)_2$ with $Os_3(CO)_{10}(\mu^2\text{-}O(CH_2)_5OH)_2$ in toluene. Structure is proposed to be an 8-carbonyl triosmium cluster with bridging alkoxide ligands and possibly agostic proton(s).

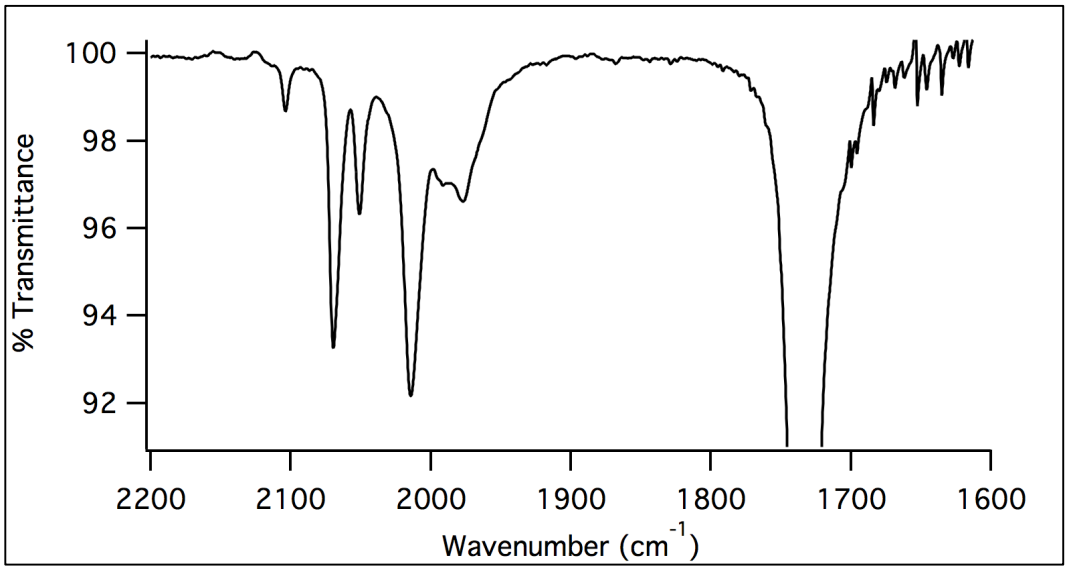

IR-14 – Infrared spectrum of product 2 from the 100-minute reaction of $Os_3(CO)_{10}(\mu^2\text{-}OEt)_2$ with $Os_3(CO)_{10}(\mu^2\text{-}O(CH_2)_5OH)_2$ in toluene. Structure is proposed to be the linked cluster $\{Os_3(CO)_{10}\}_2(\mu^2\text{-}O(CH_2)_5O)_2$.

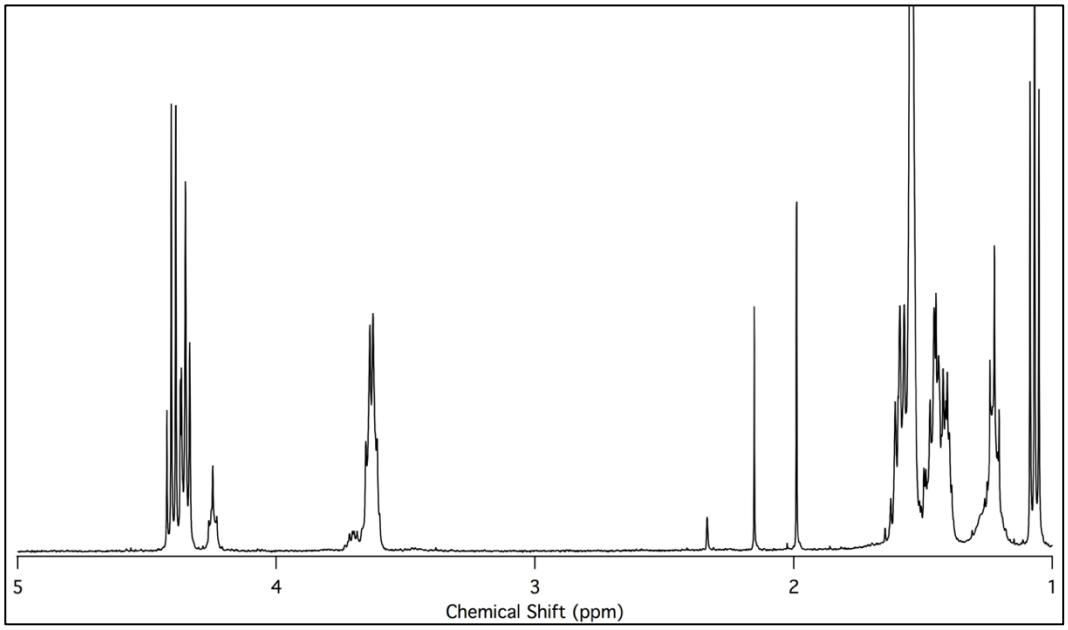

NMR-1 – ^{1}H NMR spectrum of product B from the 20-minute reaction of $Os_3(CO)_{10}(\mu^2\text{-}OEt)_2$ with 1,5-pentanediol. Structure is proposed to be the monosubstituted cluster $Os_3(CO)_{10}(\mu^2\text{-}OEt)(\mu^2\text{-}O(CH_2)_5OH)$.

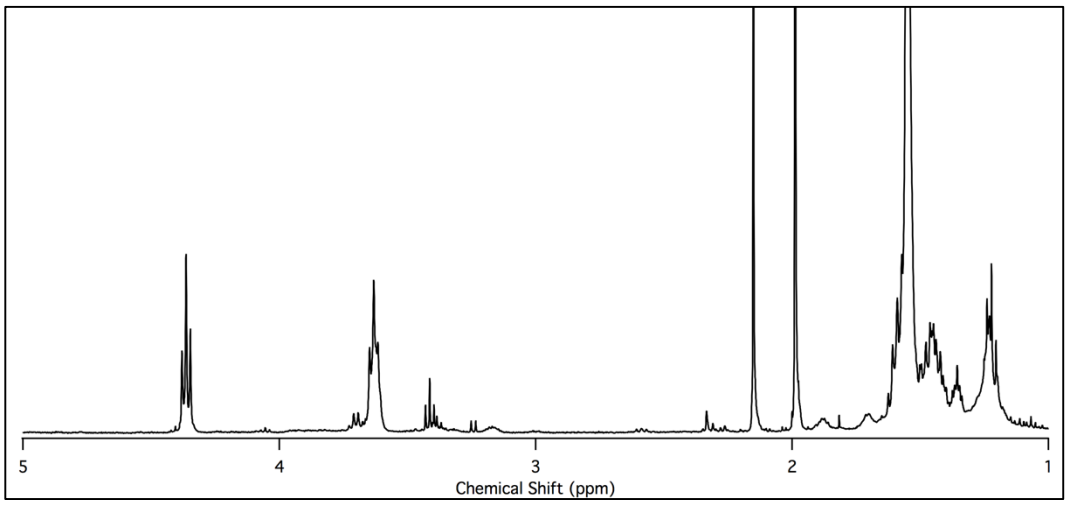

NMR-2 – ^{1}H NMR spectrum of product C from the 20-minute reaction of $Os_3(CO)_{10}(\mu^2\text{-}OEt)_2$ with 1,5-pentanediol. Structure is proposed to be the disubstituted cluster $Os_3(CO)_{10}(\mu^2\text{-}O(CH_2)_5OH)_2$.

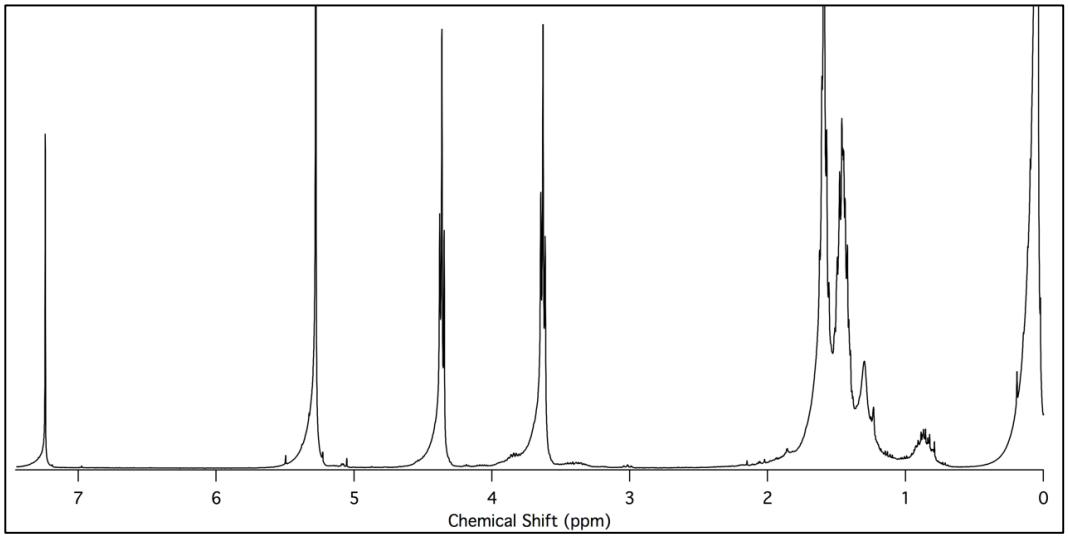

NMR-3 – ^{1}H NMR spectrum of product C from the 60-minute reaction of $Os_3(CO)_{10}(\mu^2\text{-}OEt)_2$ with 1,5-pentanediol. Structure is proposed to be the disubstituted cluster $Os_3(CO)_{10}(\mu^2\text{-}O(CH_2)_5OH)_2$.

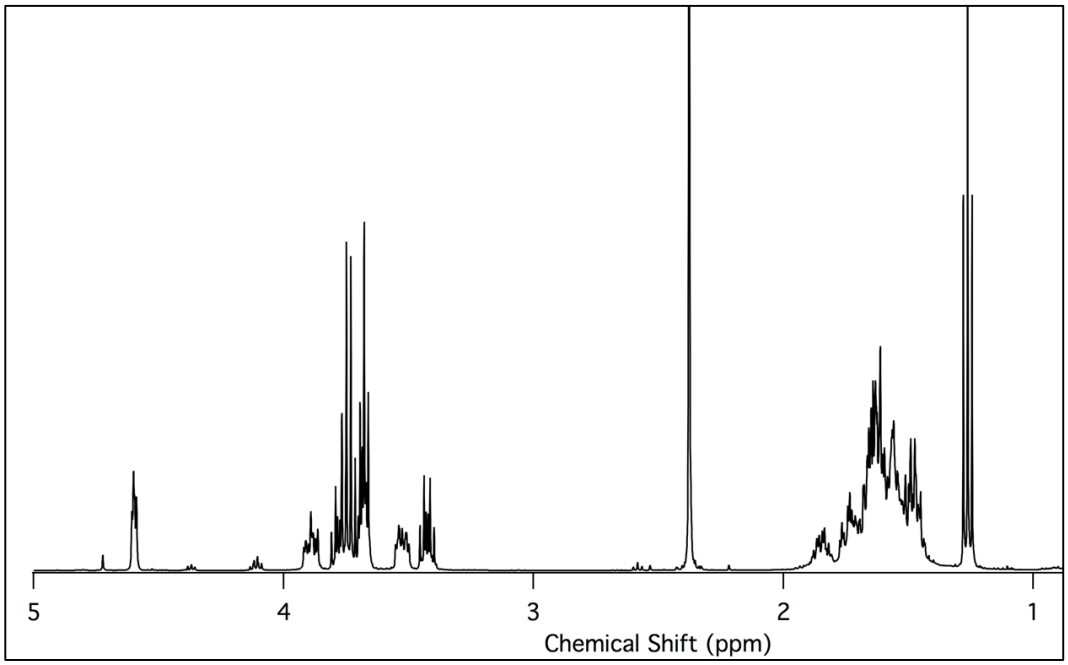

NMR-4 – ^{1}H NMR spectrum of minor cluster product and/or organic ester from the 20-hour reaction of $Os_3(CO)_{10}(\mu^2\text{-}OEt)_2$ with 1,5-pentanediol after cooling at -20 ˚C.

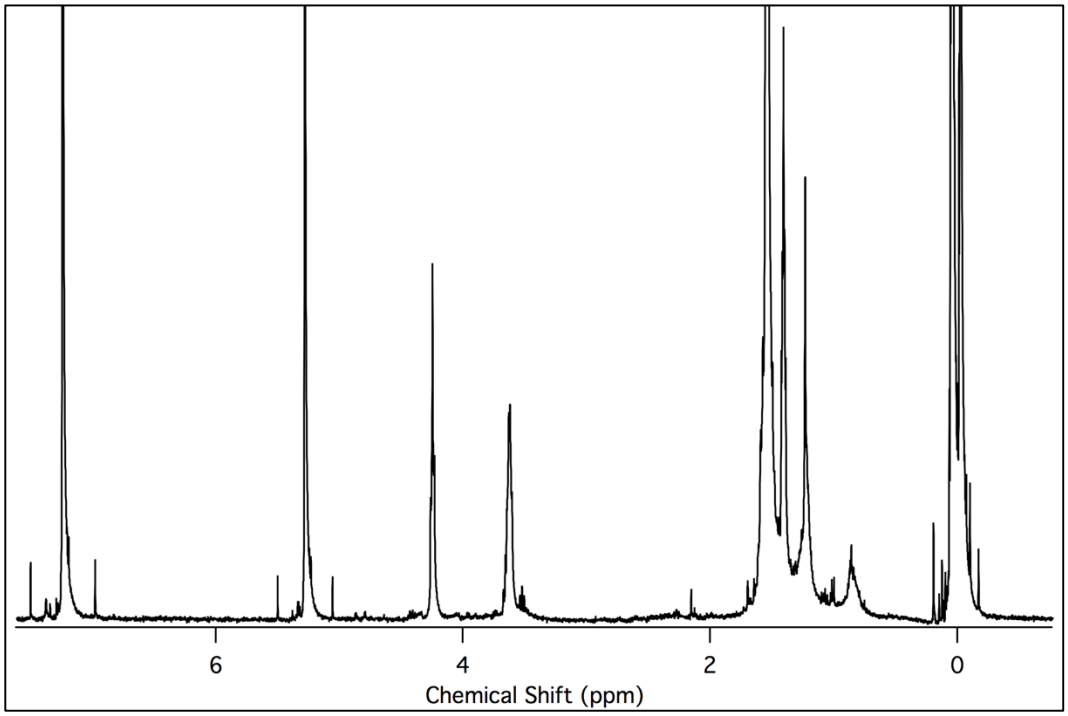

NMR-5 – ^{1}H NMR spectrum of product B from a 50-minute reaction of $Os_3(CO)_{10}(\mu^2\text{-}OEt)_2$ with 1,5-pentanediol. Structure is proposed to be the cluster $Os_3(CO)_{10}(\mu^2\text{-}Cl)(\mu^2\text{-}O(CH_2)_5OH)$.

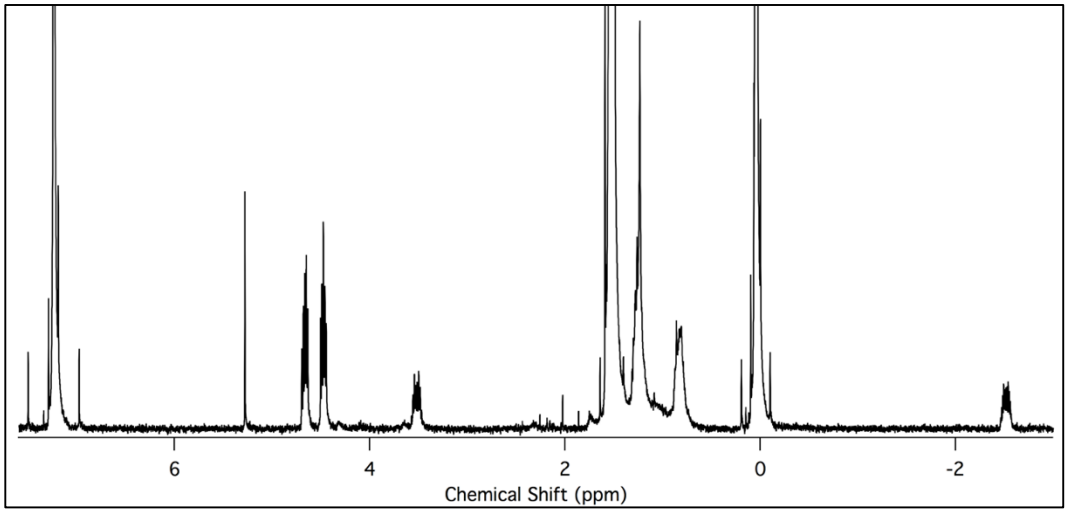

NMR 6 – ^{1}H NMR spectrum of product 1 from the 100-minute reaction of $Os_3(CO)_{10}(\mu^2\text{-}OEt)_2$ with $Os_3(CO)_{10}(\mu^2\text{-}O(CH_2)_5OH)_2$ in toluene. Structure is proposed to be an 8-carbonyl triosmium cluster with bridging alkoxide ligands and possibly agostic proton(s).

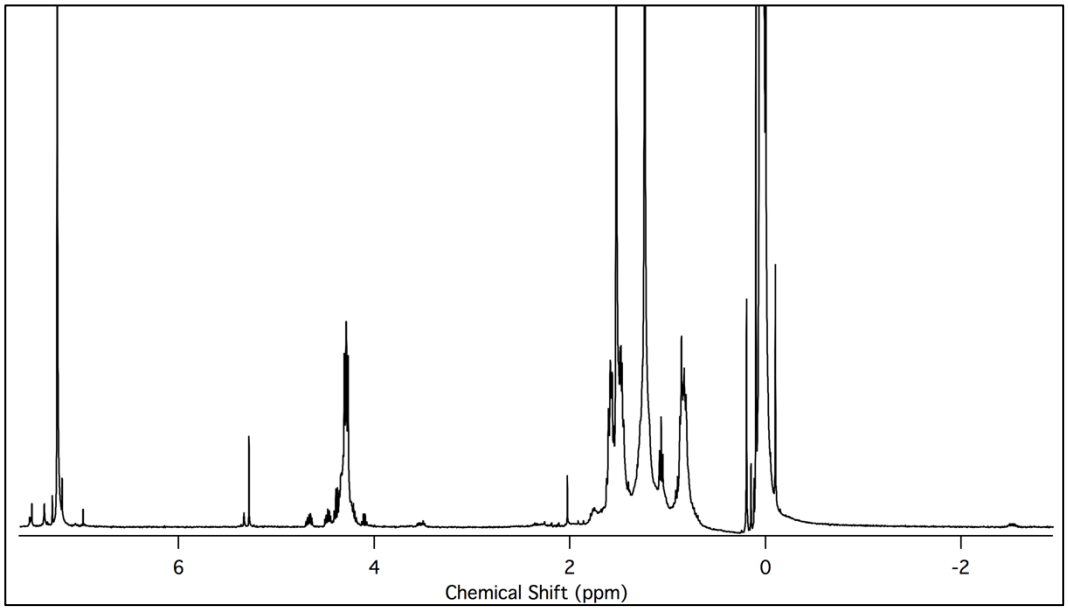

NMR 7 – ^{1}H NMR spectrum of product 2 from the 100-minute reaction of $Os_3(CO)_{10}(\mu^2\text{-}OEt)_2$ with $Os_3(CO)_{10}(\mu^2\text{-}O(CH_2)_5OH)_2$ in toluene. Structure is proposed to be the linked cluster $\{Os_3(CO)_{10}\}_2(\mu^2\text{-}O(CH_2)_5O)_2$.